

WA /
388
H-531 p3
v. 2

15.2

PAVEMENT RESEARCH
at the
WASHINGTON STATE UNIVERSITY
TEST TRACK

STATE LIBRARY
AUG 23 1972
OLYMPIA, WASH.

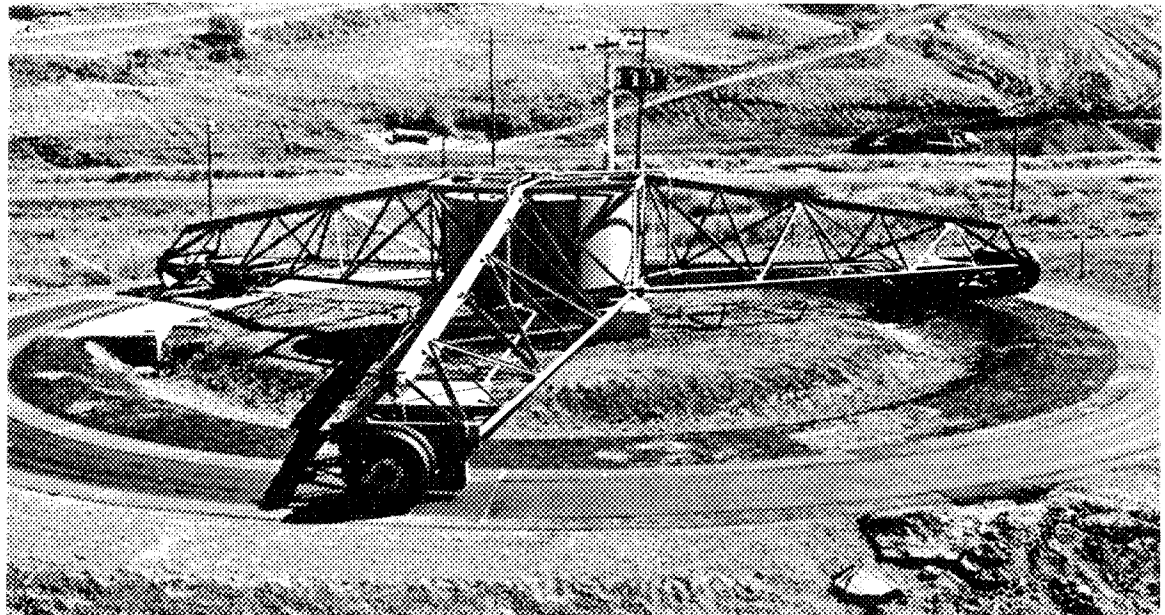
DO NOT REMOVE
From Research Office

VOLUME TWO

EXPERIMENTAL RING NO. 2: A STUDY OF UNTREATED,
EMULSION TREATED, AND ASPHALTIC-CEMENT TREATED BASES

Research Project Y-651

Highway Research Section
College of Engineering Research Division
Washington State University
Pullman, Washington



A Federal Aid Research Project in Cooperation
with the Department of Transportation
Federal Highway Administration
Bureau of Public Roads

The Washington State Department of Highways
and

The Asphalt Institute

1968

PAVEMENT RESEARCH
at the
WASHINGTON STATE UNIVERSITY
TEST TRACK

VOLUME TWO

EXPERIMENTAL RING NO. 2: A STUDY OF UNTREATED,
EMULSION-TREATED, AND ASPHALTIC-CEMENT TREATED BASES

Report to the Washington State Department of Highways
on Research Project Y-651

by

Milan Krukar and John C. Cook

Highway Research Section
College of Engineering Research Division
Washington State University
Pullman, Washington
July, 1968

In Cooperation with
U. S. Department of Transportation
Federal Highway Administration
Bureau of Public Roads

The Washington State Department of Highways
and
The Asphalt Institute

The opinions, findings, and conclusions expressed in this
publication are those of the authors and not necessarily
those of the Bureau of Public Roads.

(Highway Research Section Publication H-29)

ACKNOWLEDGMENTS

The Highway Research Staff wishes to thank the Washington State Highway Department for their financial and technical support. There were many highway department staff personnel who helped, but we want to single out the following: Carl E. Minor, Assistant Director of Planning & Research for his continued interest and support; Roger V. LeClerc, Materials Engineer who helped with the research project laboratory analysis, instrumentation and with advice; and Tom R. Marshall, Special Assignments Engineer, who spent several days in Pullman helping with construction, and also did much laboratory design analysis, all from Olympia, Washington. Sincere appreciation is due Art Sinclair, Materials Engineer from District 6, Spokane, Washington, for his unfailing help, interest and advice.

Continual financial and technical support was given the project by The Asphalt Institute, College Park, Maryland. Particular acknowledgment and thanks are given to the following individuals of that organization: Jess Buchanan, President; John M. Griffith, Director of Research and Development; Ian R. Kingham, Staff Engineer. Provision of funds and expert technical knowledge from men such as these has helped immeasurably.

Appreciation is recorded to Ron Trolle, Sales Engineer with the Chevron Asphalt Company for his continued help, interest and advice in the project, especially with the emulsion-treated bases.

The following persons, Tom R. Marshall of the Washington Highway Department, Ian R. Kingham of The Asphalt Institute, and G. W. Ring of the Bureau of Public Roads, reviewed the rough draft of this report and made many helpful suggestions many of which have been incorporated into the final report. Their efforts are greatly appreciated by the authors. However, this does not mean that they are responsible for the contents, opinions and conclusions expressed or errors which may appear in this report, for this the authors take full responsibility.

Thanks go to the secretaries, Mrs. Joan Trent, Misses Patty Wong and Judy Benes, who helped in typing and editing the various drafts of this report. The following Washington State University students, Don Averill, Ted Rees, John Cramer, Dale Barr and Dick Baker contributed to the preparation of this report by helping with evaluation of the data and with drafting.

TABLE OF CONTENTS

	Page
ACKNOWLEDGMENTS	iii
LIST OF TABLES	vi
LIST OF FIGURES	vii
ABSTRACT	xiii
INTRODUCTION	1
EXPERIMENTAL DESIGN	2
Materials	2
Subgrade	2
Crushed Surfacing Top Course	6
Special Screened Non-Fractured Aggregate	6
Asphalt Concrete Class B Aggregate	9
Construction	9
Pre-Conditioning	9
Subgrade	9
Crushed Surfacing Top Course Base--Untreated (Sections 1-4).	12
Special Asphalt-Treated Base (Sections 9-12).	12
Emulsion-Treated Base (Sections 5-8).	17
Class "B" Asphalt Concrete Wearing Course	23
Shoulders	23
Instrumentation	25
Measurement of Moisture	27
Temperature Measurements	29
Iron-constantan thermocouples	29
Thermograph	29
Stress (Pressure) Measurements	29
WSU pressure cells	29
Filpip pressure transducers	29
Strain Measurements	32
Strain gages (subgrade)	32
Strain gages (bases and surfaces)	35
Deflection Measurements	35
Dynamic	35
Rebound deflection measurements	36
Read-Out Equipment	36

	Page
PERFORMANCE OF TEST RING #2	39
Testing Periods	39
Testing Conditions	39
Design Thickness	39
Speed	40
Environmental Conditions	40
Experimental Results	47
Section Failures	47
Fall Period--1966	47
Spring Period--1967	47
Failure pattern	49
Discussion of Section Failures	51
Load Response Characteristics	66
Temperature Variables	66
Moisture Contents	66
Static Deflections	79
Dynamic Deflections	81
Strain Gage Data	94
Stress Data	96
Discussion of Results	121
Limitations of Test Track Testing	126
CONCLUSIONS	129
Major Conclusions	129
Minor Conclusions	130
PRACTICAL IMPLICATIONS FROM TEST RING #2	131
REFERENCES	133

LIST OF TABLES

Table		Page
I	Types, Sections and Thicknesses of Ring #2	3
II	Optimum Density and Moisture for Subgrade Material	5
III	Soil Characteristics and Classification	5
IV	Densities of Silt Subgrade at Final Grade	11
V	Average Field Densities of Bases at Final Grade	15
VI	Mix Design Requirements	16
VII	Emulsion-Treated Base--Moisture Contents	19
VIII	Location of Instruments Along Center Line	25
IX	Depth of LVDT Holes	36
X	Core Thicknesses and Densities	41
XI	Average Temperature Variations - Ring No. 2	44
XII	Section Condition Progress Report	48
XIII	Pavement Performance Summary - Fall and Spring Periods	52
XIV	Pavement Failure Span (PFS)	63
XV	Equivalent Thickness	64
XVI	Moisture Contents in Untreated Materials	76
XVII	Moisture Contents in Bases	76
XVIII	Subgrade Moistures at Test Completion	77
XIX	Summary of Benkelman Beam Deflection Measurements	80
XX	Summary of LVDT Deflection Maximum Measurements	87
XXI	Ratio of Shallow to Deep Dynamic Deflections	92
XXI (A)	Pavement System (PS) Vs Subgrade (S) Deflections	93
XXII	Summary of Maximum Longitudinal and Transverse Strain Gage Measurements	99
XXIII	Summary of Maximum Vertical Stresses	119
XXIV	Stress Reduction Ratios for Different Base Materials	120
XXV	Equivalencies in Terms of ATB	125

LIST OF FIGURES

Figure		Page
1	Permanent Structures and Pavement Sections Test Ring No. 2 Plan View	3
2	Schematic Profile for Ring No. Two	4
3	Density-Moisture Curves (subgrade soil characteristics).	5
4	Gradation Curve for Crushed Surfacing Top Course-- Untreated Base Sections 1-4 and Emulsion-Treated Sections 5-8	7
5	Maximum Density Curve for Crushed Surfacing Top Course	7
6	Gradation Curve for Special Non-Fractured Screened Aggregate - Special A.T.B. Sections 9-12	8
7	Combined Gradation Curve for Asphalt Concrete Class "B" Aggregate - All Sections	8
8	Leveling of the Subgrade by Maintainer	10
9	Handscreeing the Subgrade to Final Grade	10
10	The Placing of the Crushed Surface Top Course in Section 4 with a Blaw-Knox Paver	13
11	The Appearance of the Special Screened Non-Fractured Aggregate at the Test Track Stockpile	13
12	Compacting the Special Asphalt-Treated Base Sections 10-11	14
13	Appearance of the Special Asphalt-Treated Base After Rolling with Steel Roller	14
14	Attempting to Roll the Emulsion-Treated Base After a 3-Hour Curing Period	18
15	The First Two Lifts of Emulsion-Treated Base in Section 8 Being Cured by Visqueen Plastic Covering	18
16	The Appearance of the 3rd Lift of Emulsion-Treated Base in Sections 7 & 8 After Rolling	21
17	Appearance of the Emulsion-Treated Base in Section 6 After Being Cured and Rolled	21
18	A View of the Final Grade After the 3.0" Class "B" Asphalt Concrete Wearing Course Was Laid Being Checked by Straight Edge	24

Figure

19	Density of the Class "B" Mat Being Measured by the Nuclear Asphalt Gage and Scaler	24
20	Instrumentation for Section 8 - E.T.B.	26
21	Moisture Tensiometer Characteristic Curve for Palouse Silt	28
22	A Comparison of the New WSU Pressure Cell with the Old Cells Used in Ring No. 1	30
23	A Top and Side View of the WSU Pressure Cell	30
24	Calibration Curve for WSU Pressure Cell #3	31
25	Calibration Curve for Filpip Pressure Transducer #54	31
26	A View of the Size of the Filpip Pressure Transducer	33
27	This Shows the Portion of Instruments in the Subgrade	33
28	Strain Gages Mounted on Top of Emulsion-Treated Base	34
29	Mounting Strain Gages on Pavement Surface	34
30	A View of the Short LVDT Gage, the Holder and the Ferrite Core	37
31	This Shows the Long LVDT Gage, and the Inside Parts of the Holder	37
32	A Comparison of the Sizes of the Dehlen Curvature Meter, Idaho Beam, and the Soiltest Benkelman Beam	38
33	A View of the Read-Out Equipment	38
34	Speed Versus Time (Expressed in Wheel Load Repetitions)	42
35	Precipitation for Ring No. 2 Oct. '66-May '67	45
36	Average Maximum, Minimum and Average Monthly Temperature for Ring No. 2, 7-Month Period 1966-67	46
37	The Appearance of the Transverse Cracks at 100,000 Wheel Loads in 7.0 Inches of Untreated Base, Section 2	53
38	Another View of the Transverse Cracking in Section 2 Stage 2	53
39	The Appearance of Section 2 at Ultimate Failure Just Before Being Removed from Service at 206,750 Wheel Loads	53

Figure		Page
40	Subsidence in the 5.0 Inches of Emulsion-Treated Base After 133,700 Wheel Loads Stage 5	54
41	Another View of Section 6 at 133,700 Wheel Loads	55
42	The Development of Ruts and Some Transverse Cracks in the 3.5 Inches of Special Asphalt-Treated Base, Section 10 After 210,234 Wheel Loads Spring Period	55
43	Further Development of Transverse Cracks in Section 10 at 216,234 Wheel Loads	56
44	Continued Deterioration of Section 10 at 219,018 Wheel Loads	56
45	The Appearance of Section 10 at Ultimate Failure After 219,123 Wheel Loads	57
46	Continued Failure at 220,377 Wheel Loads of Section 10 After an Asphalt Overlay Was Put On	57
47	Overall Appearance of Section 9 (2.0 Inches of Special Aggregate Asphalt-Treated Base) After 208,299 Wheel Loads	58
48	Spectacular Failure of Section 9 After 208,876 Wheel Loads	58
49	The Start of Transverse Cracks in Section 11 (5.0 Inches of A.T.B.) at 231,691 Wheel Loads	59
50	The Permanent Deformation in Section 11 After 231,691 Wheel Loads	59
51	Ultimate Failure of Section 11 After 232,608 Wheel Loads .	60
52	Appearance of Section 4 (12 Inches of Untreated Base) After 232,608 Wheel Loads	60
53a	The Appearance of Section 8 (9.0 Inches of E.T.B.) After 231,693 Wheel Loads	61
53b	A View of Section 8 Showing the Permanent Deformation and Cracking at Completion of Testing at 232,608 Wheel Loads	61
54	Wheel Load Applications (Initial & Final) as a Function of Base Thickness	64
55	Air, Pavement, & Soil Daily Temperatures, Week of November 9-15, 1966	67

Figure		Page
56	Air, Pavement, & Soil Daily Temperatures, Week of November 16-22, 1966	68
57	Air, Pavement, & Soil Daily Temperatures, Week of November 23-29, 1966	69
58	Air, Pavement, & Soil Daily Temperatures, Week of April 19-25, 1967	70
59	Air, Pavement, & Soil Daily Temperatures, Week of May 3-9, 1967	71
60	Air, Pavement, & Soil Daily Temperatures, Week of May 10-16, 1967	72
61	Air, Pavement, & Soil Daily Temperatures, Week of May 17-23, 1967	73
62	Moisture Contents with Time	75
63	Variation of Moisture Contents in Subgrade with Depth . .	75
64	A View of the Subgrade in Section 1 After the Pavement Was Removed	78
65	The Appearance of Subgrade in Section 10 & 11 After the Existing Test Section Had Been Removed	78
66	Deflections Vs. Wheel Loads	81
67	Temperature Vs. Deflections (Benkelman Beam)	81
68	Dynamic Deflections Against Transverse Distance for LVDT #1 & 2 in Section 2 (7.0" of Untreated Crushed Stone	84
69	Dynamic Deflection Variations with Transverse Distance . .	85
70	Dynamic Deflections Against Transverse Distance for LVDT Gages #3 & 4 - Section 6 (5.0" E.T.B.)	85
71	Dynamic Deflections, Section 8	88
72	Dynamic Deflections, Section 10	88
73	Dynamic Deflection with Respect to Wheel Loads	89
74	Effect of Different Speeds on Deflections, Section 2-- LVDT #2, November 4, 1966	91

Figure		Page
75	Dynamic Deflection Ratio $\frac{\text{Shallow}}{\text{Deep}}$	91
75 (A)	Deflections - Pavement System (PS) Vs Subgrade (S)	93
76	Section 8--9.0" Emulsion-Treated Base, Surface Longitudinal Strain Gage B-5-L	100
77	Surface Longitudinal Strain Gage B-5-L (Section 8-- Emulsion-Treated Base = 9.0")	100
78	Surface Transverse Strain Gage B-6-T, (Section 8-- Emulsion-Treated Base = 9.0")	101
79	Surface Transverse Strain Gage B-6-T (Section 8--Surface)	101
80	Longitudinal Strain Gage C-7-L, Section 8	102
81	Longitudinal Strain Gage C-7-L, Section 8	102
82	Surface Transverse Strain Gage B-6-T, Section 8	103
83	Longitudinal Strain Gage C-7-L, Section 8	103
84	Transverse Strain Gage C-8-T, Section 8	104
85	Transverse Strain Gage C-8-T, Section 8	104
86	Transverse Strain Gage C-8-T, Section 8	105
87	Longitudinal Strain, Section 8, D-5-L	106
88	Longitudinal Strain, Section 8, D-5-L	106
89	Transverse Strain, Section 8, D-6-T, Depth 3"	107
90	Transverse Strain, Section 8, D-6-T, Depth 3"	107
91	Longitudinal Strain Gage D-9-L, Section 8	108
92	Longitudinal Strain Gage D-9-L, Section 8	108
93	Transverse Strain Gage D-10-T, Section 8	109
94	Transverse Strain Gage D-10-T, Section 8	109
95	Maximum Strain Vs. Depth--Section 8, 9" Emulsion- Treated Base	110
96	Longitudinal Strain Gage B-9-L, Section 10, Surface	110
97	Transverse Strain Gage B-10-T	110

Figure		Page
98	Longitudinal Strain Gage C-9-L, Section 10, 3.0" Depth . .	112
99	Transverse Strain Gage C-10-T	112
100	Longitudinal Strain Gage E-1-L, Section 10, 6.5" Depth . .	113
101	Transverse Strain Gage E-2-T	113
102	Maximum Values of Strain Measures as Wheels Were Moving Longitudinally with Respect to Lateral Wheel Position Section 10	114
103	Vertical Stresses Measured by Filpip Transducers with Respect to Lateral Wheel Position	116
104	Vertical Stress Vs. Speed--WSU Pressure Cell	117
105	Vertical Subgrade Stress as a Function of Base Material, Depth and Environment	118
106	Transverse Vertical Stress Distribution, Section 6: 5.0" E.T.B.	118

ABSTRACT

This report describes the results obtained from Experimental Ring No. 2, the first ring of a three-ring test series on treated bases, at the Washington State University Test Track. This experiment was concerned with studying the effects of controlled wheel load repetitions on untreated, emulsion, and special aggregate asphalt-treated bases of four varying thicknesses. Construction, instrumentation, results, and conclusions are described and drawn.

Benkelman beam, LVDT, strain gages, pressure cells and moisture tensiometers were used to measure deflections, strains, stresses and moisture. Maximum values are tabulated. Temperatures were also recorded.

Testing can be divided into two time periods - fall of 1966 and spring of 1967. Values obtained from instruments show that different conditions existed during those testing periods, and that deflections, strains and stresses were two to four times higher in the spring than in the fall. Modes of failure were also different.

Equivalencies between the different base materials were established. Other conclusions were drawn. Since this is a continuing experiment, it should be emphasized that results and conclusions are subject to change, depending upon data from the remaining experimental rings.

EXPERIMENTAL PAVEMENT RING #2

INTRODUCTION

Experimental pavement Ring #2, the second ring built under contract Y-651, was the first of these rings of a continuing pavement experiment designed to test bases constructed from different materials varying in thicknesses in order to study their strengths and determine their relative equivalencies.

Each ring consists of 12 sections constructed from three different base materials which are subdivided into four sections of varying base thickness. Crushed rock base is used as the standard control for comparison purposes.

The three rings were to be constructed during the summer and tested under different environmental conditions. Ring #2 was constructed the summer of 1966 and tested the fall of 1966 and spring of 1967; Ring #3, built the summer of 1967, was tested the fall of 1967 and spring of 1968. Ring #4 will be constructed the summer of 1968 and tested the fall of 1968 and spring of 1969. Therefore, the following results from Ring #2 are tentative and subject to modification depending upon findings from Rings #3 and #4.

This part of the report is concerned with a description of Ring #2 and the experimental results. This ring has provided invaluable experience and data for future rings. The data collected has helped in evaluating the performance of other rings and has resulted in modification of future experiments.

This project was conceived and initiated by the Highway Research Section, College of Engineering, Research Division, Washington State University. Financing is a joint undertaking among the University, the Washington State Highway Department; the Bureau of Public Roads of the Federal Highway Administration, Department of Transportation, as a HRP federal aid research project; and the Asphalt Institute, which provided professional guidance in design planning and in evaluation of results.

EXPERIMENTAL DESIGN

Since the 260-foot centerline circumference of the test track limits the number of bases that can be tested at any one time, it was decided that 12, 18-foot test sections separated by 3.7-foot transition zones would provide the necessary length without causing boundary conditions. This division permits testing of three base types at four thickness levels in any one-ring experiment. The inclusion of several thicknesses of each base type was considered necessary for proper evaluation of the performance of several base types. The degree of thickness was chosen to provide estimated pavement lives from several hundred up to 2 million wheel load applications of 10,000 pounds. The actual load per set of duals, however, is 10,600 pounds.

The subgrade, surfacing, and other variables were kept constant, while base types and thickness were varied. A subbase was not used so as to keep the pavement layers at a minimum and to simplify the analysis of the theoretical system.

Although a random distribution of base types of varying thicknesses might have been preferable (1),* sections of the same base type were grouped to facilitate construction with standard construction equipment.

The location and dimensions of the pavement sections of Ring #2 are shown in Fig. 1. Table I lists the base types and thicknesses. The thicknesses of the sections and transition zones are shown schematically in Fig. 2. The subgrade soil, type A-6(10), was common to all sections.

Materials

Subgrade

The subgrade soil, a clay-silt A-6(10) known locally as Palouse silt, was the same type as used in Ring #1 and is described in detail in the first part

*Figures in parentheses refer to specific reports in the References.

PLAN VIEW

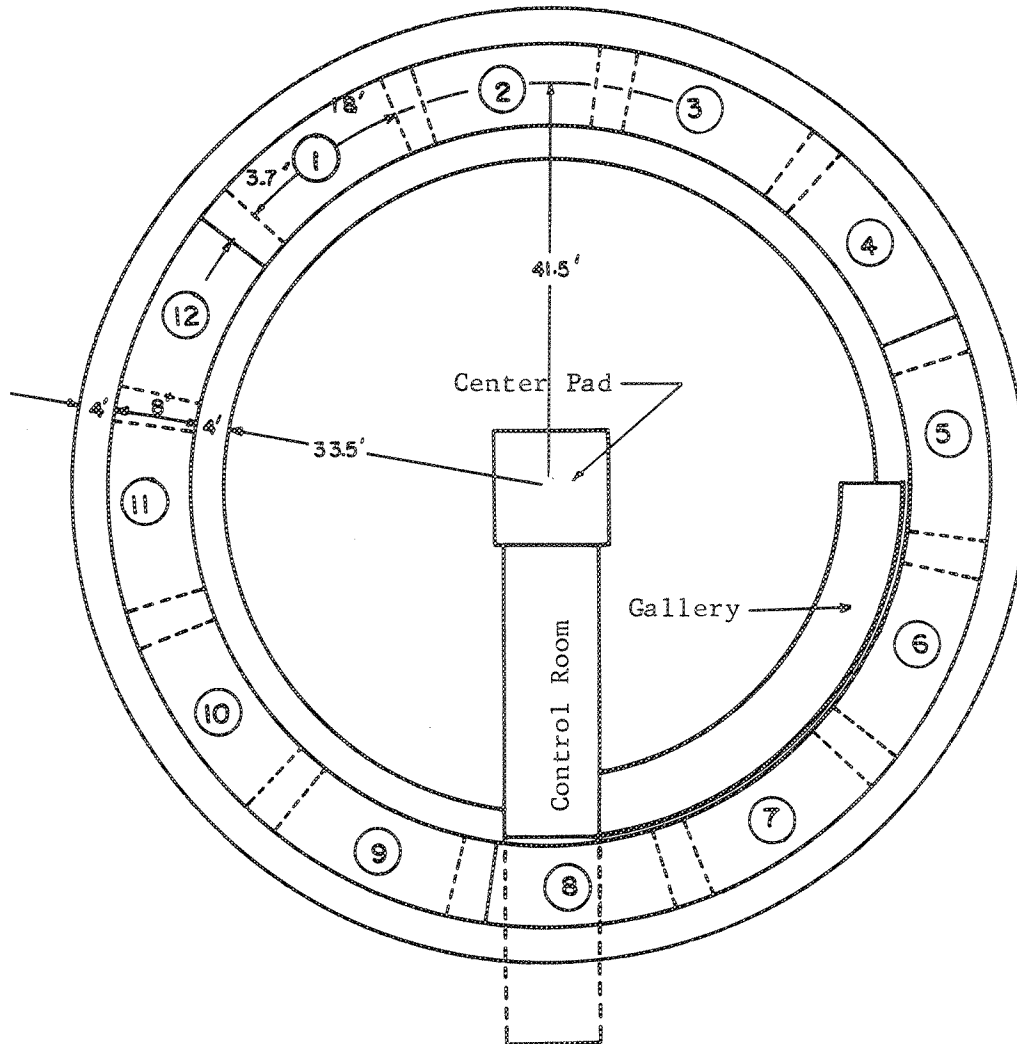


FIGURE 1.--PERMANENT STRUCTURES AND PAVEMENT SECTIONS
TEST RING NO. 2

TABLE I: TYPES, SECTIONS AND THICKNESSES OF RING #2

Type of Base	Sections	Thickness Levels--Inches			
		A	B	C	D
Crushed Surfacing Top Course	1 - 4	4.5	7.0	9.5	12.0
Emulsion-Treated Top Course	5 - 8	3.0	5.0	7.0	9.0
Special Aggregate Asphalt-Treated	9 - 12	2.0	3.5	5.0	6.5
Wearing Course-- Class "B" Asphalt	All Sections	3.0			

Scale: 1" = 20'

Highway Research Section
Washington State University
June 2, 1966

FIGURE 2. --- SCHEMATIC PROFILE FOR RING NO. TWO

SECTION 1-4 UNTREATED CRUSHED SURFACING TOPCOURSE

SECTION 5-8 EMULSION TREATED CRUSHED SURFACING TOPCOURSE

SECTION 9-12 SPECIAL ASPHALT TREATED BASE -- NON-FRACTURED SCREENED AGGREGATE

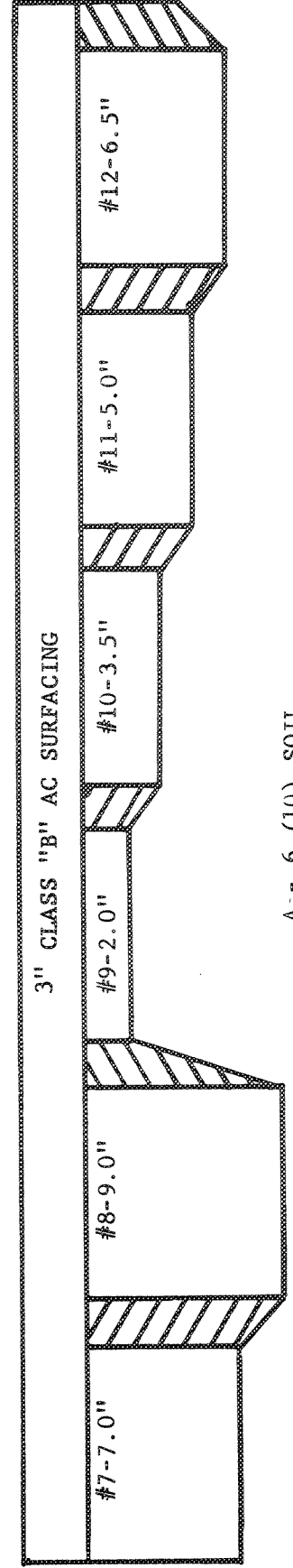
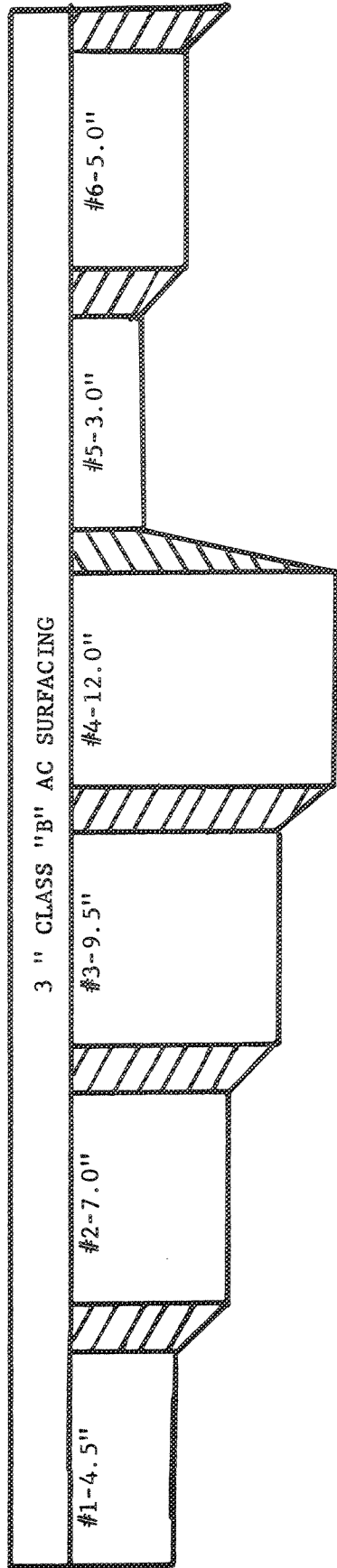


FIGURE 3.--DENSITY - MOISTURE CURVES
(Subgrade Soil Characteristics)

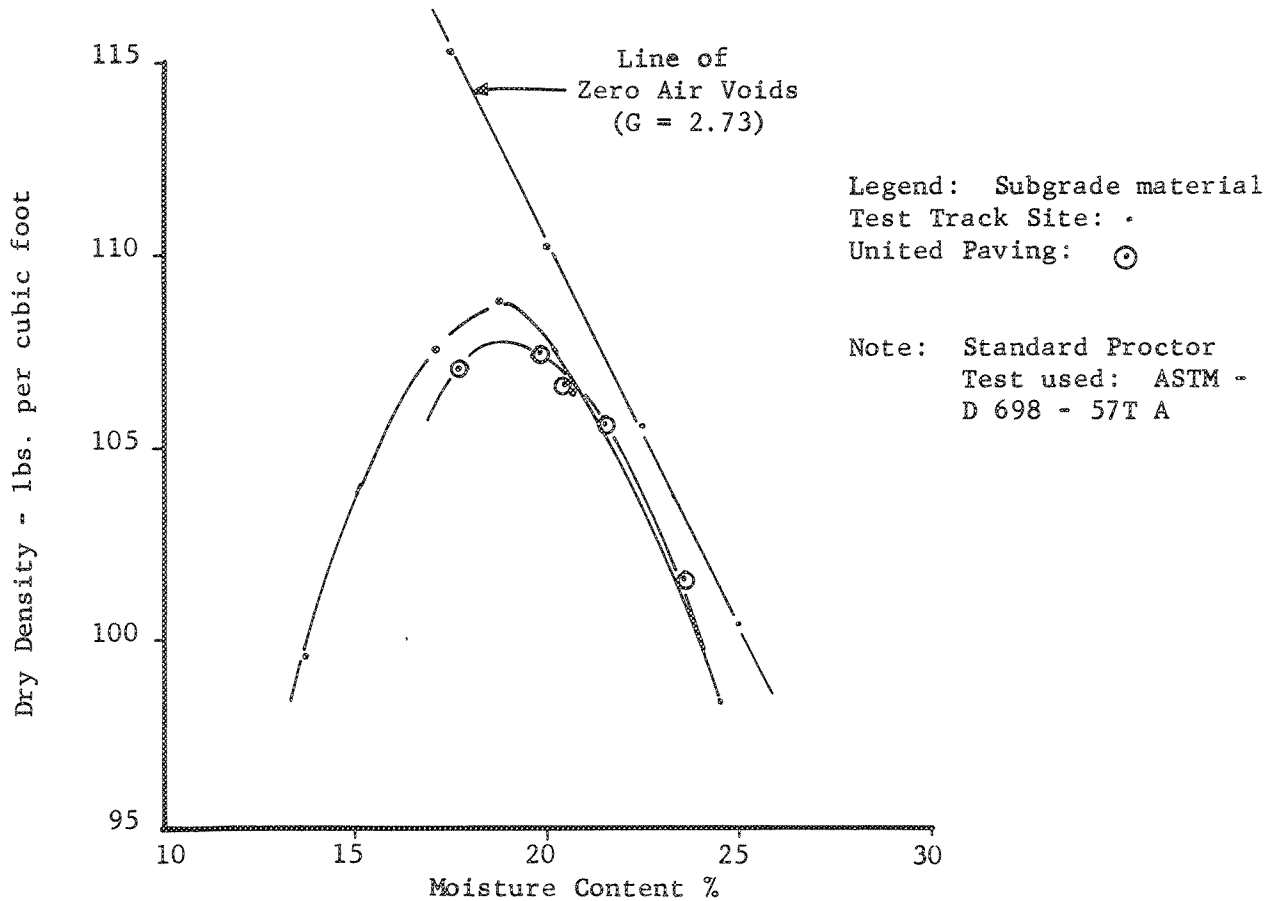


TABLE II: OPTIMUM DENSITY AND MOISTURE
FOR SUBGRADE MATERIAL

Source	Max. Optimum Dry Density	Optimum Moisture
Test Track	108.8	18.8
United Paving	107.8	18.8

TABLE III: SOIL CHARACTERISTICS AND CLASSIFICATION

Soil	Specific Gravity S.G.	Liquid Limit L.L.	Plastic Limit P.L.	Plasticity Index P.I.	Highway Res., Board Class.	Airfield Classifi- cation
Clay-silt	2.73	34.9	20.2	14.7	A - 6 (10)	CL

Stabilometer "R" Value = 16
pH Factor = 6.1

of this report. Soil moisture-density curves are shown in Fig. 3 and Table II. Characteristics and classifications are shown in Table III. Some of the soil came from the contractor's local pit and the curve for this soil is also shown in Fig. 3. The slight difference in density may be attributed to a difference in the clay contents of the two silts or to testing variance.

Crushed Surfacing Top Course

The basaltic aggregate, hauled from United Paving's Geiger Pit in Spokane and stockpiled at the test track, met Washington State Highway specifications (2) for crushed surfacing top course. This rock was used for the untreated bases in sections 1 to 4 as standard control and for the emulsion-treated base aggregate in sections 5 through 8. Figure 4 shows the gradation curve for this aggregate. Figure 5 represents the maximum density curve which can be obtained with this aggregate.

Special Screened Non-Fractured Aggregate

This aggregate was specially blended at the Fort Wright site of Central Pre-Mix of Spokane under the supervision of Washington State Highway personnel. The coarse aggregate came from the Fort Wright gravel pit and the fine aggregate from their Mead sand pit. This blended aggregate was trucked to Pullman and stockpiled at the test track site for use with asphalt cement for the special asphalt-treated bases in sections 9 through 12 (3).

It is a river-run gravel and contains less than 5% freshly fractured surfaces. Figure 6 shows the gradation curve for this aggregate. Fig. 11 (photo) shows its appearance and size. Although this type of aggregate is uncommon in Eastern Washington, it is prevalent on the west side of the state. Since good aggregate is becoming scarce in the populated western areas of the state, the highway department wants to make use of more readily available glacial gravels-- and therefore has included them for study as base aggregates.

FIGURE 4.--GRADATION CURVE FOR CRUSHED SURFACING TOP COURSE--UNTREATED BASE SECTIONS 1 - 4 AND EMULSION TREATED SECTIONS 5 - 8

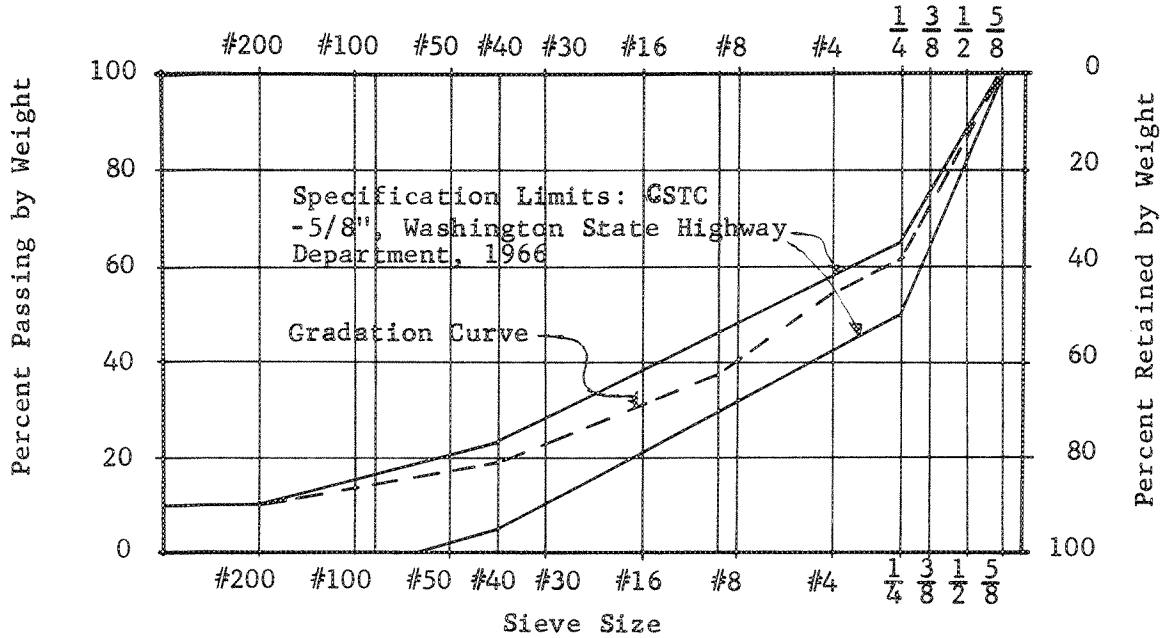


FIGURE 5.--MAXIMUM DENSITY CURVE FOR CRUSHED SURFACING TOP COURSE

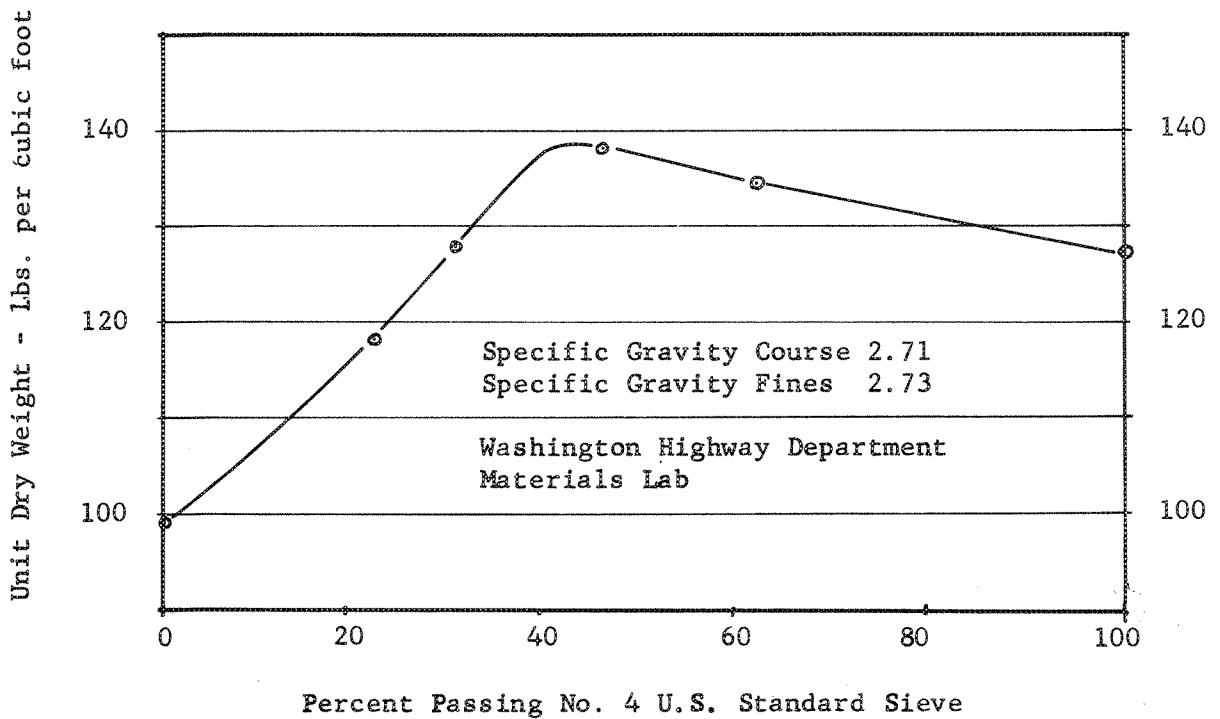


FIGURE 6.--GRADATION CURVE FOR SPECIAL NON-FRACTURED SCREENED AGGREGATE - SPECIAL A.T.B. SECTIONS 9 - 12

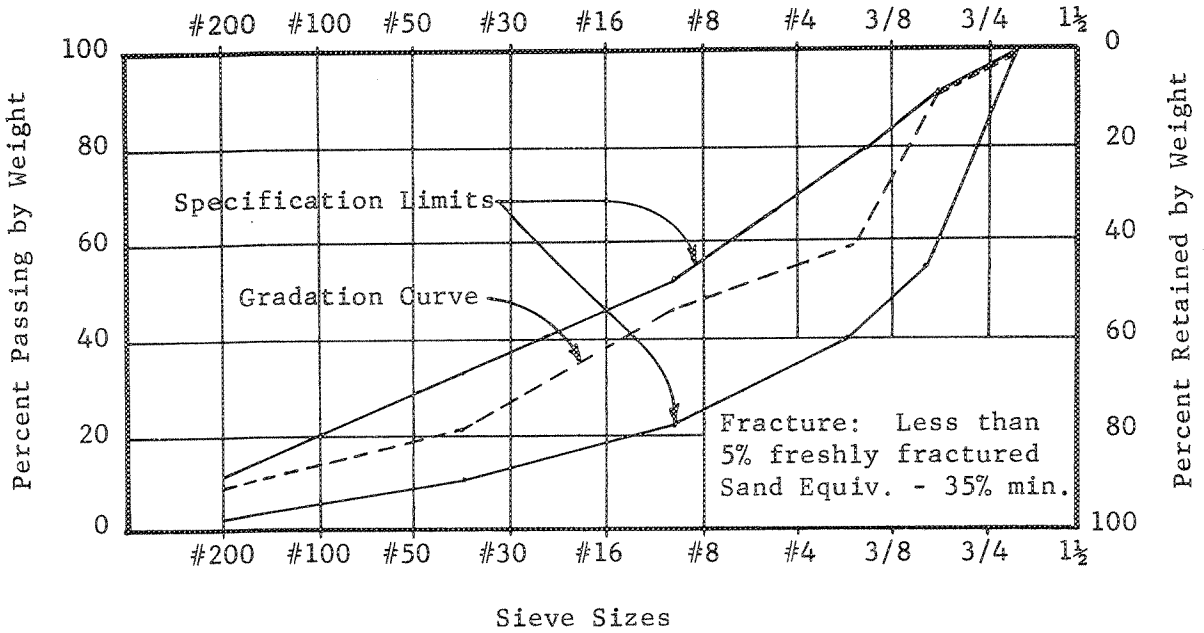
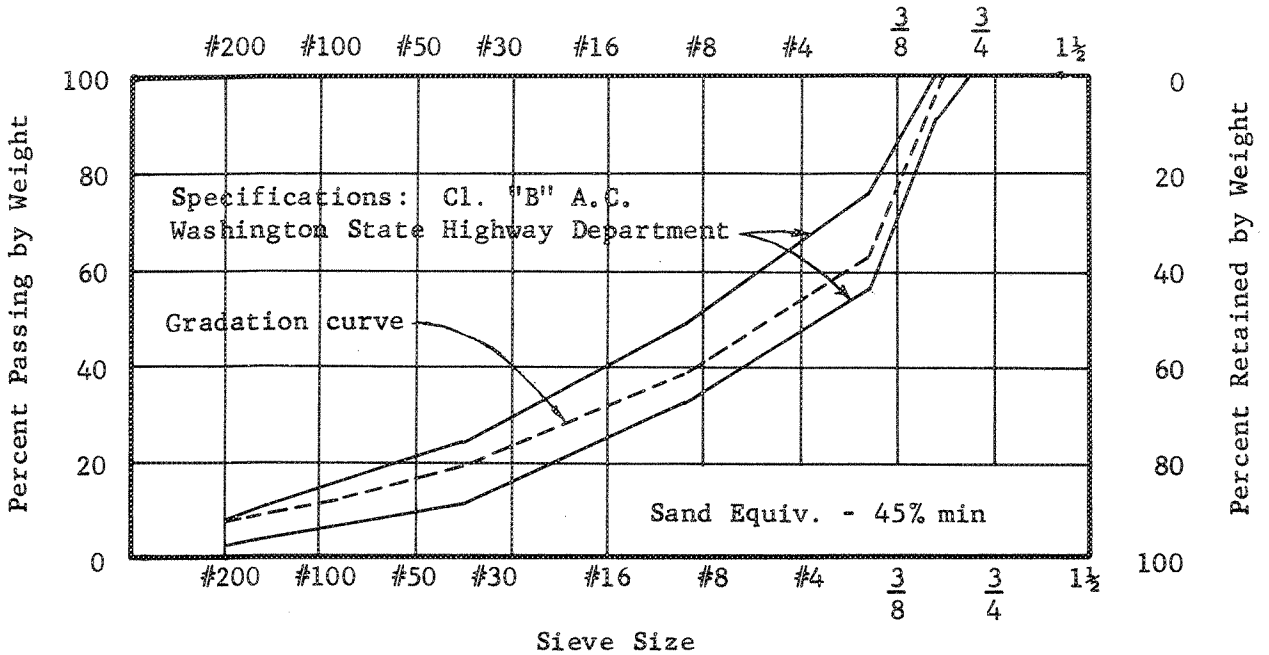


FIGURE 7.--COMBINED GRADATION CURVE FOR ASPHALT CONCRETE CLASS "B" AGGREGATE - ALL SECTIONS



Asphalt Concrete Class B Aggregate

This aggregate came from United Paving's Geiger Pit in Spokane and was blended to meet Washington State Highway specifications (2). It is a basalt rock similar to the crushed surfacing top course. The combined gradation curve is shown in Fig. 7 and in Table VI.

Construction

Pre-Conditioning

United Paving, Inc. of Pullman, Washington, the only bidder on the project, began construction on August 9, 1966. The existing pavements, treated bases, and crushed rock were removed in one and one-half days. The top 12 inches of the subgrade was reconditioned and recompacted with a 5-ton Huber steel roller. A weak area, found in Section 5, was dug out to a depth of 3 feet, filled with dry silt, then recompacted in layers with a 10-ton, 9-tired pneumatic Galion roller. Densities and moisture contents were taken in each section by a Nuclear-Chicago density and moisture gage and checked with sand-cone tests.

Subgrade

The subgrade was brought up in 4-inch lifts loose depth, watered, and compacted with a steel roller. Each lift was checked for density and moisture. The subgrade was brought up to rough final grade, blue tops placed, then each section cut and filled to final grade (as shown in Fig. 8). This was a departure from specifications which required bringing the subgrade to a common elevation and then cutting it down to the desired elevation. The reason for this was that the contractor found it was easier to fill than to cut a good grade in the Palouse silt, which has a tendency to break up and cut into chunks and lumps. The moisture contents were kept low as possible since

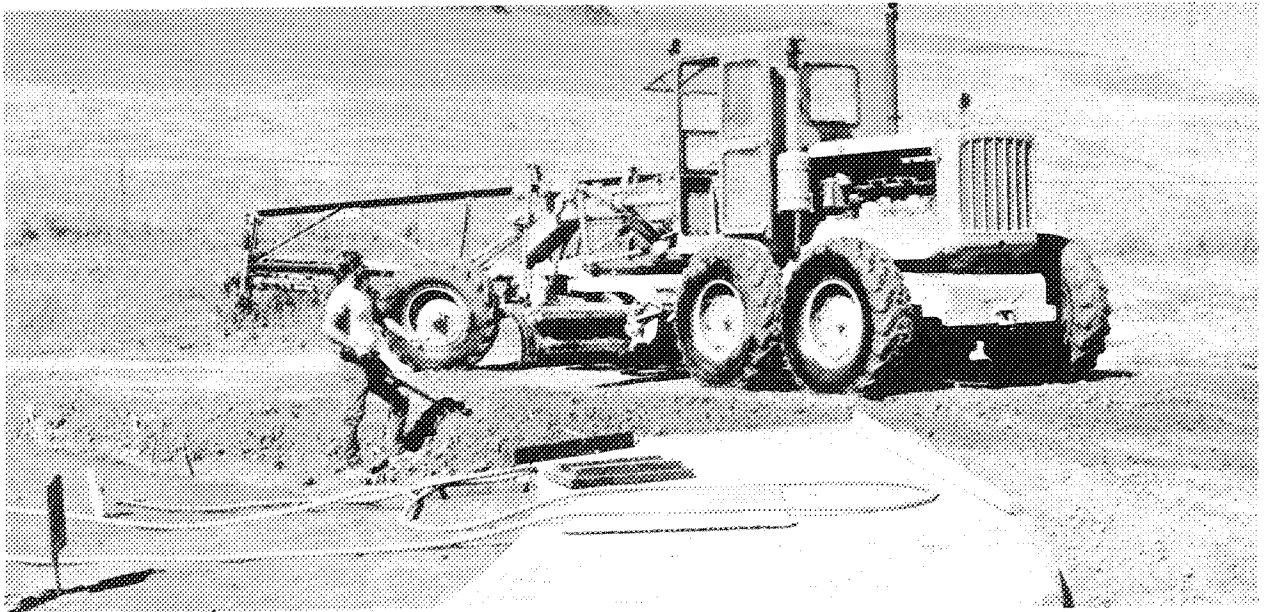


FIGURE 8.--LEVELING OF THE SUBGRADE BY MAINTAINER.

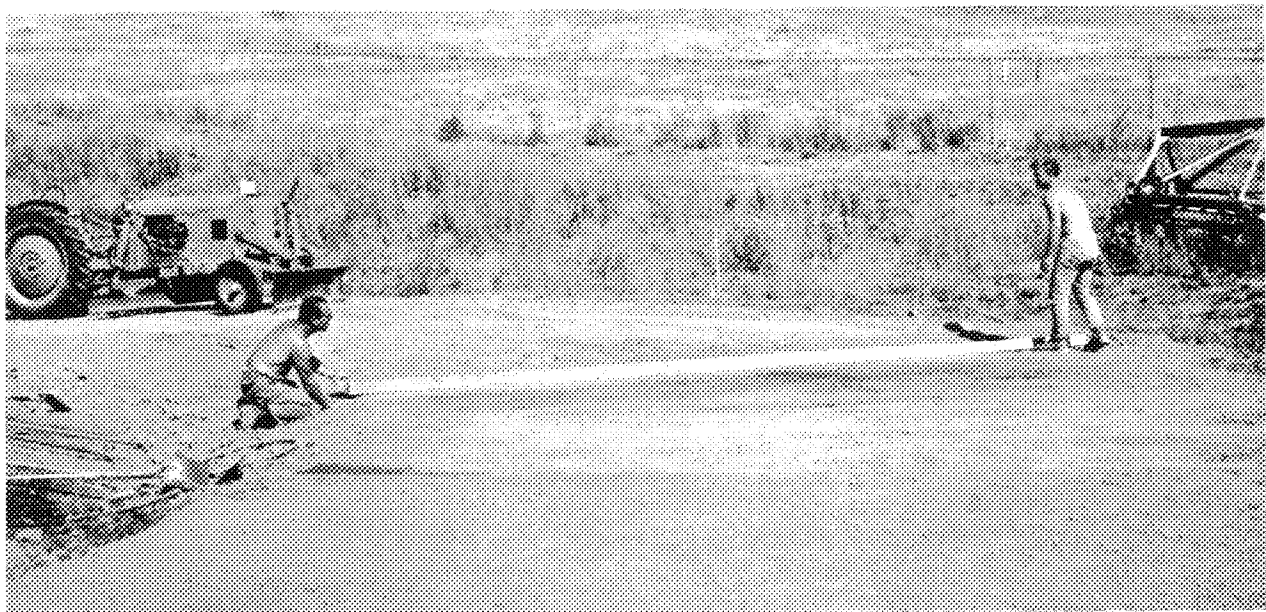


FIGURE 9.--HANDSCREEDING THE SUBGRADE TO FINAL GRADE.

TABLE IV
DENSITIES OF SILT SUBGRADE AT FINAL GRADE

Section	Dry Density lbs/cu. ft.	Moisture Content %	Per Cent of Maximum Density *	Per Cent of Optimum Moisture Content *
1	109.2	11.6	102.0	61.0
2	105.5	17.1	98.6	90.0
3	104.5	12.4	97.7	65.3
4	104.0	13.5	97.2	71.0
5	106.5	11.9	99.5	62.6
6	110.5	12.7	103.3	66.8
7	107.0	12.9	100.0	67.9
8	111.5	13.7	104.2	72.1
9	108.5	12.0	101.4	63.2
10	106.5	12.2	99.5	64.2
11	107.0	12.6	100.0	66.3
12	102.7	14.4	96.0	75.8
Average	107.0	13.1	100.0	69.0

Maximum Density = 107 lbs/cu. ft. Optimum Moisture Content = 19%

* Standard Proctor Test used: ASTM - D698-57TA

a slight increase in moisture made the Palouse silt unworkable. Table IV shows the dry densities and moisture contents obtained in each section.

Fine-grading began August 18 and was completed by noon, August 24. Although a Huber blade was used for cutting and spreading silt, much hand work had to be done. The Palouse silt, which tends to agglomerate, had to be broken up extensively and spread to bring the subgrade to final elevation. Each section was checked repeatedly for grade and elevation by straight-edge to a rigid $\pm\frac{1}{4}$ " tolerance (as shown in Fig. 9), and by rod and level to insure proper base thickness. Densities and moisture contents were checked periodically for proper compaction levels (see Table IV). A weak area was located in section 4 similar to that in section 5. Since it occurred mainly outside the pavement centerline and outside the wheel paths, nothing except more rolling was done to correct it, but the location was noted for future reference. Instrumentation of the subgrade began August 25.

Crushed Surfacing Top Course Base--Untreated (Sections 1-4)

Laying of the crushed top course in sections 1 to 4 began September 1. The aggregate was processed and laid in three lifts with a Blaw-Knox paver (as shown in Fig. 10). Each lift was compacted with a 5-ton Huber steel roller--with compaction being controlled by nuclear density methods. On the last lift, both a steel and pneumatic tired roller were used for compaction. The base was found to contain 9.4% moisture, making it too wet to work, so it was allowed to cure. The final density obtained is shown in Table V. It was later checked for grade and elevation and cut and filled where necessary.

Special Asphalt-Treated Base (Sections 9-12)

These sections were laid the afternoon of September 1 and the morning of September 2. Figure 6 shows the gradation for this special non-fractured aggregate; Fig. 11 (photo) shows its appearance; and Table VI shows the mix design

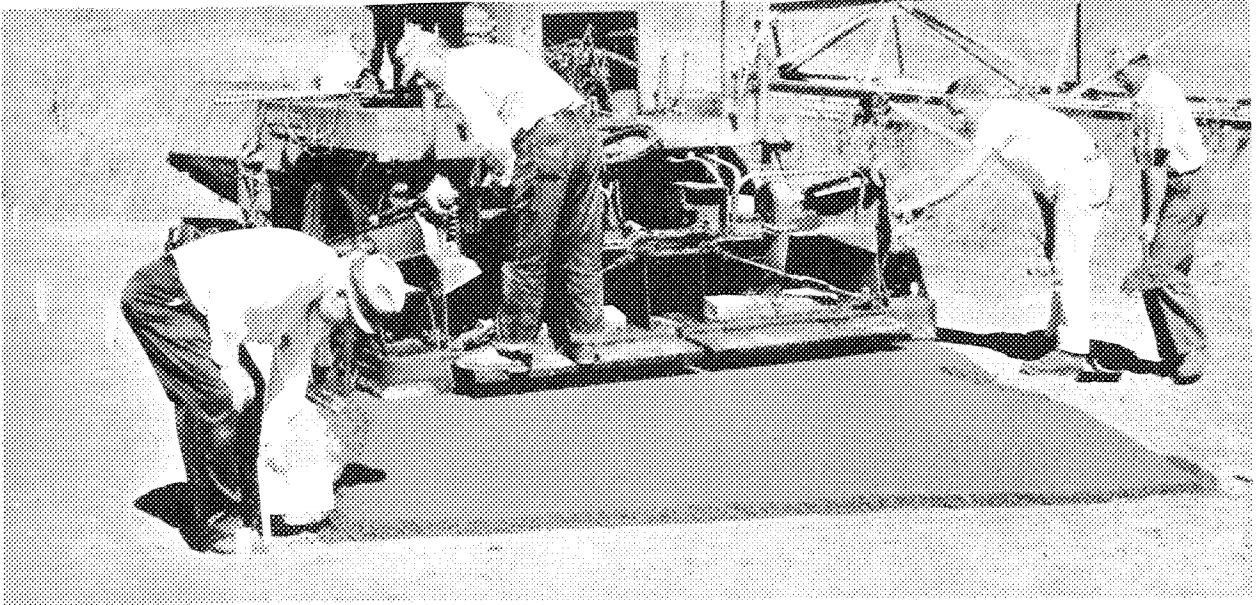


FIGURE 10.--THE PLACING OF THE CRUSHED SURFACE TOP COURSE IN SECTION 4 WITH A BLAW KNOX PAVER.

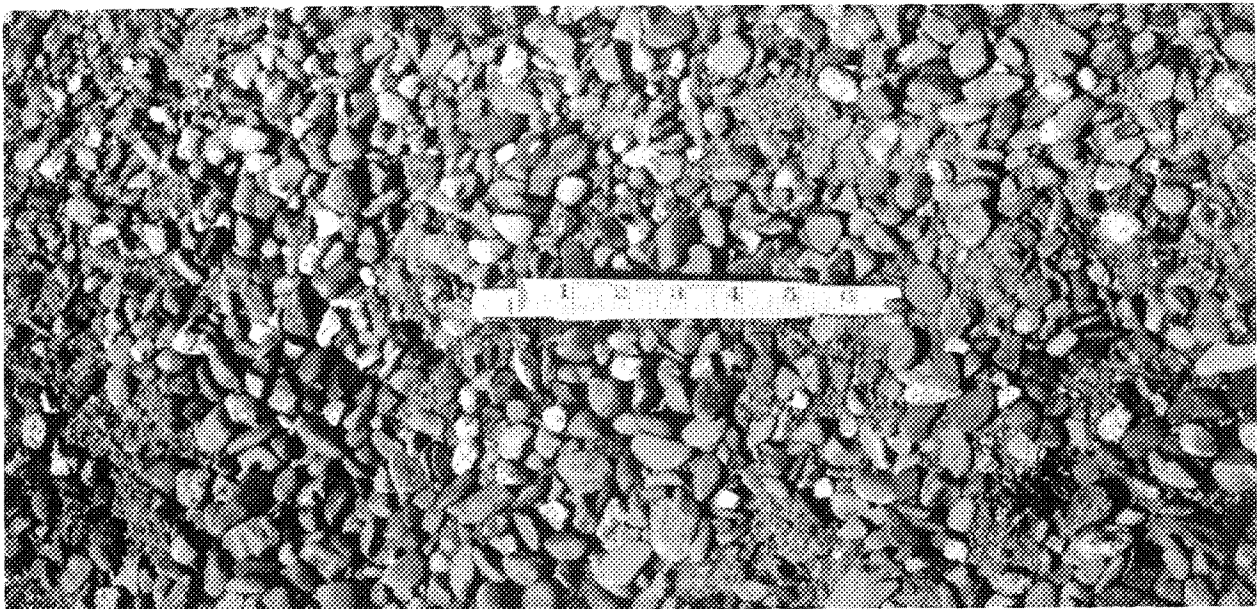


FIGURE 11.--THE APPEARANCE OF THE SPECIAL SCREENED NON-FRACTURED AGGREGATE AT THE TEST TRACK STOCKPILE.

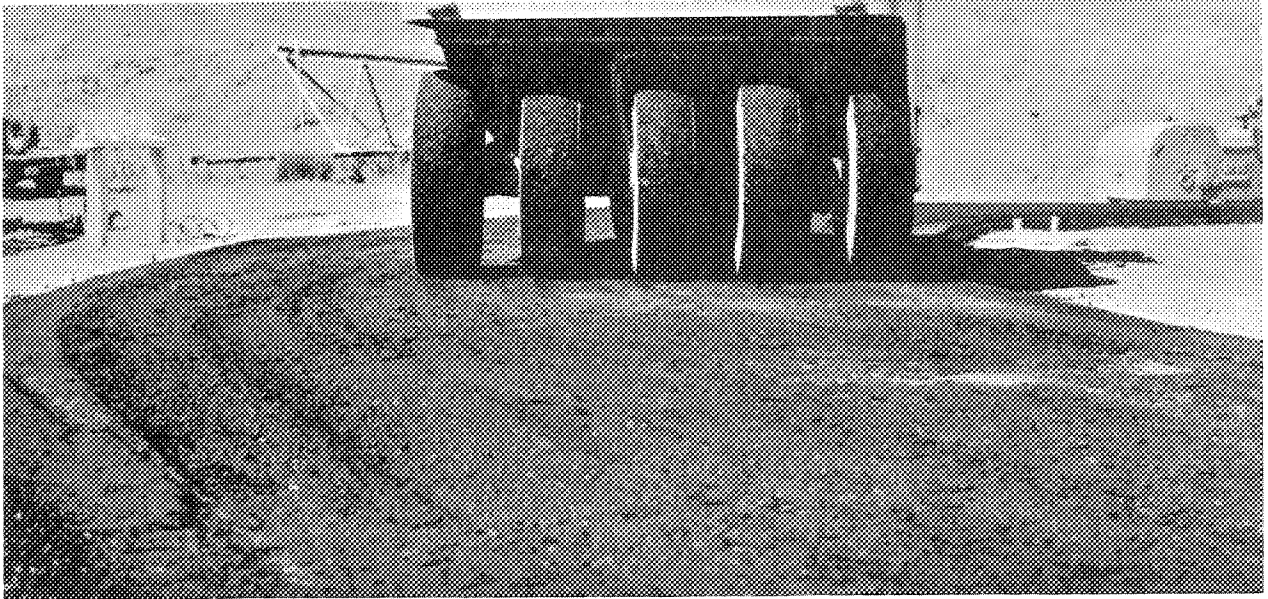


FIGURE 12.--COMPACTING THE SPECIAL ASPHALT-TREATED
BASE SECTIONS 10-11. NOTE THE FLATTENED EDGES.



FIGURE 13.--APPEARANCE OF THE SPECIAL ASPHALT-TREATED
BASE AFTER ROLLING WITH STEEL ROLLER.

TABLE V
AVERAGE FIELD DENSITIES OF BASES AT FINAL GRADE

Type of Base	Sections	Average Dry Density (a) lbs/cu. ft.	Standard Laboratory Density lbs/cu. ft.	Per Cent of Standard
C.S.T.C. ^b	1 - 4	137.7	137.0	100.5 ^f
E.T.B. ^c	5 - 8	139.0	140.4	99.0 ^f
Spec. A.T.B. ^d	9 - 12	141.8	148.5	95.5 ^h
Cl. "B" A.C. ^e	1 - 12	148.4	152.0	97.6 ^h

^aBy nuclear density methods

^bCrushed surface top course--untreated.

^cEmulsion-treated base (C.S.T.C.)

^dSpecial asphalt-treated base.

^eClass "B" asphalt concrete wearing course.

^fSpecifications call for 95% of standard density.

^hSpecifications call for 93% of standard density.

TABLE VI: MIX DESIGN REQUIREMENTS

Sieves-% Passing	Emulsion-Treated Base (C.S.T.C.)		Special Asphalt-Treated Base (Non-Fractured)		Cl. "B" A.C. Wearing Course	
	Specified	From * Extraction	Specified	From * Extraction	Specified	From * Extraction
2" Square			100	100		
1" Square						
5/8" Square	100	100	56-90	100	100	100
1/2" Square		99	40-78	90	90-100	97
1/4" Square	50-65	64	22-52	59	55-75	65
U.S. No. 10		30	8-32	44	32-48	39
U.S. No. 40	8-23	19		21	11-24	20
U.S. No. 80		15		10	6-15	13
U.S. No. 200	10 max.	10	2-9	6	3-7	8
Sand Equivalent % Min.	40		35			
% Fractures			5% max.	3% max.	75% min.	
Penetration Grade A.C.	SS-Kh		60-70	60-70	85-100	85-100
Amount of A.C. %	5.0	3.5	2.8	3.0	5.3	5.2
Stabilometer "S" Valves	Emulsion	Residue				
Cohesimeter "C" Valve	30	32	20	28	30	29
Modified Immersion Com- pression (MIC) Test-% Ret.	100	200	50	158	100	260
Wt. Per Cu. ft. of Mix	70		70		70	
Voids-Volume in Mix	140.4	148.3**	148.5	145.8	152.0	158.8
Rice Density						3.6
						162.3

* Extracted and tested by the Washington Highway Department, Materials Laboratory at Olympia, Washington

** Compacted at room temperature, tested at 140°F.

required and obtained. This aggregate was hot mixed with 3%, 60/70 penetration asphalt at the United Paving plant in 3,000-pound batches and laid in four lifts with a Blaw-Knox paver. Each lift was rolled with a steel and pneumatic-tired roller (as shown in Fig. 12) and the densities measured by nuclear density methods.

Some difficulty was experienced in obtaining the correct grade with the paver and a fifth lift was necessary to correct grade deficiencies. Since no berms were used to hold the sides, the edges moved transversely when the base was rolled, causing an overrun. Small surface transverse cracks appeared as the base was rolled with the steel roller. These cracks were caused by the continuous turning of the roller, which induced tension and separation of the surface of the asphalt base (Fig. 13). Table V shows the final average density measured and is compared with the required or laboratory density.

Emulsion-Treated Base (Sections 5-8)

The first lift was laid with a Blaw-Knox paver on the Morning of September 2. The aggregate was the same as that used for the untreated bases. The gradation and density curves are shown in Figs. 4 and 5, and the design mix requirements are tabulated in Table VI. The asphalt emulsion SS-Kh was diluted with water on a 50-50 basis, instead of adding water to the mix. The aggregate, which was not predried, and 5% of the diluted emulsion were cold-mixed in 3,000-pound batches. The loose thickness of this first lift was $4\frac{1}{2}$ inches in section 8 (9.0 inches of ETB) and $2\frac{3}{4}$ inches in section 7 (7.0 inches of ETB). After a three-hour curing period, the sections were rolled with a 5-ton Huber steel roller. As water was still pumping out of section 8, compacting operations were halted and the emulsion base was allowed to cure overnight. This condition is shown in Fig. 14.

The next morning inspection and more rolling revealed that section 8 was still wet and spongy while section 7 had cured fairly well. A second lift was

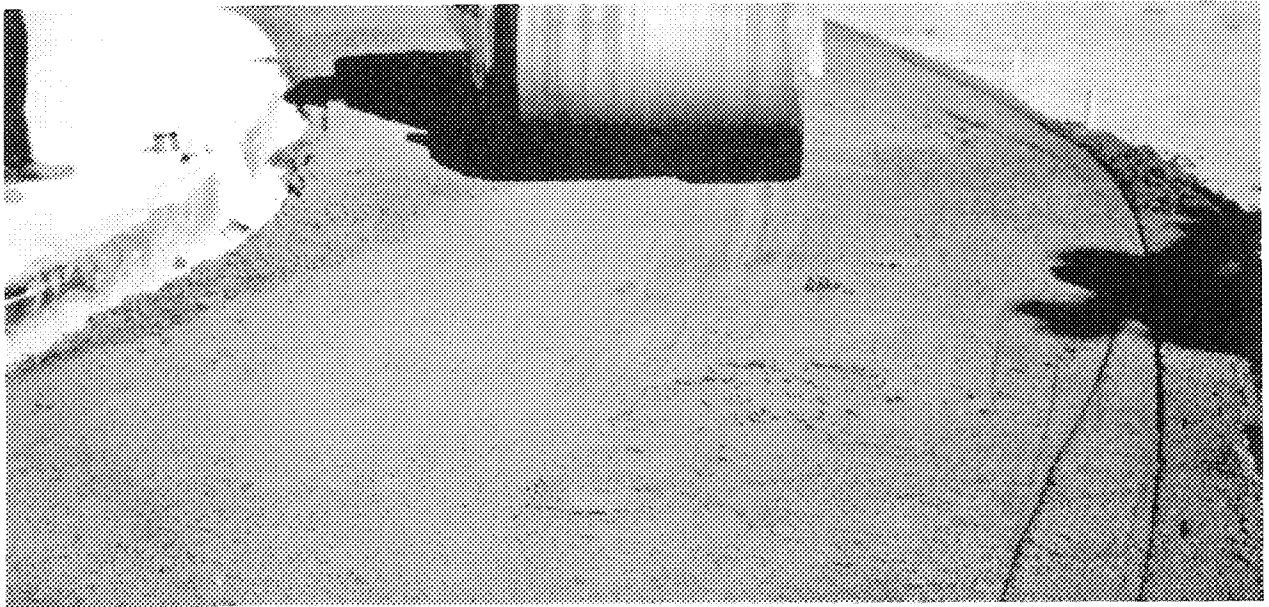


FIGURE 14.--ATTEMPTING TO ROLL THE EMULSION-TREATED BASE AFTER A 3-HOUR CURING PERIOD. NOTE THE PICK-UP OF THE MATERIAL AND THE WET AREAS.

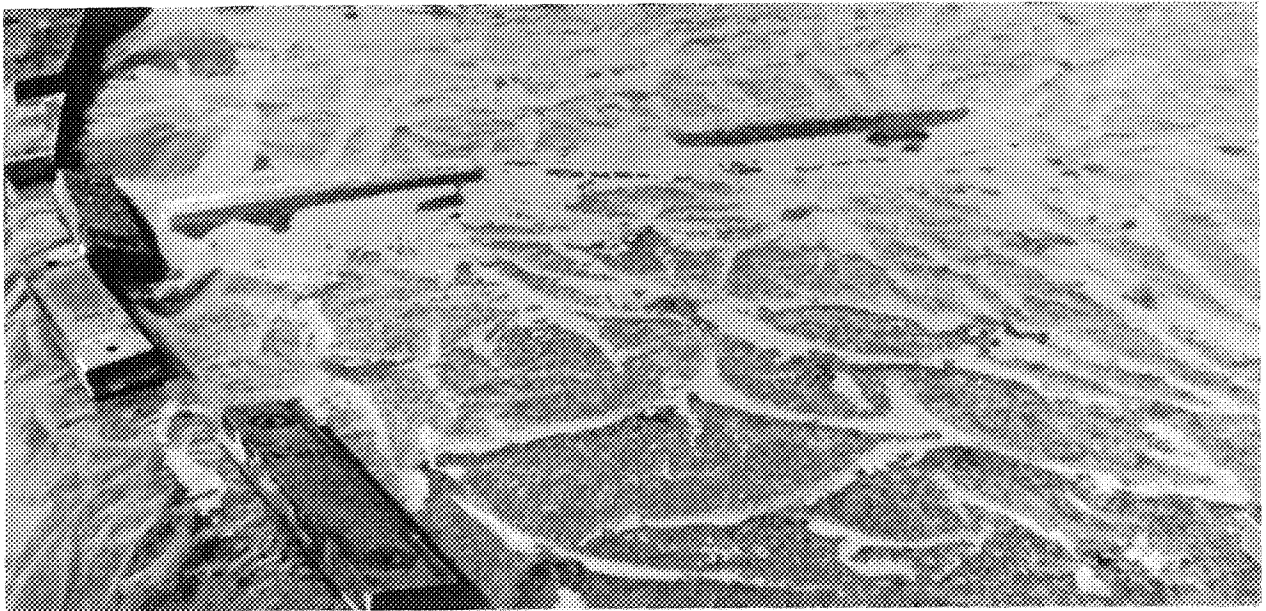


FIGURE 15.--THE FIRST TWO LIFTS OF EMULSION-TREATED BASE IN SECTION 8 BEING CURED BY VISQUEEN PLASTIC COVERING. NOTE THE CONDENSED MOISTURE ON THE BOTTOM OF THE PLASTIC.

TABLE VII
EMULSION-TREATED BASE--MOISTURE CONTENTS

Lift	Loose Thickness Inches	Section	% Moisture from Time 1st Lift Was Laid Time in Days				
			1st	2nd	5th	12th	15th
1	4-1/2	8	13.7	--	6.8	4.7	--
	2-3/4	7	--				
2	2-3/4	8-6	--	11.4	4.9 ^a	--	--
3	3	8-5	--	--	--	10.9 ^b	--
4	3/4	8-5	--	--	--	--	6.4

^aThis was the 4th day after being laid down.

^bExample: This was the moisture content of 3rd lift at laying, 12 days after the 1st lift was put on, that is, on September 2.

placed on sections 6, 7 and 8 using a batch of emulsion base material mixed the day before and which had been stored overnight in a truck protected with a canvas. Laboratory analysis showed that the moisture content had dropped from 13.7 to 11.4% overnight (Table VII). The second lift was steel rolled after an hour of curing, then rolled later in the afternoon. On Sunday evening, another attempt was made to compact the sections with little noticeable success. Another attempt was made to compact sections 7 and 8 the following Tuesday, September 6, but the sections were still too soft. Nuclear density readings indicated that the top two inches of the emulsion base had crusted over while the bottom four inches were still wet and soft; this was especially noticeable in section 8.

To facilitate the curing process a series of $\frac{1}{2}$ -inch diameter holes were punched in the emulsion base in section 8 on Wednesday. This operation confirmed the fact that the top lift had crusted over, leaving the bottom lift soft and moist. The section was covered with a sheet of visqueen plastic to draw out the moisture (Figure 15). After four days enough moisture had been drawn out for the bottom lift to be considered cured.

On Monday, September 12, after the application of a slight tack coat of emulsion SS-1 on the emulsion base surface, the third lift was placed on sections 5, 6, 7 and 8. This mix differed in that the aggregate was partially dried then mixed with the diluted SS-Kh emulsion asphalt. The temperature of this mix was 100°F at placing and contained 10.9% water, a 3% reduction in water content. Rolling began after an hour of curing and immediately some pumping and shoving occurred in sections 7 and 8. (See Fig. 16) On section 5 where the lift was laid on the dry subgrade, curing was very rapid and there was no problem with compaction.

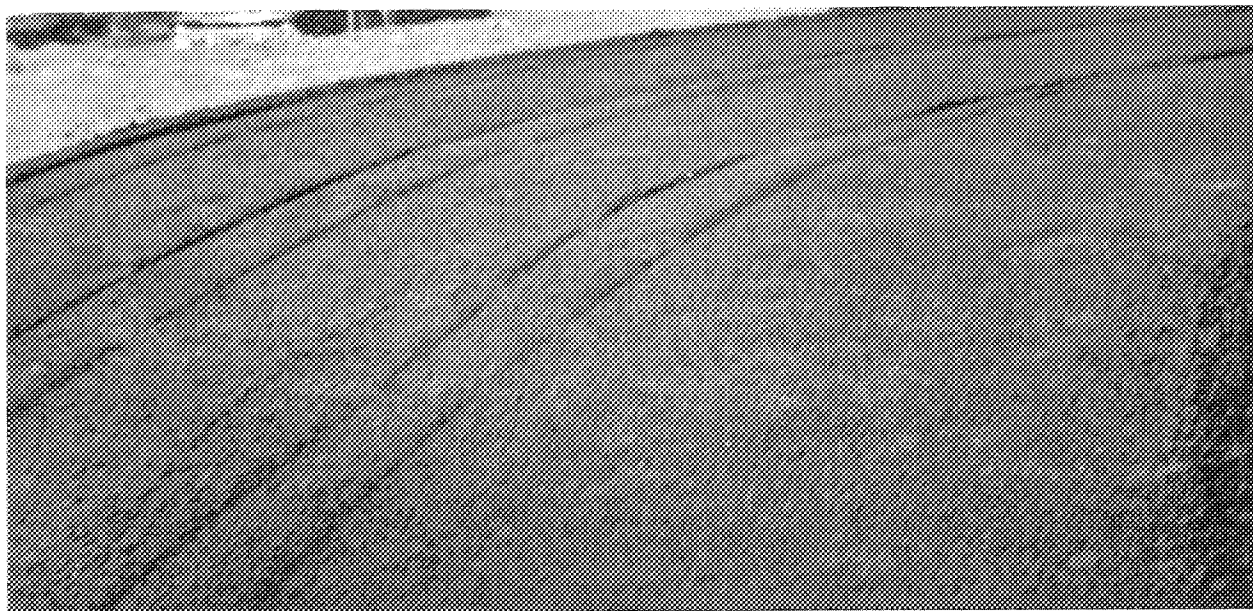


FIGURE 16.--THE APPEARANCE OF THE 3RD LIFT OF EMULSION-TREATED BASE IN SECTIONS 7 AND 8 AFTER ROLLING. PICTURE WAS TAKEN 2 HOURS AFTER LAYING.

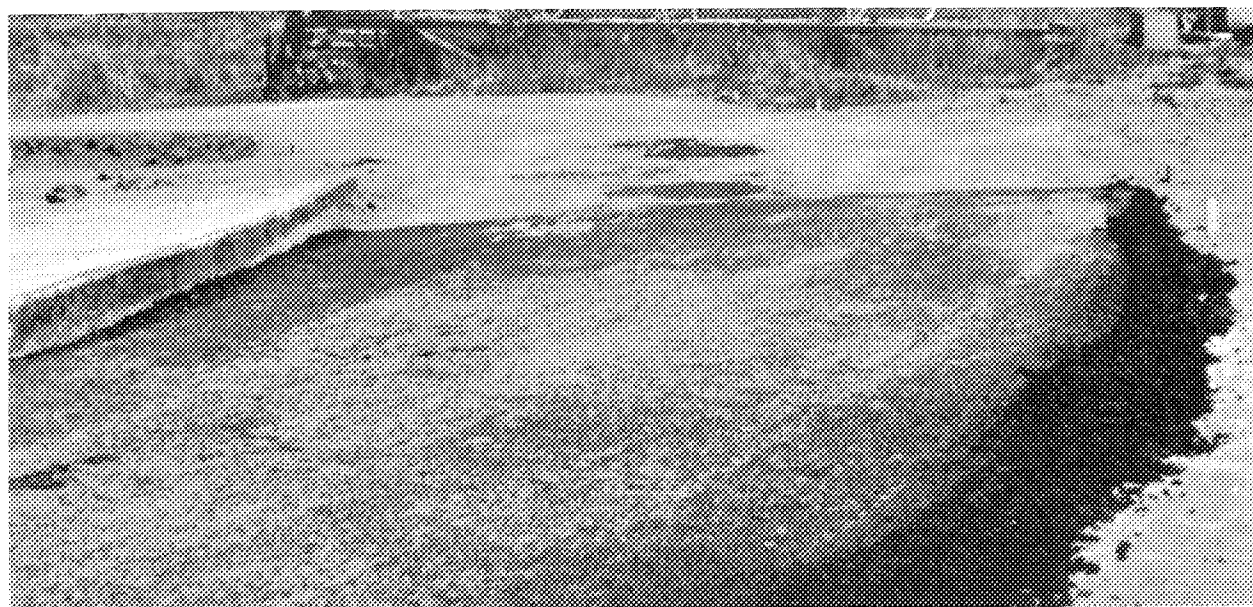


FIGURE 17.--APPEARANCE OF THE EMULSION-TREATED BASE IN SECTION 6 AFTER BEING CURED AND ROLLED. NOTE THE GRANULAR APPEARANCE OF EMULSION.

On September 14, the pneumatic-tired roller was used to break up the crust and to help aerate the emulsion base. Soft spots were evident in sections 7 and 8 which had the thickest emulsion layers. The next day, the emulsion base was rolled with a steel roller leaving very few soft spots. A light tack coat of SS-1 was applied and a final correction layer was put on. This last lift was different in that the aggregate and the undiluted SS-Kh emulsion were mixed without pre-drying or pre-wetting except in the pug. The moisture content of this mix was 6.4%. Setting of this final lift occurred very rapidly and compaction was achieved with very little rolling effort. Table VII indicates moisture contents and the curing time as compared with the first lift. It shows that moisture content and thickness of lift are important in the curing of the emulsion-treated base. Final grade was checked by straight-edge and rod and level. Final densities were obtained by nuclear density methods.

Some questions need to be answered about the emulsion-treated bases. The principle one is why did it take so long to set up. Table VII shows that the moisture content and thickness of the lift are part of the answer. The thinner and drier lifts cured more rapidly than the thicker ones. There also was 4.8% moisture in the crushed surfacing top course stockpile. This moisture plus the water added to the SS-Kh made the emulsion-treated mix too wet. This combination of thick lifts and excess water created the curing problem, the crusting of the surface retained this excess moisture. This situation was solved partially by punching holes through the crust and drawing out the moisture with the plastic sheet. The problem was avoided in Ring 3 by using 2-3/4 inch lifts and an emulsion mix of 9.0% total fluids containing 6.64% water (4). Also, the cool nights during September did not facilitate the curing process. These difficulties resulted in a three-week delay.

Class "B" Asphalt Concrete Wearing Course

The wearing course was placed in two lifts the afternoon of September 20 and the asphalt-treated bases were tacked with SS-1 emulsion. The course and fine aggregates were mixed with blending sand then hot-mixed with 5.3%, 85/100 penetration grade asphalt. Figure 7 and Table VI give the gradation and mix designs. The lifts were then rolled with a 4-ton steel roller followed by a 7-ton pneumatic-tired roller. The top lift was finished by extra rolling with a steel roller. The grade was checked with a straight-edge and rod and level as shown in Fig. 18. Densities were measured with nuclear equipment (Fig. 19) and are tabulated in Table V.

Shoulders

Shoulders of crushed surfacing top course aggregate were put in place on September 28 and 29. A waterproofing tack coat was sprayed on the inside shoulders and ditch.

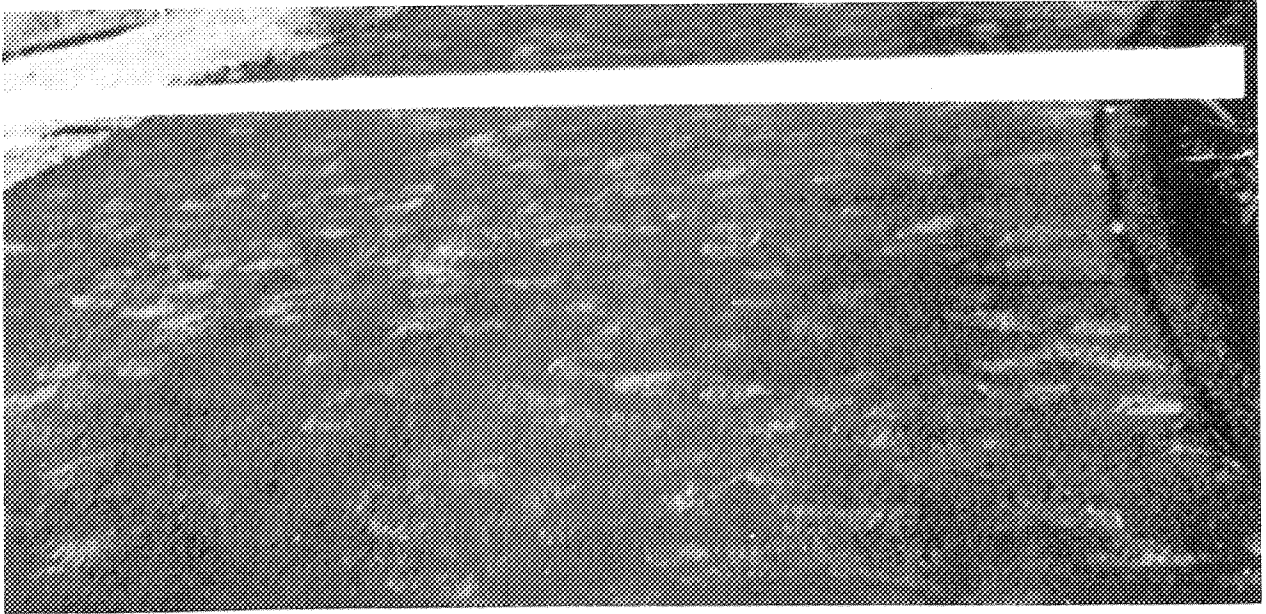


FIGURE 18.--A VIEW OF THE FINAL GRADE AFTER THE 3.0" CLASS "B" ASPHALT CONCRETE WEARING COURSE WAS LAID BEING CHECKED BY STRAIGHT-EDGE. NOTE THE GROOVES LEFT IN THE MAT FOR INSTRUMENTATION.

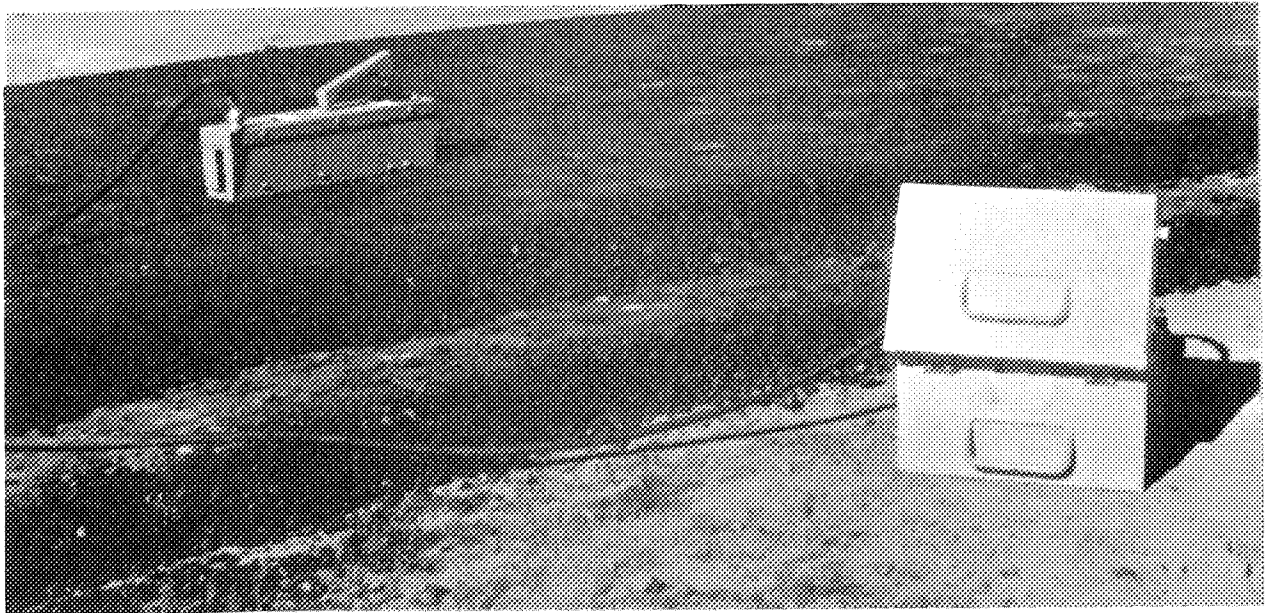


FIGURE 19.--DENSITY OF THE CLASS "B" MAT BEING MEASURED BY THE NUCLEAR ASPHALT GAGE AND SCALER.

Instrumentation

Instruments to measure stresses, strains, temperature, dynamic deflection, and moisture were installed in the different layers of the pavement structure in similar positions used in the San Diego County Experimental Base Project (5). Figure 20 shows the depth and location of some of the instruments in one section. Table VIII shows the type of instrumentation installed and their location in various sections.

TABLE VIII
LOCATION OF INSTRUMENTS ALONG CENTER LINE

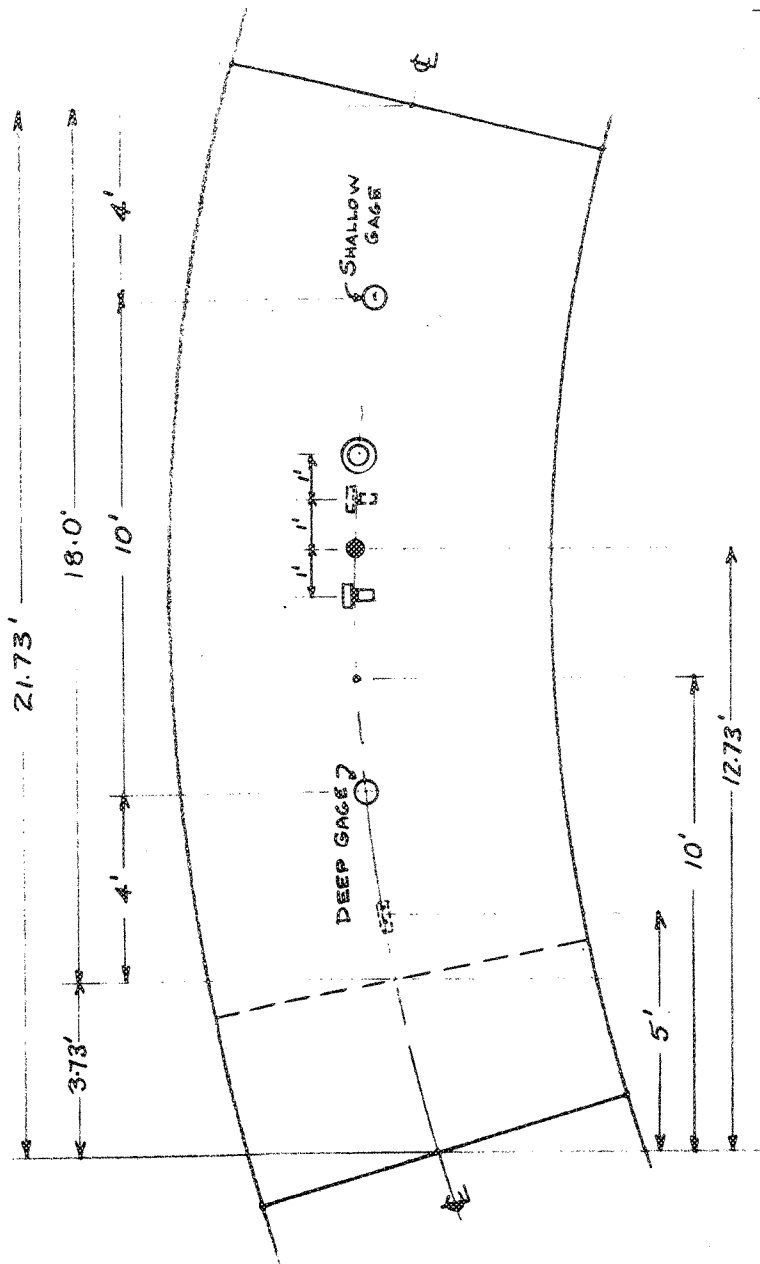
Type of Instrument	Subgrade		Base	Surface
	Below	On Top	On Top	On Top
	Sections	Sections	Sections	Sections
Moisture probes	1-3, 5, 6, 8, 9-11 ^a	--	--	--
WSU cell	--	8	6 & 8	--
Filpip cells	--	1-12	2, 4, 6, 8, 10, 12 ^c	--
Thermocouples	1-12	1-12	1-12	1-12
Strain Gages	--	1, 2, 6, 8, 10 ^b	2, 6, 8, 10, 12 ^b	1-12 ^b
LVDT	--	--	--	2, 6, 8, 10 ^d

^aIn Sections 2, 6, and 10 three moisture probes were installed.

^bThe strain gages were installed in pairs; one longitudinal to the direction of travel and the other transverse. Spares were also installed except on the surface.

^cA Filpip transducer was installed in Section 8 in the middle of the base thickness.

^dOne shallow and one deep LVDT gage was installed in these sections.



LEGEND

- LVDT
- ⊙ WSU CELL
- FILPIP CELL
- ⊥ STRAIN GAGE
- THERMOCOUPLE
- ◻ MOISTURE CELL

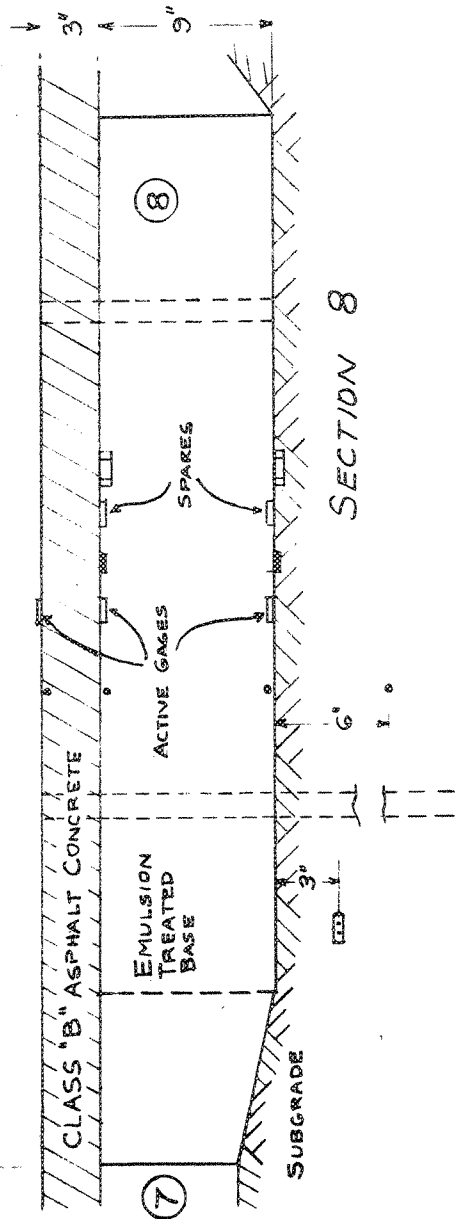


FIGURE 20. ...
 HIGHWAY RESEARCH SECTION
 RING No. 2 Y-651
 WASHINGTON STATE UNIVERSITY
 JULY 28, 1966
 M. KRUKAR
 INSTRUMENTATION FOR SECTION 8 - E.T.B.

SCALE: HORIZONTAL 1" = 4.0'
 VERTICAL 1" = 1.0'

Note: The positions of the deep and shallow LVDT gages have been reversed.

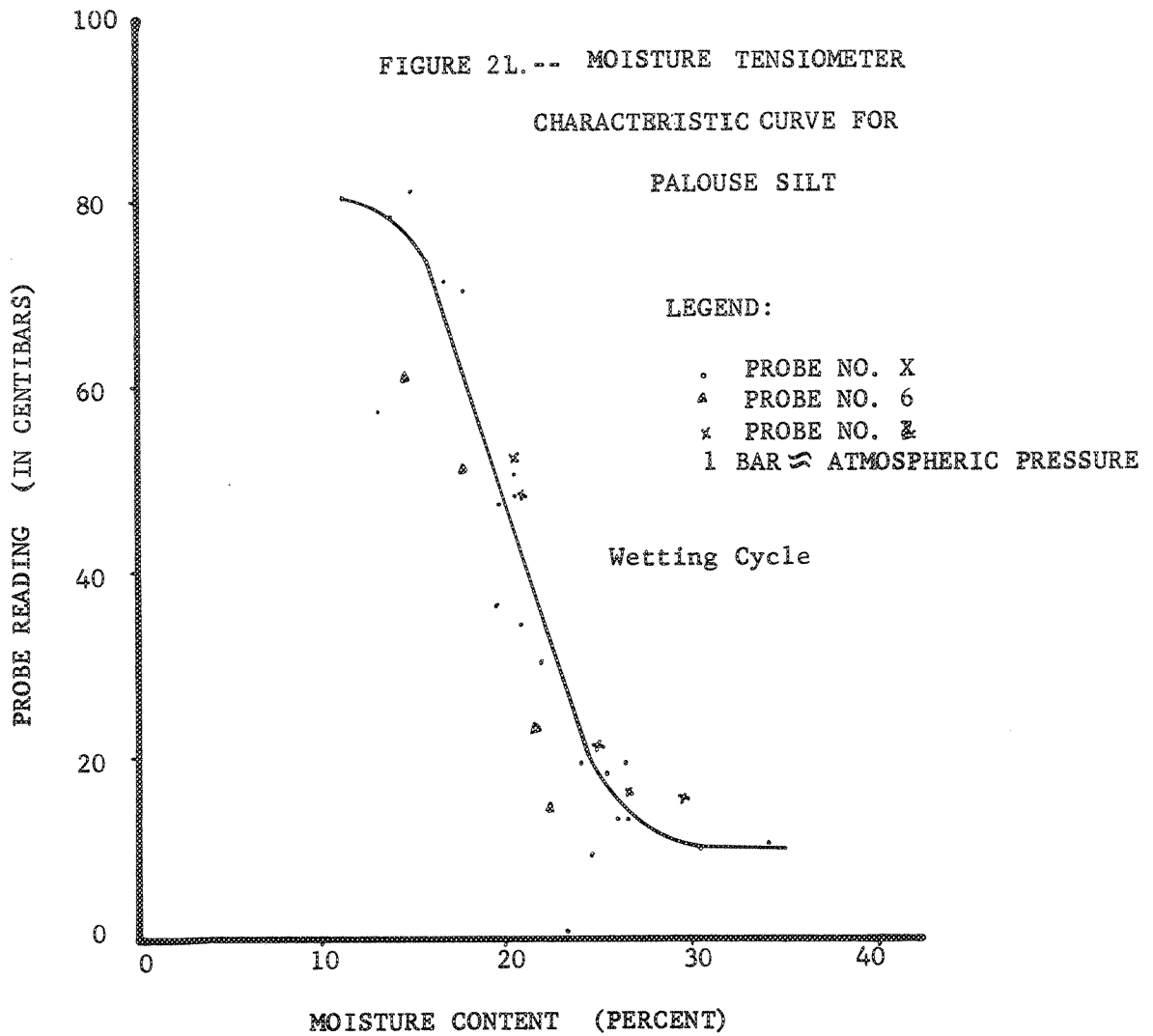
All the instruments, with the exception of the thermocouples, moisture probes, and some pressure cells, were wired into an amplifier, manual switching panel, and recorder. The other instrument readings were taken visually and recorded manually. Deflection measurements were measured with a Benkleman beam and the Idaho beam.

Measurement of Moisture

The moisture in the subgrade during construction was measured by nuclear methods. To measure the amount and movement of water in the silt subgrade, 15 moisture tensiometer probes were installed. These probes work on the principle that moisture tension between the soil particles causes soil suction. Porous ceramic cups filled with water are attached by long capillary-like copper tubing to a Bourdon dial gage. As the surrounding soil dries out, tension within the water film draws the water from the porous cup. This suction registers in centibars on the Bourdon gage. High readings on the dial indicate dry soil.

Several moisture probes were calibrated in the laboratory on the wetting cycle. The calibration graphs for these probes exhibit a hysteresis effect (6); one curve for the drying cycle and another for the wetting cycle. The calibration curve for the wetting cycle is shown in Fig. 21.

Holes for the probes were bored with an auger. Twenty-four hours before installation, the ceramic cups were saturated with de-aired distilled water. The ceramic probes were installed in pre-wetted probes in a vertical position to make filling and removal of air bubbles easier. They were then filled with distilled water and purged. The copper leads were buried in 2 to 6-inch deep trenches and covered with soil. All leads were placed so the gages would be on the outside shoulders of the track to facilitate reading. Special holders and protective boxes housed the 15 gages.



Temperature Measurements

Iron-constantan thermocouples:--Forty-eight Leeds and Northrup iron-constantan thermocouples type 20-50-4, were installed in four different positions in each section (Fig. 20). Each wire was insulated with silicone impregnated asbestos with the overall insulation consisting of single-glass braid, impregnated with silicone-resin. The ends were bared, sanded clean, crimped together, and waterproofed with a silicone seal before installation. The thermocouples were then hooked up to a switch box, which was connected to a direct-reading potentiometer. Some problems developed with the thermocouple insulation causing erratic readings.

Thermograph:--After trouble developed with the thermocouples in Section 8 (9.0 inches of ETB), a two-probe automatic recording Belfort Instrument Thermograph was installed. One probe was installed 3 inches below surface and the other 12 inches below surface. This instrument recorded temperature continuously for the duration of the test.

Stress (Pressure) Measurements

WSU pressure cells:--These cells are similar to those used in Ring #1 and are shown in Figs. 22 and 23. Calibration of these cells was accomplished in an air pressure chamber. A typical calibration unit is shown in Fig. 24. During ring construction the subgrade and the base where they were to be placed was leveled then covered with a layer of fine silica sand. The cells were placed in position and covered with another layer of fine silica sand to protect the cell from any pressure points that might develop from the aggregates in the base. The system was connected to a manometer board.

Filpip pressure transducers:--Filpip pressure transducers are thin, flexible, low inertia, vibration damped, vacuum sealed sensors. They are constructed of embossed alloy steel plates separated by a dielectric and sealed under vacuum.



FIGURE 22.--A COMPARISON OF THE NEW WSU PRESSURE CELL WITH THE OLD CELLS USED IN RING NO. 1.

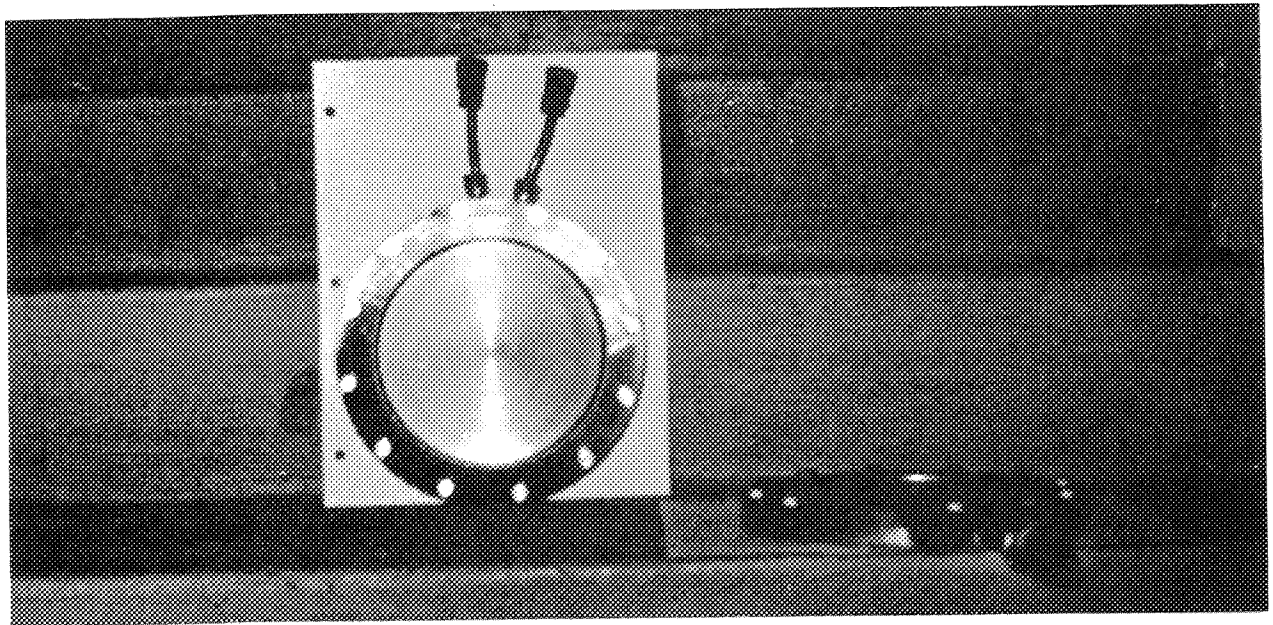
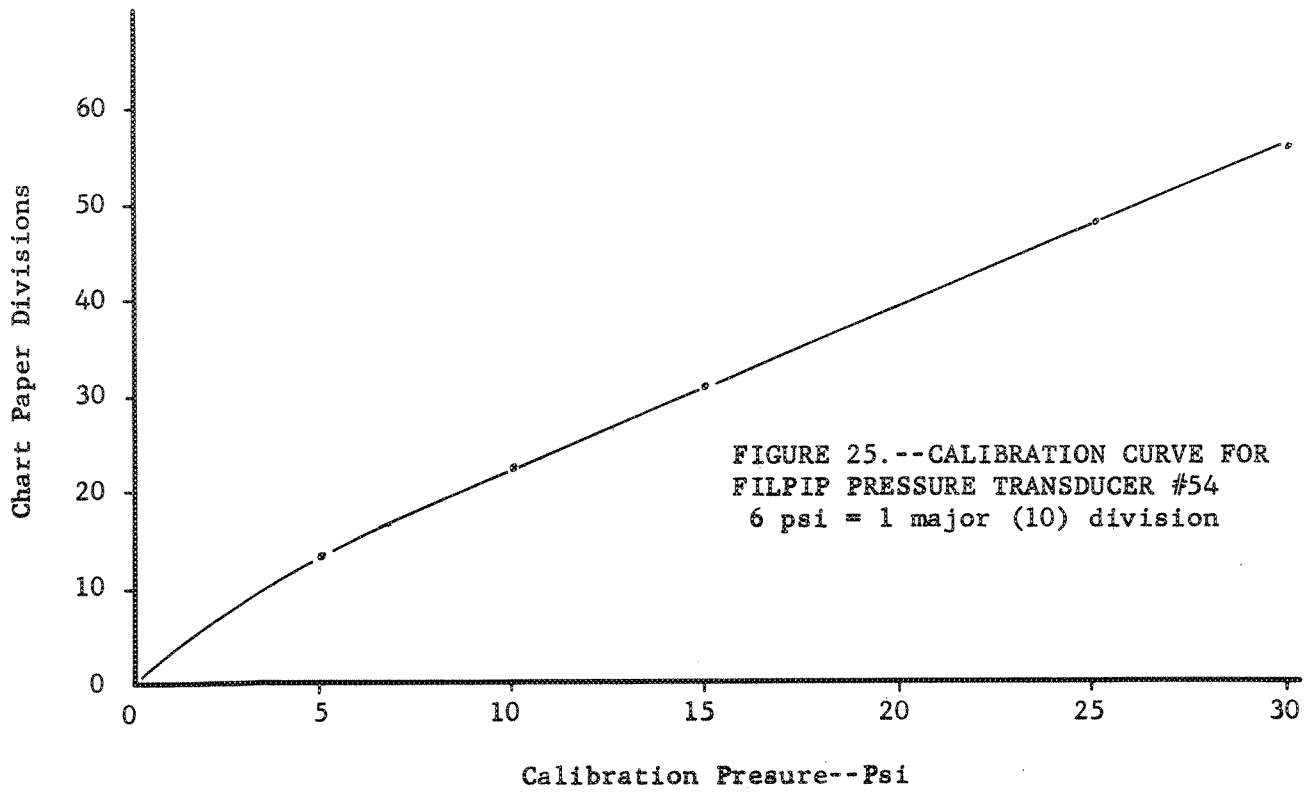
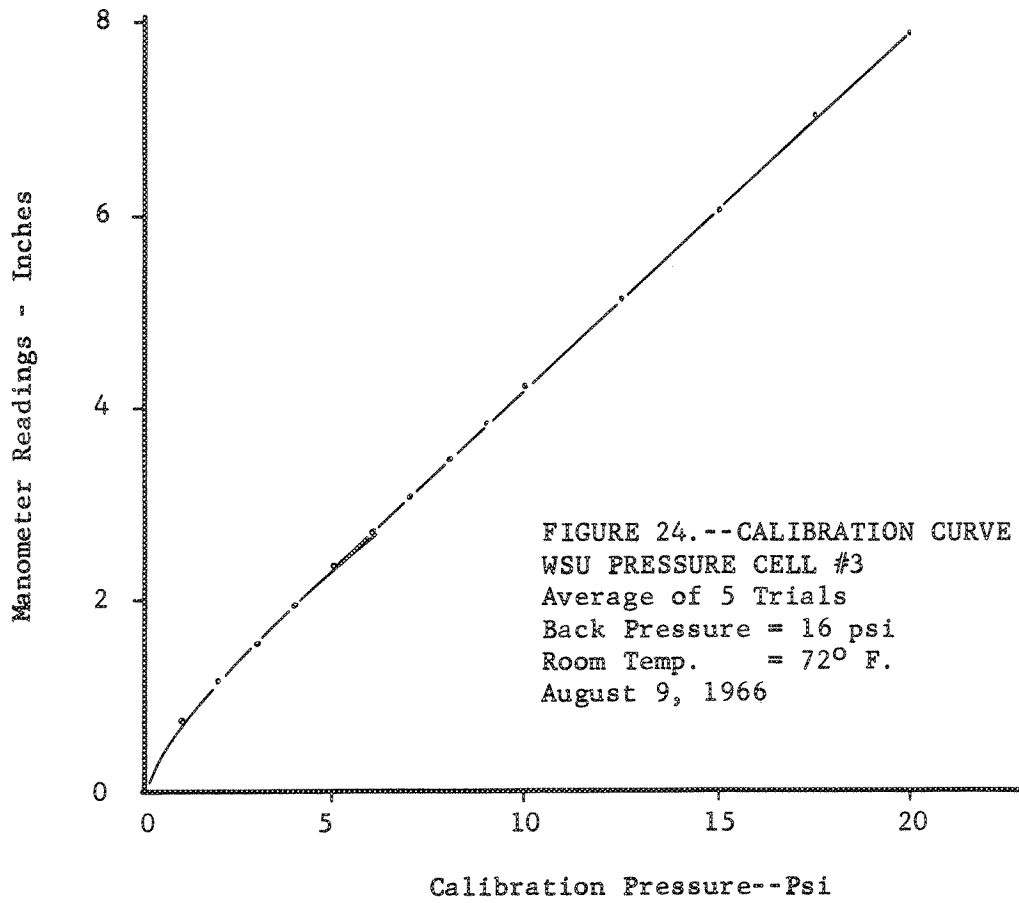


FIGURE 23.--A TOP AND SIDE VIEW OF THE WSU PRESSURE CELL.



Under external pressure the plates deform elastically to bring the plates closer together. The separation of the plates is determined through measurement of electrical capacitance. A total of 20 Filpip transducers were prepared and calibrated in an air chamber in the laboratory. A typical curve is shown in Fig. 25. The leads from the transducers were encased in a 20-foot tough plastic casing for protection from aggregates and temperature. Half of the gages were mounted with a silicone seal on a small plastic platform, then covered with a protective silicone seal coat and Ottawa sand. The other ten cells were left unprotected. The cells with the plastic platforms were placed directly on the subgrade and base without any preparation and leads were stapled to keep the gages horizontal. The unprotected gages were laid in a thin bed of silica sand, the leads stapled to hold the gage in a horizontal position, and then covered with the silica sand. This is shown in Fig. 26. All transducers were then connected to the switching unit and the recorder.

Strain Measurements

Shinkoh polyester SR-4 #P-20 strain gages were used for the measurement of strain. Strain gages in longitudinal and transverse positions were installed on the surface, bases, and subgrades as shown in Table VII and Fig. 20.

Strain gages (subgrade):--The problem of installing strain gages on loose material, such as the subgrade, was resolved by using extensometers (Fig. 27). These consist of 2- to 10-inch, 3/8-inch diameter dowels joined by an 8-inch long, 3/4-inch wide, 8-mil thick steel shim stock. Strain gages and connector blocks were epoxyed on this shim stock with the manufacturer's epoxy and coated with a silicone seal waterproofing. The extensometers were placed in position (one running longitudinally and the other transversely) and stretched taut. They were then hooked up to a 6-foot length of Teflon-coated wiring connected to Belden strain gage wire. All connections around the strain gages were coated

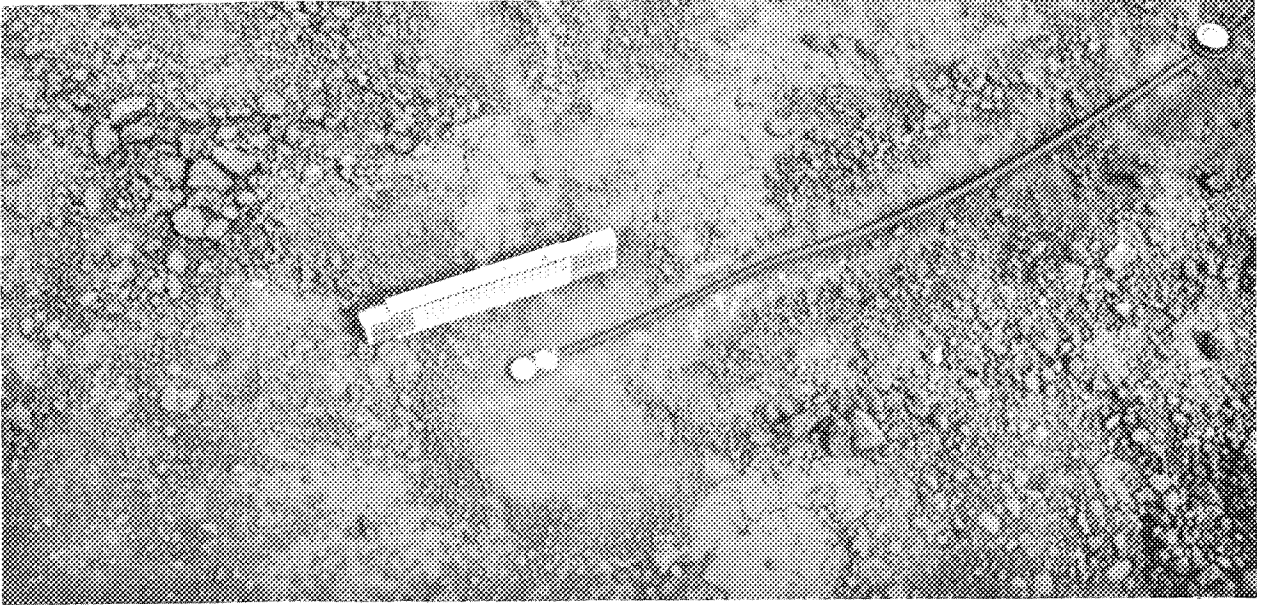


FIGURE 26.--A VIEW OF THE SIZE OF THE FILPIP PRESSURE TRANSDUCER.

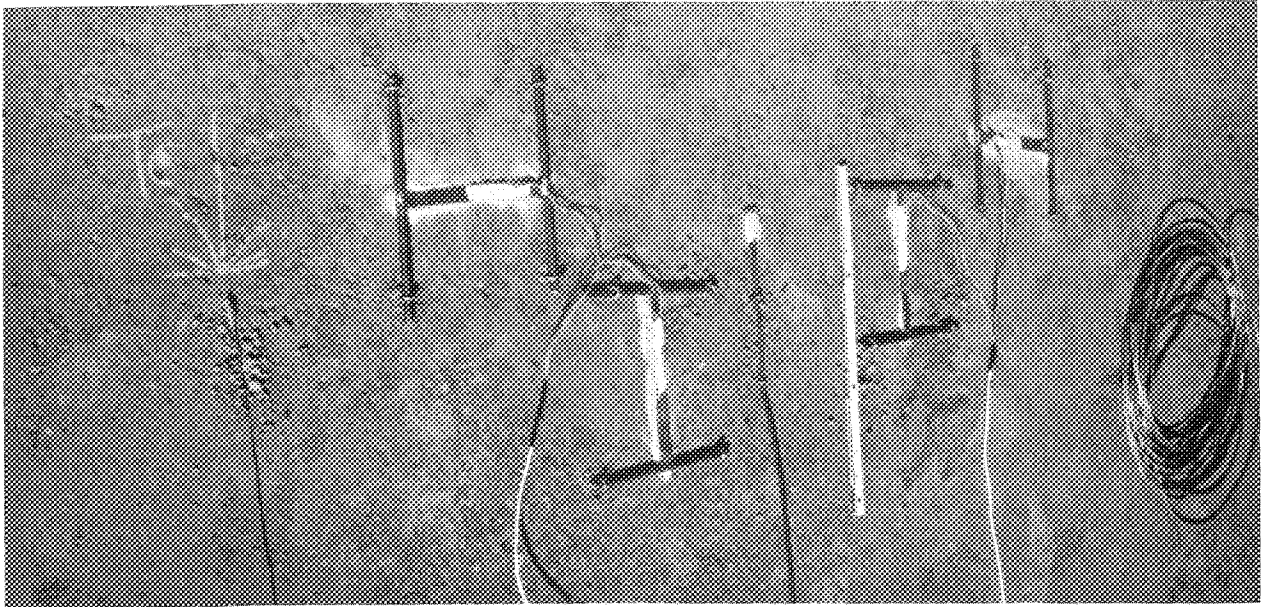


FIGURE 27.--THIS SHOWS THE PORTION OF INSTRUMENTS IN THE SUBGRADE. NOTE THE STRAIN GAGE EXTENSIOMETERS, THE FILPIP TRANSDUCER, AND THE THERMOCOUPLE.

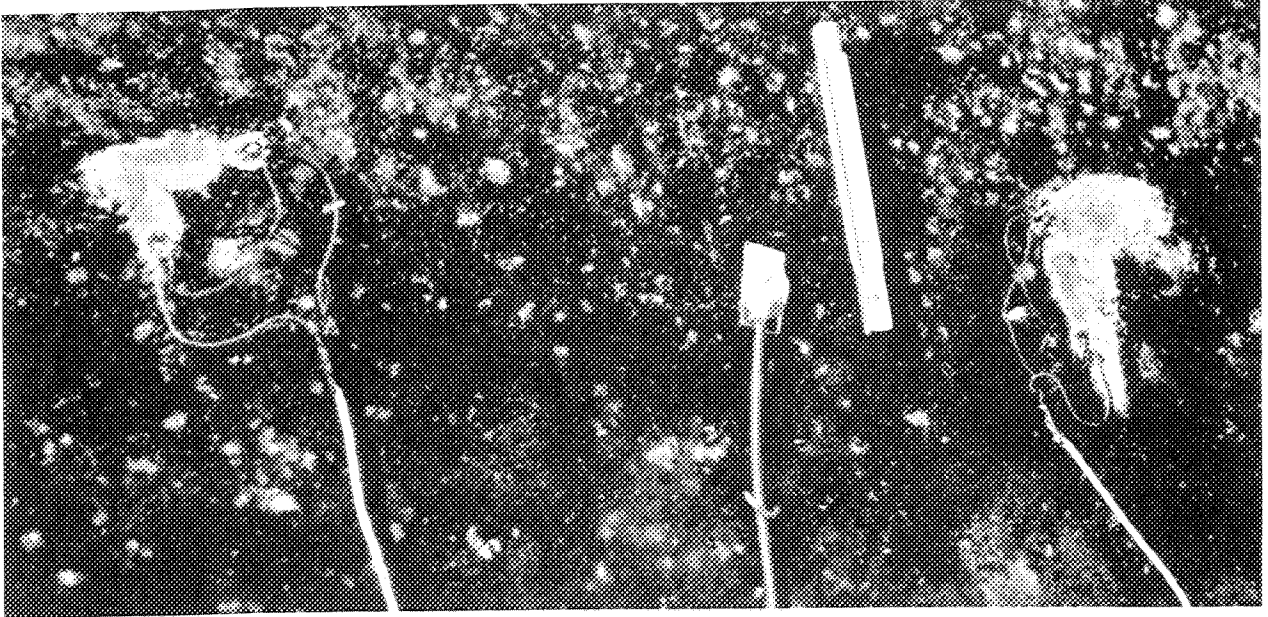


FIGURE 28.--STRAIN GAGES MOUNTED ON TOP OF EMULSION-TREATED BASE. THE FILIPIP TRANSDUCER LIES BETWEEN BOTH PAIRS OF STRAIN GAGES.

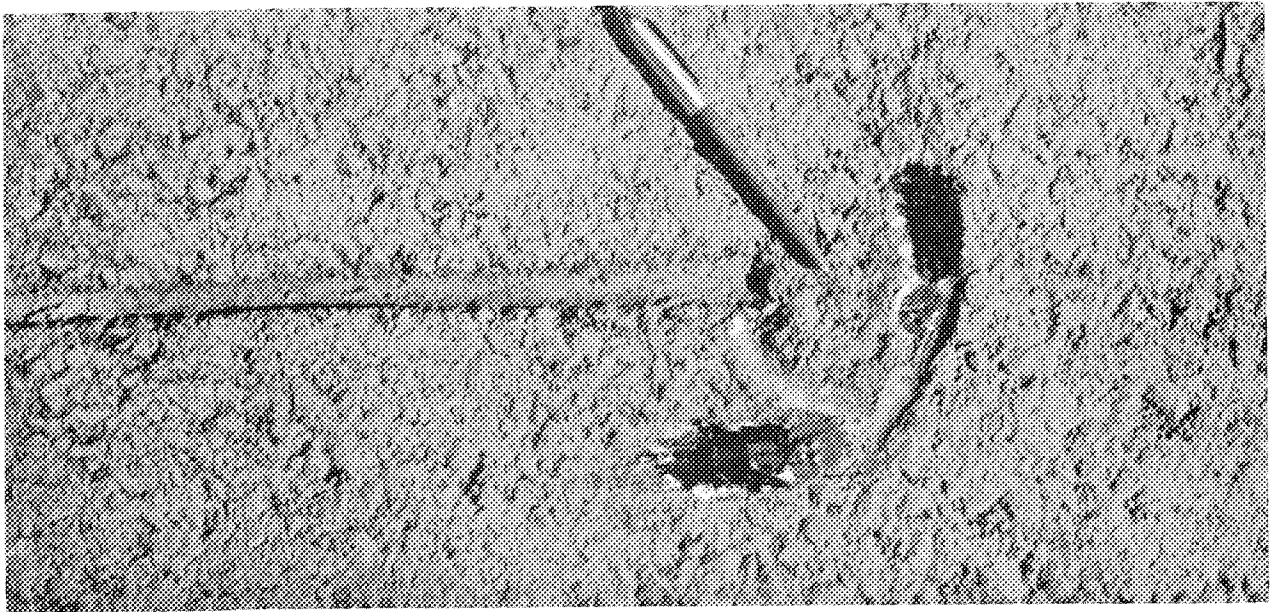


FIGURE 29.--MOUNTING STRAIN GAGES ON PAVEMENT SURFACE. NOTE GROOVE IN PAVEMENT.

with a silicone seal and a thin layer of hot asphalt mix was packed over it (7).

Strain Gages (bases and surfaces):--Extensometers were used in the placement of strain gages on top of the untreated base (7). For mounting on the asphalt and emulsion bases, the surface was prepared by filling it with a silicone seal to level the surface and give consistency of strain to the gage. After curing, the surface was sanded where necessary and the gage and mounting block were epoxied (as shown in Fig. 28) then connected with Belden strain gage wire. All gages and connecting wires were waterproofed with a tack coat of SS-1 emulsified asphalt mixed with fines.

At pavement surface, grooves were made by inserting wooden dowels during the rolling process (Fig. 29). The asphalt surface was then ground down and smoothed. The gages were epoxied under pressure with the standard strain gage epoxy. Figure 29 shows the grooves and the gages in position. Belden strain gage wire was placed in the groove, and the wire and the gages were covered with bituminous joint filler for water and wear protection.

One strain gage was mounted on an asphalt block and buried in the ground to act as a temperature compensating gage, meaning that each gage had to be balanced individually as it was switched on.

Deflection Measurements

Dynamic:--Four short 585 DT-100 and four long 585 DT-500 Sanborn Linear Variable Differential Transformers (LVDT) gages measured dynamic deflections. The short LVDT's measured deflection of the wearing course and base with respect to the subgrade, while the long gages measured the dynamic displacement of the total system. Holders for the gages were constructed at the Research Division's machine shop (Figs. 30 & 31).

Four deep and four shallow holes were diamond drilled through the asphalt and then augered to final depth placement of the gages and holders (see Table

IX). The gages, which were calibrated before and after installation to insure proper readings, were then connected to the switching panel and recorder.

TABLE IX
DEPTH OF LVDT HOLES

Type of Base LVDT Holes	Section & Base Type			
	Untreated	Emulsion Treated		Spec. Asphalt Treated
	2 (7.0")	6 (5.0")	8 (9.0")	10 (3.5")
Shallow (inches)	10	8	12	6.5
Deep (feet)	15.19	6.36	4.00	16.18

Rebound deflection measurements:--These were measured with a Soil Test Benkelman beam, Dehlen curvature meter, and Idaho Highway beam (Fig. 32). The Dehlen curvature meter was too large to slip between the tires and the dial was impossible to read under our field conditions. The curvature basin appeared to be too large for the Idaho beam to work effectively. Readings near the end of testing were taken, five per section, at different locations, to obtain an average deflection value.

Read-Out Equipment

A Brush amplifier with input boxes for strain and LVDT gages was utilized. Several manual switching panels were made by the Electrical Science section, WSU, to work with the B & K switcher. The system was manually operated and each Filpip transducer, strain gage, and LVDT gage was individually switched into the system. The strain gages were also balanced.

The thermocouples were switched in manually and readings were taken from the direct reading potentiometer. Manual switching is time consuming and it is hoped to eventually obtain an automatic system. The read-out equipment is shown in Fig. 33.

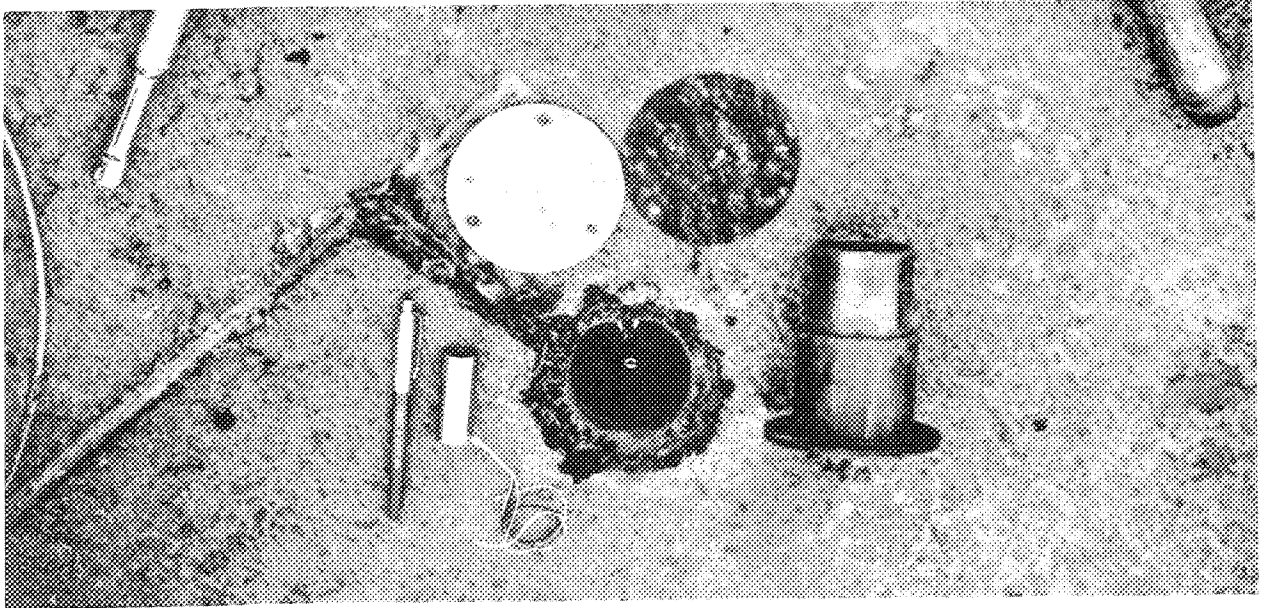


FIGURE 30.--A VIEW OF THE SHORT LVDT GAGE, THE HOLDER AND THE FERRITE CORE. NOTE THE GROOVES.

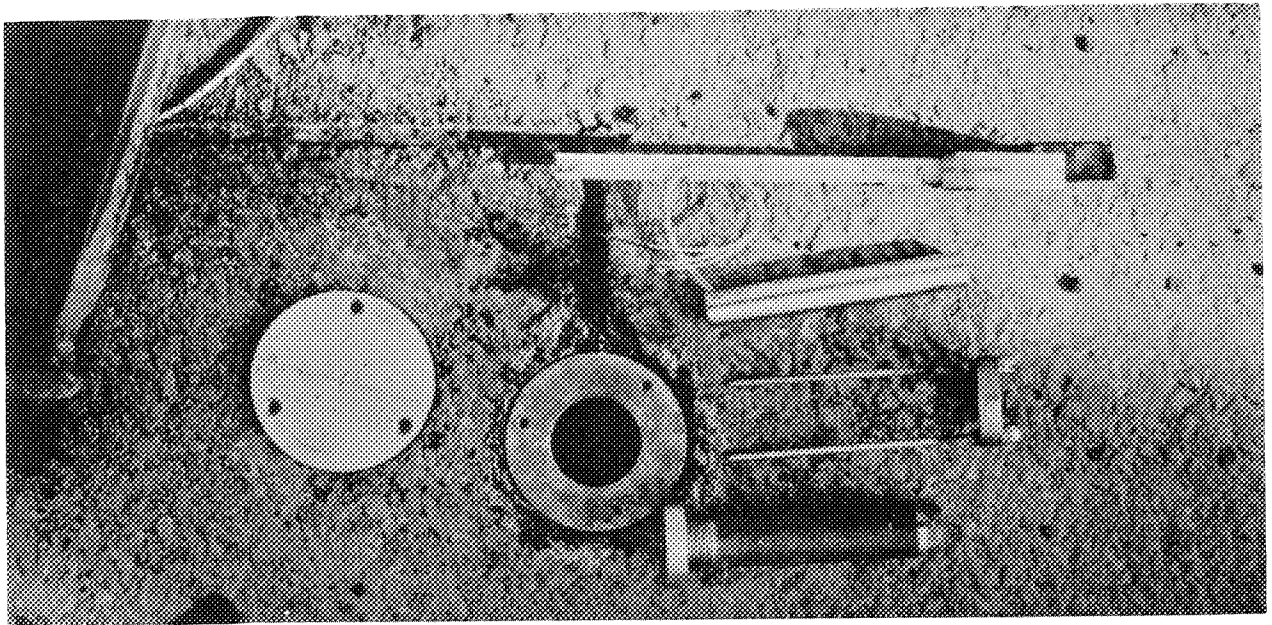


FIGURE 31.--THIS SHOWS THE LONG LVDT GAGE AND THE INSIDE PARTS OF THE HOLDER.

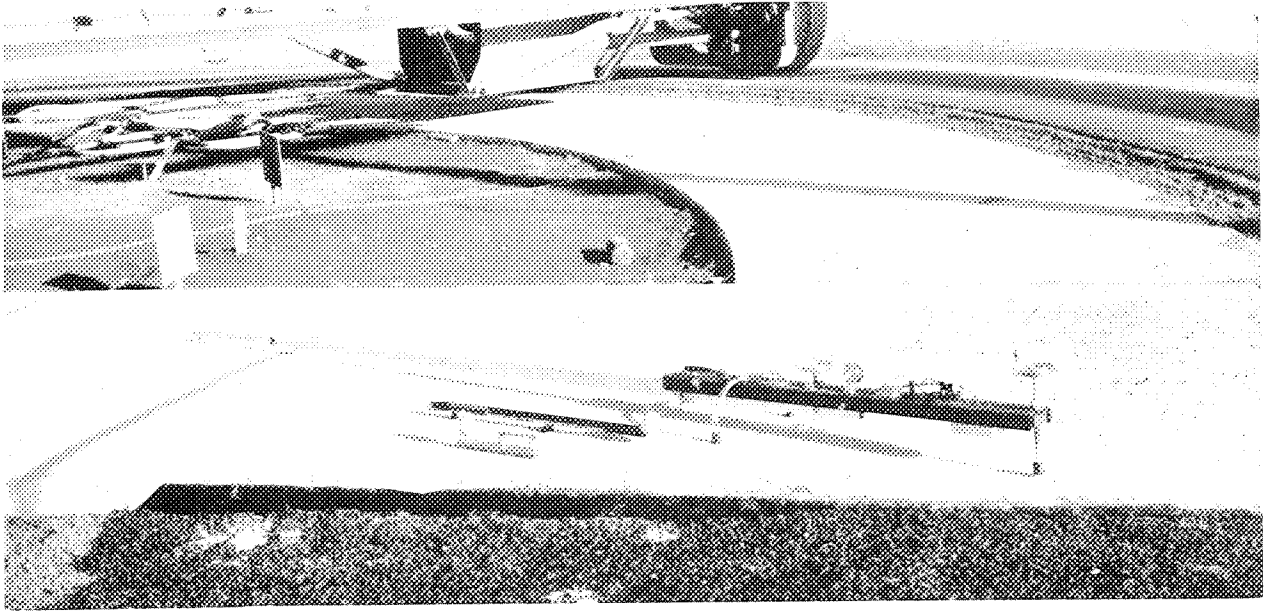


FIGURE 32.--A COMPARISON OF THE SIZES OF THE DEHLEN CURVATURE METER, IDAHO BEAM, AND THE SOILTEST BENKELMAN BEAM.

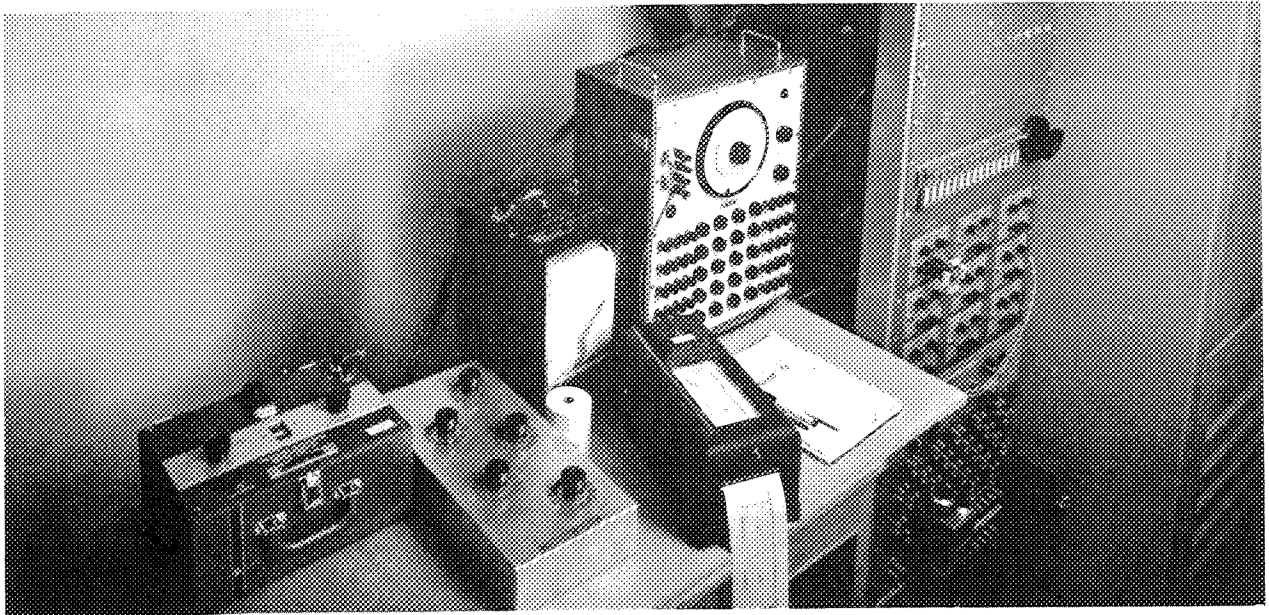


FIGURE 33.--A VIEW OF THE READ-OUT EQUIPMENT SHOWING THE BRUSH AMPLIFIER AND INPUT BOXES, MANUAL SWITCHING PANELS, B & K AUTOMATIC SWITCHING PANEL, BRUSH RECORDER, THERMOCOUPLE SWITCHING BOX AND DIRECT READING POTENTIOMETER.

PERFORMANCE OF TEST RING #2

Testing Periods

Testing began October 31, 1966 and was suspended December 31, 1966 due to the advent of winter. During this period, a total of 205,425 wheel loads and 68,475 revolutions were applied. Testing was done on a 7-day, 24-hour basis whenever possible. Signs of distress appeared in all the untreated base sections 1-4, all the emulsion-treated base sections 5-8, but no signs of distress were evident in the special aggregate asphalt-treated bases, sections 9-12. Sections 2 and 3 (7.0 and 9.5 inches of untreated base, respectively) and sections 5 and 6 (3.0 and 5.0 inches of emulsion-treated base, respectively) were declared failed. The operating speed had been lowered from 25 mph to 5 mph at closure (8,9).

Full time testing was resumed on April 6, 1967, after several of the failed sections had been replaced and weather conditions improved. All testing was stopped on May 31 after 232,608 wheel loads and 77,536 revolutions. At this time all sections showed various degrees of distress, and all sections, with the exception of Section 12 (6.5 inches of asphalt-treated base), were declared failed (8,9).

Testing Conditions

Design Thickness

Special care was taken during construction to ensure that the proper specified base and wearing course thicknesses would be achieved. The subgrade was brought to the desired elevation, and was checked by rod and level. Even so, it was difficult to achieve the proper thicknesses. Cores were drilled before and after testing and thicknesses were checked along with densities. Table X shows the measured thicknesses and the deviations from design thicknesses.

Densities of the cores were also measured and compared to laboratory and nuclear densities. It should be noted that it was impossible to obtain complete cores from the emulsion-treated bases. Field experience with emulsion-treated bases indicates that over 8 months of curing may be necessary before complete cores of the emulsion-treated bases can be obtained.¹

Speed

Attempts were made to keep as many of the variables as constant as possible during the testing periods. The speed of the apparatus was kept at 20 mph until the break-up of the sections required reduction of speed for protection of the apparatus. Figure 34 shows speed versus wheel load applications. The graph illustrates the fact that as the number of wheel loads was increased (thus increasing the pavement roughness), the speed was reduced accordingly. The graph also shows approximately when the first signs of distress occurred in the different sections.

Environmental Conditions

Since the testing pavement center is not under cover, it is open to all the elements of weather and hence subject to all the variable effects caused by a changing environment.

All testing was done during a total of some 51 days - 29 days in November-December and 22 days in April-May. The testing period has been divided into two parts--the fall period of November, 1966 and the spring period of April-May, 1967.

During the fall period (November-December, 1966), unusually large amounts of precipitation were recorded (especially during the two middle weeks of November), saturating the subgrade. Figure 35 shows the amounts of precipitation

¹Conversation with Chevron Asphalt Technical Engineers, Lloyd Coyne and Ron Trolle.

TABLE X: CORE THICKNESSES¹ AND DENSITIES

Section	Type	Design Thickness (in.)	Core Thickness (in.)	Deviation From Design (in.)	Average Nuclear Density lbs/cu.ft.	Core Density lbs/cu.ft.	Laboratory Density lbs/cu.ft.	Deviation From Lab lbs/cu.ft.
2	Cl. "B"	3.0	2.78	-0.22	148.4	152.9	152.0	+0.9
4	Cl. "B"	3.0	2.94	-0.06	148.4	155.4	152.0	+3.4
6 ²	Cl. "B"	3.0	2.91	-0.09	148.4	152.2	152.0	+0.2
8 ²	Cl. "B" E.T.B.	3.0 9.0	2.88	-0.12	148.4 139.0	152.3 147.5	152.0 140.4	+0.3 +7.1
10 ⁴	Cl. "B" Spec. ATB	3.0 3.5	2.94 3.63	-0.06 +0.13	148.4 141.8	150.3 146.5	152.0 148.5	-1.7 -2.0
11 ⁴	Cl. "B"	3.0	2.94	-0.06	148.4	149.8 ³	152.0	-2.2
12 ⁴	Cl. "B" Spec. ATB	3.0 6.5	3.12 6.38	+0.12 -0.12	148.4 141.8	154.2 143.2	152.0 148.5	+2.2 -5.3

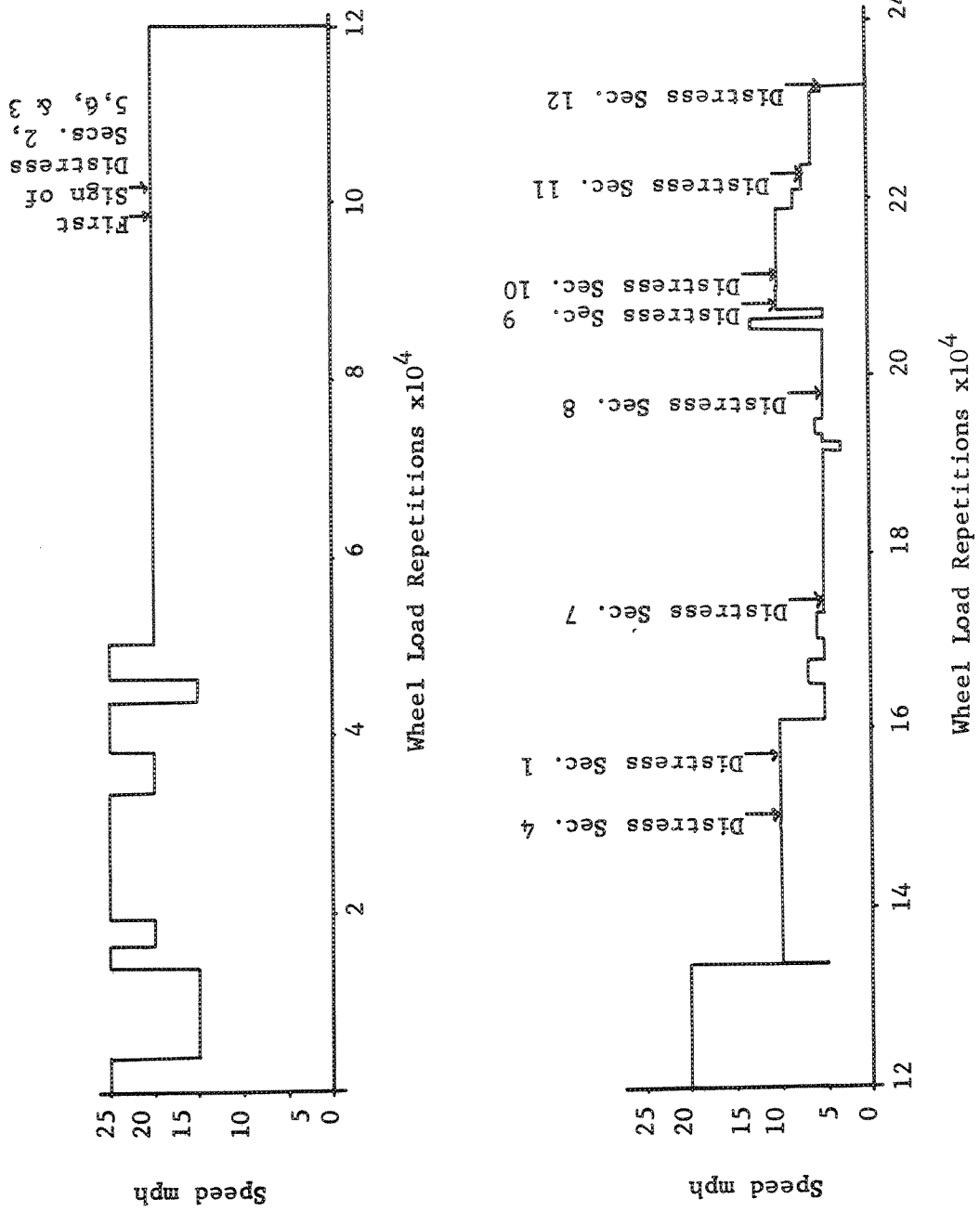
¹ Cores were taken prior to start and at end of testing. Core diameters were 2½", 3½", and 5.0".

² It was impossible to obtain complete cores of emulsion-treated bases.

³ The total density, including part of the special ATB.

⁴ Indicates poor bond between the different layers of the special asphalt-treated base.

FIGURE 34. --SPEED VERSUS TIME (EXPRESSED IN WHEEL LOAD REPETITIONS)



that occurred during the existence of Ring #2.

During this period, thermograph copper constantan probes recorded a downward trend in ambient temperature (see Fig. 36). The deep probe #1 was less sensitive to daily temperature changes than the shallow probe #2 due to depth.

Testing was resumed the spring of 1967 (April-May) after the weather became drier and air and soil temperatures started to rise. After heavy precipitation during January, 1967, the precipitation during February was low. Precipitation rates increased in March and stayed at a fairly constant level during April and May. Air and soil temperatures started to increase although minimum daily temperatures did not rise as rapidly as the maximum temperatures. The difference between maximum and minimum temperatures became pronounced during this period (shown in Fig. 36).

The significance of these temperature differences results in the division of the period into two time and temperature zones. The fall period from November to December, 1966, was wet and cold with very little difference between the maximum and minimum temperatures. The spring period from April-May, 1967, was relatively dry after a very wet March. Rising temperatures with large daily temperature differences between the average maximum and minimum temperatures typified the spring period (Fig. 36 and Table XI).

TABLE XI: AVERAGE TEMPERATURE VARIATIONS - RING NO. 2

Year	Month	Temperature* - °F								
		Ambient			3" Below Surface			12" Below Surface		
		Max.	Min.	Variation	Max.	Min.	Variation	Max.	Min.	Variation
1966	Nov.	47.0	33.0	14.0	40	33	7	42	41	1
	Dec.	40.0	31.0	9.0	34	30	4	38	38	0
1967	Jan.	40.5	30.0	10.5	34	30	4	36	35	1
	Feb.	45.0	30.0	15	38	30	8	37.5	37	.5
	Mar.	44.0	30.0	14.0	35	32	3	40	39	1
	Apr.	51.0	31.5	19.5	54	36	18	48	46	2
	May	63.0	39.0	24.0	73	48	25	60	57	3

*Average maximum and minimum monthly temperatures

FIGURE 35.--
Ring #2

Rainfall

Oct. 1966 - May 1967

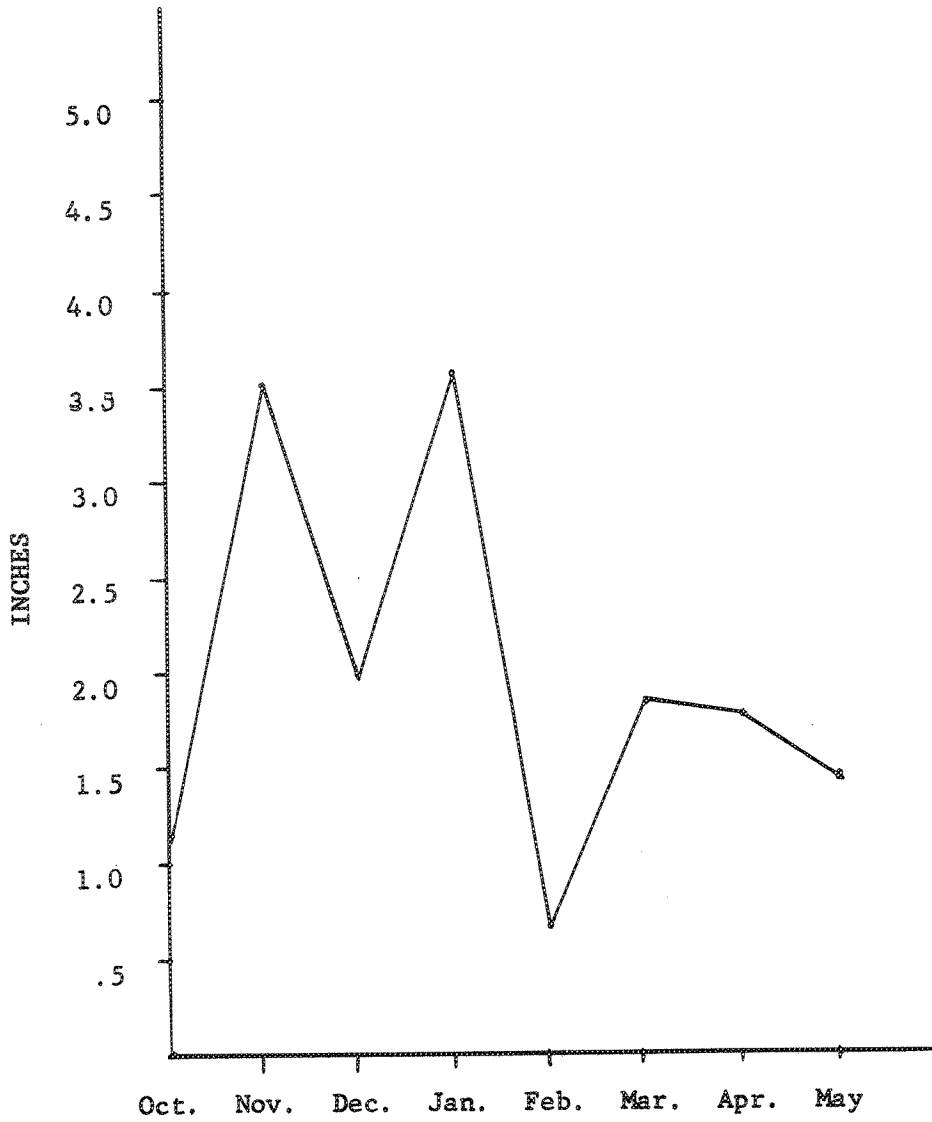
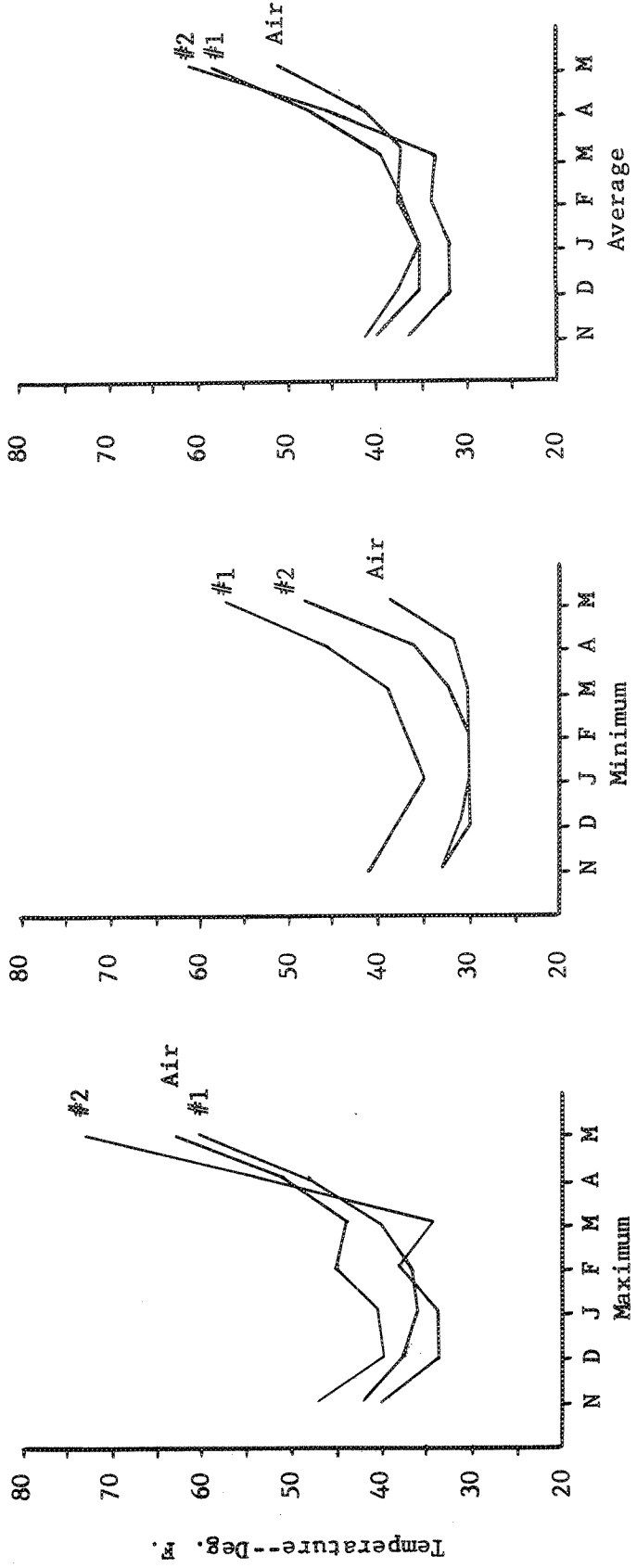


FIGURE 36. -- AVERAGE MAXIMUM, MINIMUM, AND AVERAGE MONTHLY TEMPERATURES FOR RING NO. 2 7-MONTH PERIOD 1966-67

Legend:
 Air (10)
 Probe #1 12" Below Surface
 Probe #2 3" Below Surface



Experimental Results

Section Failures

Fall Period--1966:--During this period of testing, several sections started to show signs of distress and ultimately failed. Signs of distress occurred in sections 5 and 6 (3.0 and 5.0 inches of emulsion-treated base, respectively) and section 2 (7.0 inches of untreated base) at about 99,000 wheel loads; section 3 (9.5 inches of untreated base) at 100,000 wheel loads; section 4 (12.0 inches of untreated base) at 153,411 wheel loads; section 1 (4.5 inches of untreated base) at 157,203 wheel loads; section 7 (7.0 inches of emulsion-treated base) at 175,581 wheel loads; and finally section 8 (9.0 inches of emulsion-treated base) at 198,811 wheel loads.

Testing was halted after 205,425 wheel loads. At this time, sections 5, 6, 2, and 3 were declared failed. These had to be removed and replaced before testing could be resumed in the spring. Table XII shows the pavement conditions, the first signs of distress, and when failure was declared.

The fall period was a time of steady rain with ambient ground temperatures of above and below freezing within a few degrees. Environmental conditions probably contributed significantly to the early distress of the pavements.

Spring Period--1967:--Sections continued to develop signs of distress and section failures increased. Distress appeared in sections 9, 10, 11, and 12, (2.0, 3.5, 5.0, and 6.5 inches of special asphalt-treated base) and at 208,299; 211,320; 216,039; and 231,204 wheel loads, respectively.

Sections 1, 7, 9, 10, and 11 were declared failed during this testing period as shown in Table XII. At the end, only section 12 was in relatively good condition. Testing was halted at 232,608 wheel loads.

The spring period was characterized by decreasing amounts of precipitation and rising air and ground temperatures. Temperature differences between the

TABLE XII: SECTION CONDITION PROGRESS REPORT

Base Type	Section	Base Thickness (inches)	First Appearance of Distress		Section Declared Failed		Condition at 232,608 Wheel Loads
			Wheel Loads	Date	Wheel Loads	Date	
Crushed Surfacing Top Course (CSTC) Untreated	1	4.5	157,203	11-22-66	210,270	4-13-67	Replaced
	2	7.0	99,000	11-14-66	205,425	12- 5-66	Replaced
	3	9.5	100,000	11-14-66	206,748	3- 5-67	Replaced
	4	12.0	153,411	11-18-66	232,608	5-29-67	Transverse cracking extensive. Permanent settlement.
Emulsion Treated (CSTC)	5	3.0	99,000	11-14-66	199,233	11-30-66	Replaced
	6	5.0	99,000	11-14-66	199,233	11-30-66	Replaced
	7	7.0	175,581	11-24-66	230,856	5-19-67	Replaced
	8	9.0	197,811	12- 1-66	232,608	5-29-67	Transverse cracks. Extreme deflection and ruts.
Special Aggregate Asphalt Treated	9	2.0	208,299	4-10-67	208,896	4-10-67	Replaced
	10	3.5	211,320	4-25-67	221,451	5- 4-67	Transverse cracks extensive
	11	5.0	216,039	4-26-67	232,608	5-29-67	Failed. Transverse cracks and longitudinal crack. Deep ruts.
	12	6.5	231,204	5-22-67			Tiny cracks.

extremes (maximums and minimum) rose and environmental conditions were not as severe as during the fall period.

Failure Pattern: The failure patterns of the sections for the two periods had enough similarity so that a general failure pattern could be established. Pavement distress seemed to follow this pattern:

1. Ruts become pronounced.
2. Visible flexing of the pavement section.
3. The appearance of a few transverse cracks of varying lengths and the pumping of mud through them. Since pumping depends upon wetness, cracking and pumping may or may not occur simultaneously, depending upon environmental conditions.
4. The transverse cracks lengthen and increase in frequency with or without pumping.
5. The appearance of a longitudinal crack along the wheel path center, with some noticeable permanent pavement subsidence and pumping. Pumping may or may not increase depending upon the weather.
6. Alligator cracking appearance and more settlement.
7. Longitudinal cracks appear at edge of the wheel path, with extensive subsidence of the traveled part of the pavement. The untraveled part of the pavement may bulge.
8. It becomes necessary to fill in the distressed sections to keep the frame from dragging. At this point the section is declared failed.

This is the usual distress pattern although there may be variations and omissions, depending upon the time period. During the fall period, the first two patterns were not as evident as in the spring period. This may be due to the pavement temperature differences. During the spring, steps 5 and 6 were often by-passed, and instead a sudden longitudinal shear failure often occurred either on the inside or outside edge of the dual tires. As mentioned before, pumping of mud was a function of the environment. The different distress steps are shown in Figs. 37 to 41 for the fall period and Figs. 42 to 54 for the spring period.

In the fall, the failure pattern usually followed these steps:

1. Some visible flexing of the pavement section.
2. The appearance of a few transverse cracks of varying lengths and the pumping of mud through them. Since pumping depends upon wetness, cracking and pumping may or may not occur simultaneously, depending upon environmental conditions.
3. The transverse cracks lengthen and increase in frequency with or without pumping.
4. The appearance of a longitudinal crack along the wheel path center, with some noticeable permanent pavement subsidence and pumping. Pumping may or may not increase depending upon the weather.
5. Alligator cracking appearance and more settlement.
6. Longitudinal cracks appear at edge of the wheel path, with extensive subsidence of the traveled part of the pavement. The untraveled part of the pavement may bulge.
7. It becomes necessary to fill in the distressed sections to keep the frame from dragging. At this point the section is declared failed.

In the spring, the failure pattern differed somewhat and usually followed these steps:

1. Ruts became pronounced.
2. Very visible flexing of the pavement.
3. The appearance of a few transverse cracks of varying lengths and the pumping of mud through them. Since pumping depends upon wetness, cracking and pumping may or may not occur simultaneously, depending upon environmental conditions.
4. The transverse cracks lengthen and increase in frequency with or without pumping.
5. Longitudinal shear cracks appear at the edge of the dual tires. Some alligator cracking pattern may occur, but is not fully developed.
6. Extensive settlement occurs followed by a longitudinal shear crack on the inside or outside edge of dual tires. The untraveled part of the pavement may bulge.
7. It becomes necessary to fill in the distressed section to keep the frame from dragging. At this point, the section is declared failed.

Discussion of Section Failures

Failures which occurred in the fall and those which occurred in the spring showed some interesting contrasts. Table XII was rearranged into Table XIII to show the number of wheel applications for the different time periods, the time of first distress, and failure. Table XIV shows the amount of wheel loads needed to cause "ultimate" failure after the first appearance of cracking. "Ultimate" failure, as used here, means that the failure of the pavement was taken beyond practical limits reached in regular highway usage; in other words, on a regular highway the pavement would have been repaired long before the "ultimate" failure point was ever reached. "Ultimate" failure is shown in Figs. 39, 45, 46, 48, and 51.

During the fall period, transverse cracks began at random and increased with wheel applications. The number of wheel load applications to reach "ultimate" failure was large as compared to the spring period. The failure mode followed was that as outlined in the previous sections, although rutting and visible pavement deflections were not as evident or prominent as during the spring.

In contrast, sections 9, 10, and 11 containing the asphalt-treated bases which failed at the resumption of testing in the spring, failed spectacularly. Once initial cracking appeared, "ultimate" failure occurred very rapidly as shown in Table XIV and Figures 42-50.

Differences between failures occurring during the two periods was noticeable. During the spring period, shear cracks occurred at the edge of the wheel path. The alligator cracking pattern was not as fully developed as in the sections which failed in the fall. Failure in the fall was slower and progressive, following the failure mode steps mentioned before. The spring failure bypassed some of the failure mode steps and occurred rapidly and spectacularly. Pave-

TABLE XIII: PAVEMENT PERFORMANCE SUMMARY - FALL & SPRING PERIODS

Base Type	Section	Base Thickness Inches	First Appearance of Cracking			Section Failure				
			Date	Wheel Load Applications Fall	Spring	Total	Date	Wheel Load Applications Fall	Spring	Total
Crushed	1	4.5	22/Nov/66	157,203		157,203	13/Apr/67	205,425	4,845	210,270
Stone	2	7.0	14/Nov/66	99,000		99,000	5/Dec/66	205,425		205,425
Untreated	3	9.5	14/Nov/66	100,000		100,000	5/Mar/67	205,425	1,323	206,748
	4	12.0	18/Nov/66	153,411		153,411	29/May/67	205,425	27,183	232,608
	5	3.0	14/Nov/66	99,000		99,000	30/Nov/66	199,233		199,233
Emulsion	6	5.0	14/Nov/66	99,000		99,000	30/Nov/66	199,233		199,233
Treated	7	7.0	24/Nov/66	175,581		175,581	19/May/67	205,425	25,431	230,856
	8	9.0	1/Dec/66	197,811		197,811	29/May/67	205,425	27,183	232,608
Special	9	2.0	10/Apr/67	*	2,874	208,299	10/Apr/67	205,425	3,471	208,896
Aggregate	10	3.5	25/Apr/67	*	5,895	211,320	4/May/67	205,425	16,026	221,451
Asphalt	11	5.0	26/Apr/67	*	10,614	216,039	29/May/67	205,425	27,183	232,608
Treated	12	6.5	22/May/67	*	25,779	231,204	*	*	*	*

*Section did not crack or fail in the time period indicated.

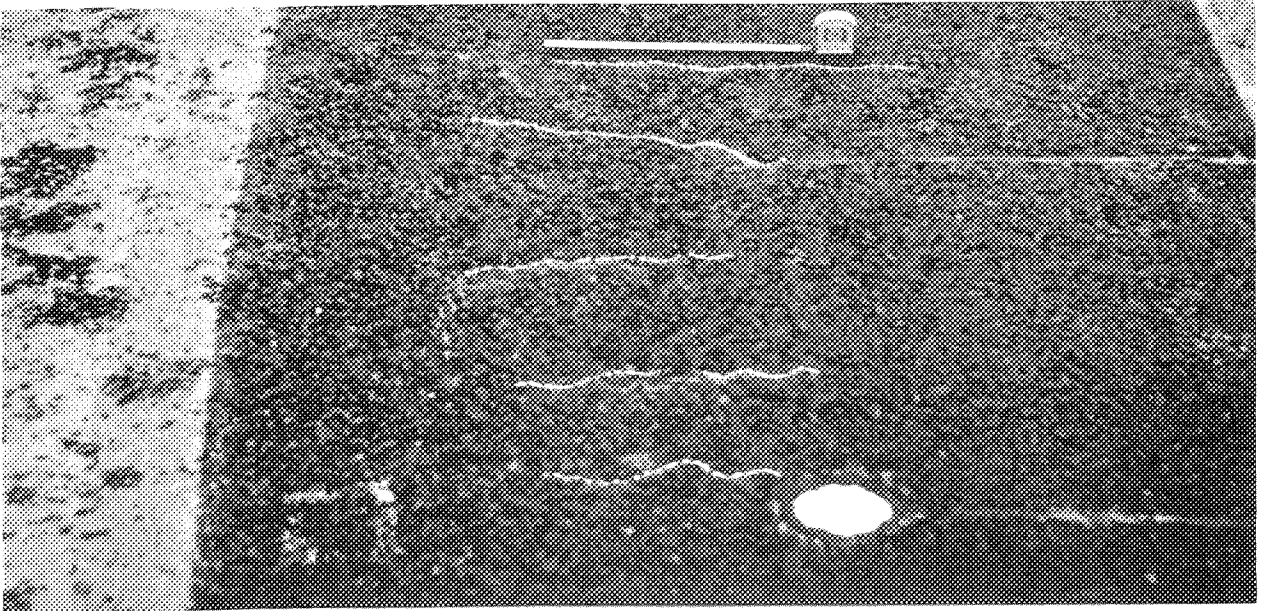


FIGURE 37.--THE APPEARANCE OF THE TRANSVERSE CRACKS AT 100,000 WHEEL LOADS IN 7.0 INCHES OF UNTREATED BASE, SECTION 2. THIS OCCURRED DURING THE FALL PERIOD.

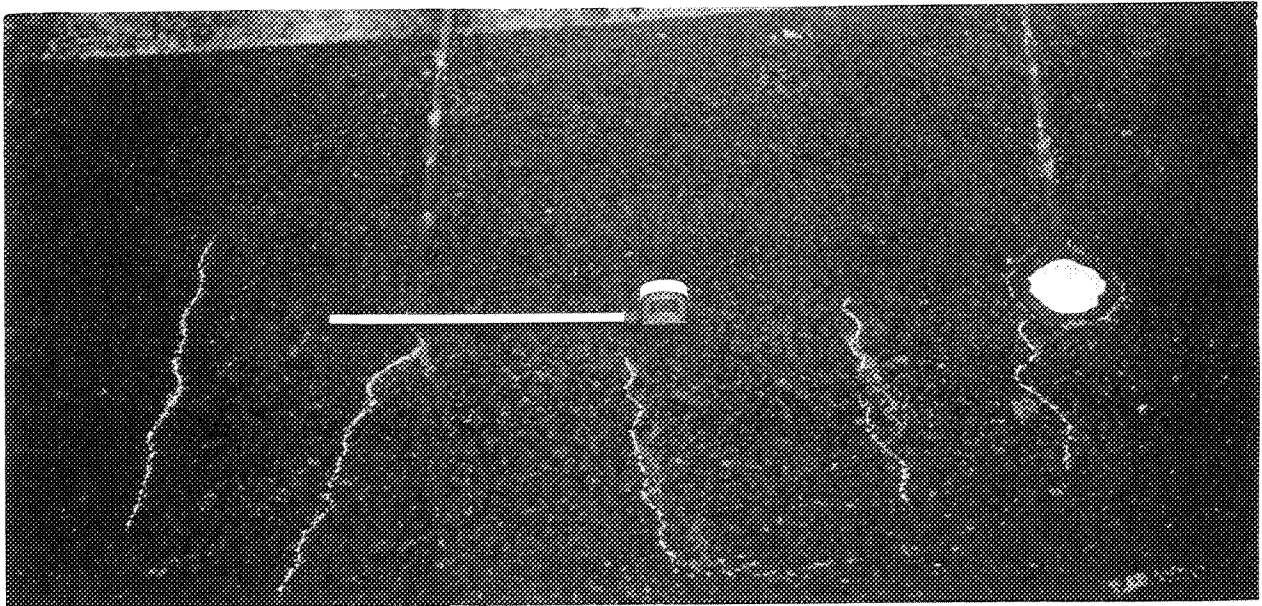


FIGURE 38.--ANOTHER VIEW OF THE TRANSVERSE CRACKING IN SECTION 2. NOTE THE PUMPING OF MUD THROUGH THE CRACKS. THIS IS STAGE 2.

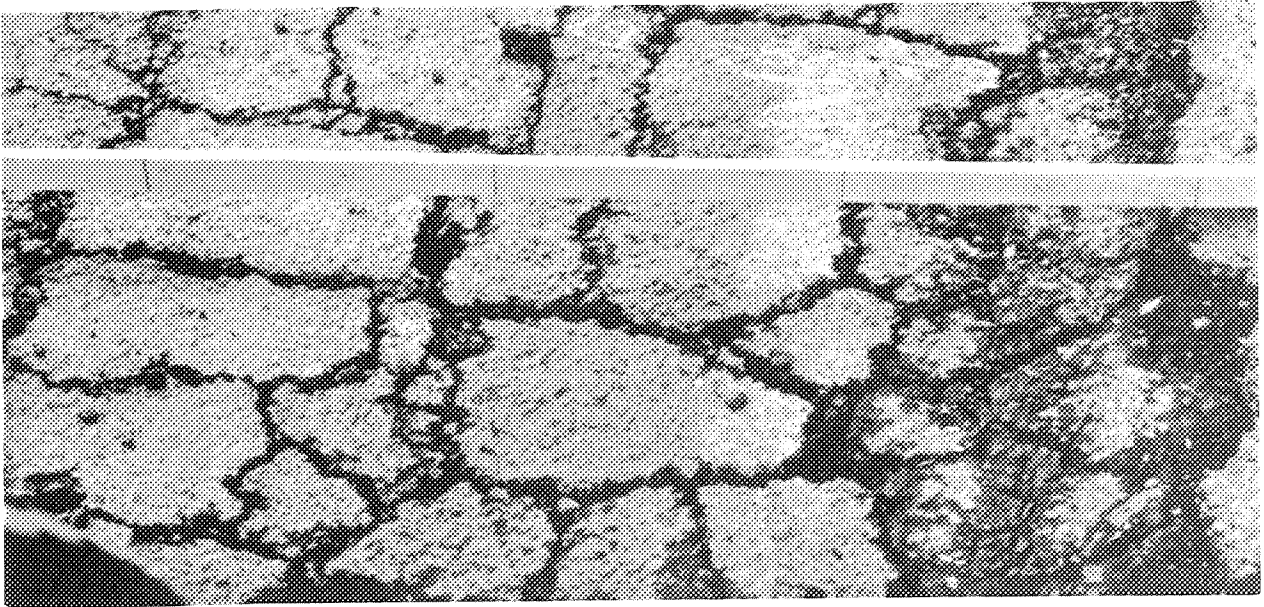


FIGURE 39.--THE APPEARANCE OF SECTION 2 AT ULTIMATE FAILURE JUST BEFORE BEING REMOVED FROM SERVICE AT 206,750 WHEEL LOADS. NOTE THE ALLIGATOR CRACKING PATTERN AND THE LONGITUDINAL CRACKING ALONG THE WHEEL PATH. THIS IS STAGE 7.

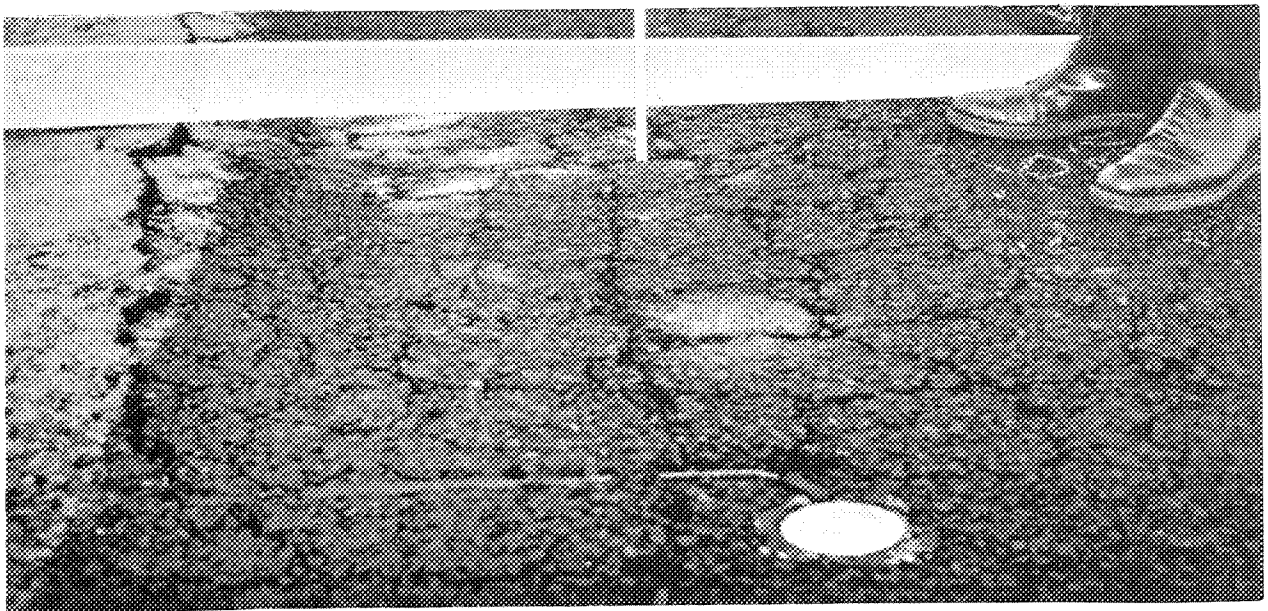


FIGURE 40.--SUBSIDENCE IN THE 5.0 INCHES OF EMULSION-TREATED BASE AFTER 133,700 WHEEL LOADS. NOTE THE ALLIGATOR CRACKING PATTERN AND THE LONGITUDINAL CRACKS IN THE CENTER AND IN WHEEL PATH. THIS IS STAGE 5.

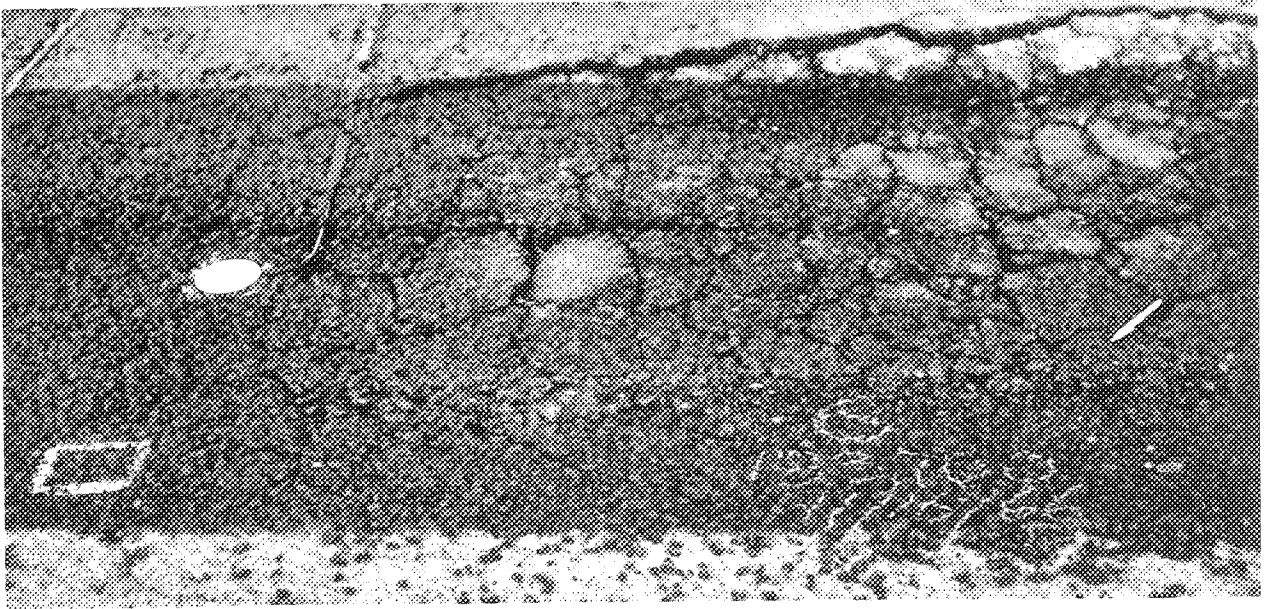


FIGURE 41.--ANOTHER VIEW OF SECTION 6 AT 133,700 WHEEL LOADS.

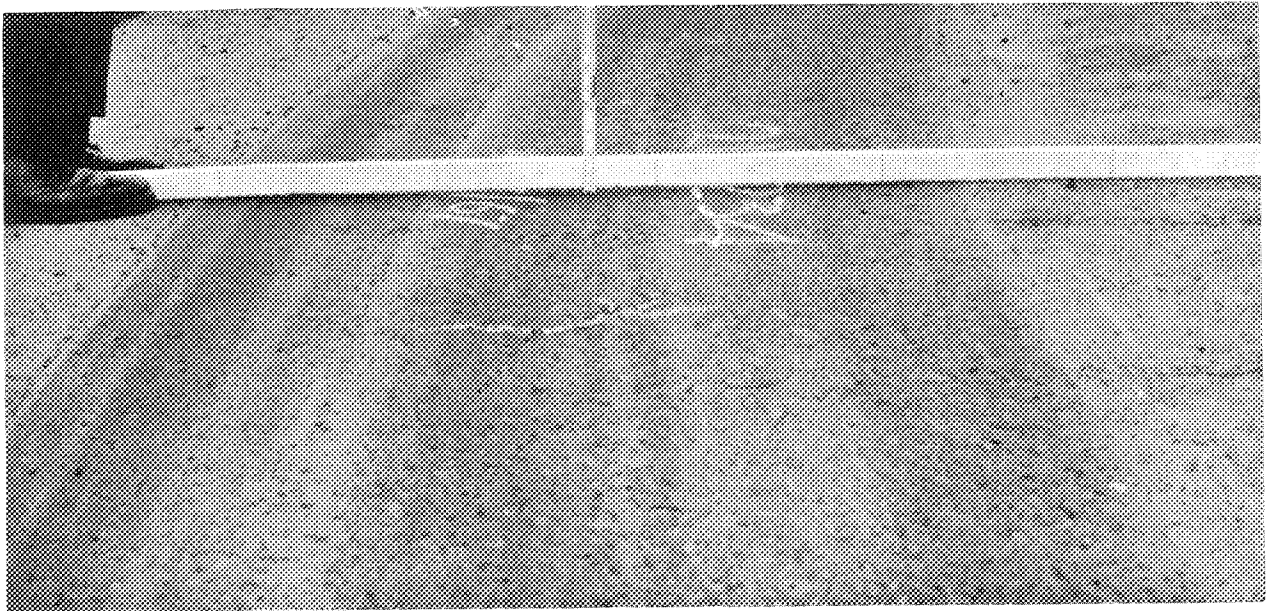


FIGURE 42.--THE DEVELOPMENT OF RUTS AND SOME TRANSVERSE CRACKS IN THE 3.5 INCHES OF SPECIAL ASPHALT-TREATED BASE, SECTION 10 AFTER 210,234 WHEEL LOADS. THIS WAS IN THE SPRING PERIOD.

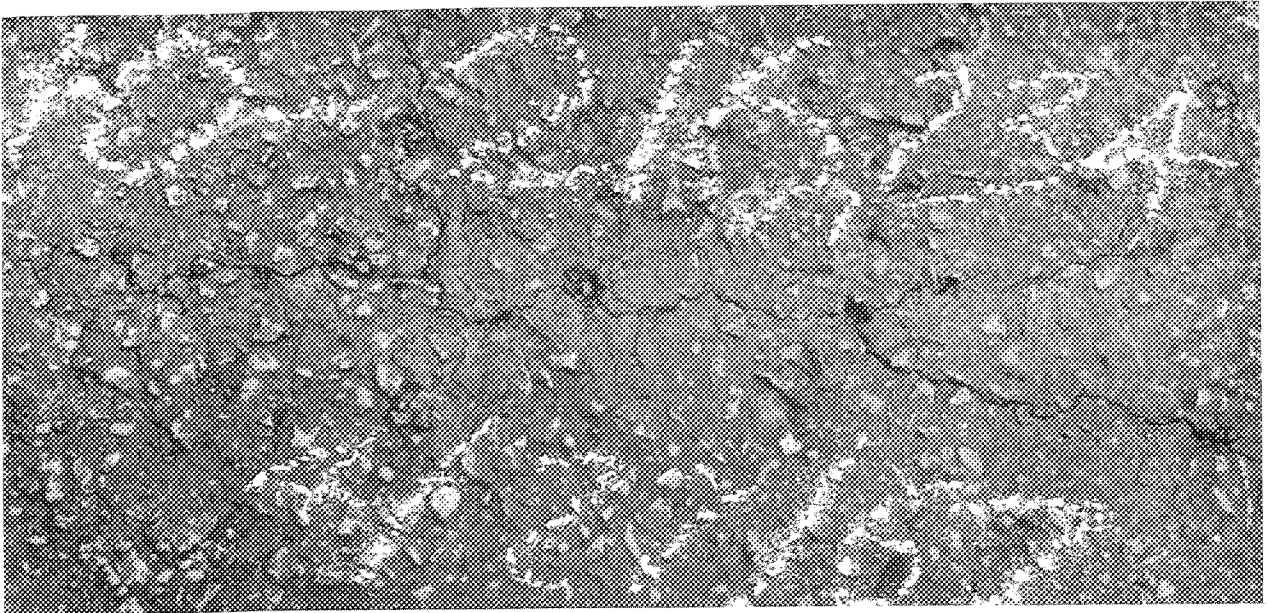


FIGURE 43.--FURTHER DEVELOPMENT OF TRANSVERSE CRACKS
IN SECTION 10 AT 216,234 WHEEL LOADS.

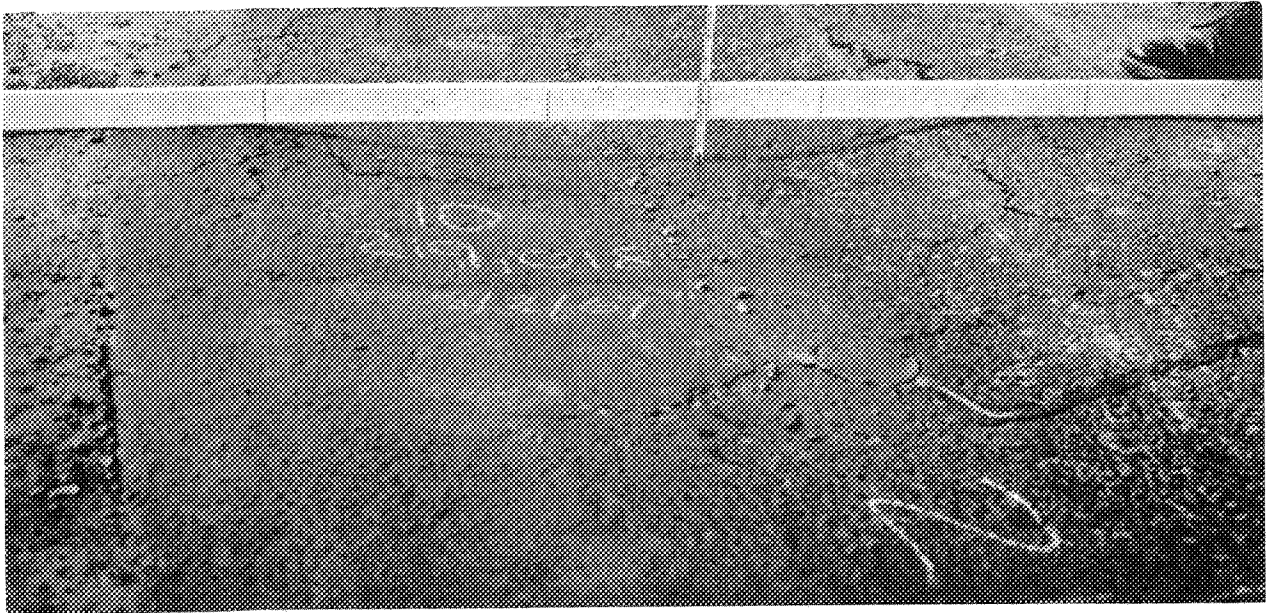


FIGURE 44.--CONTINUED DETERIORATION OF SECTION 10 AT
219,018 WHEEL LOADS. NOTE THE DEFORMATION AND LONGITUD-
INAL CRACKING.

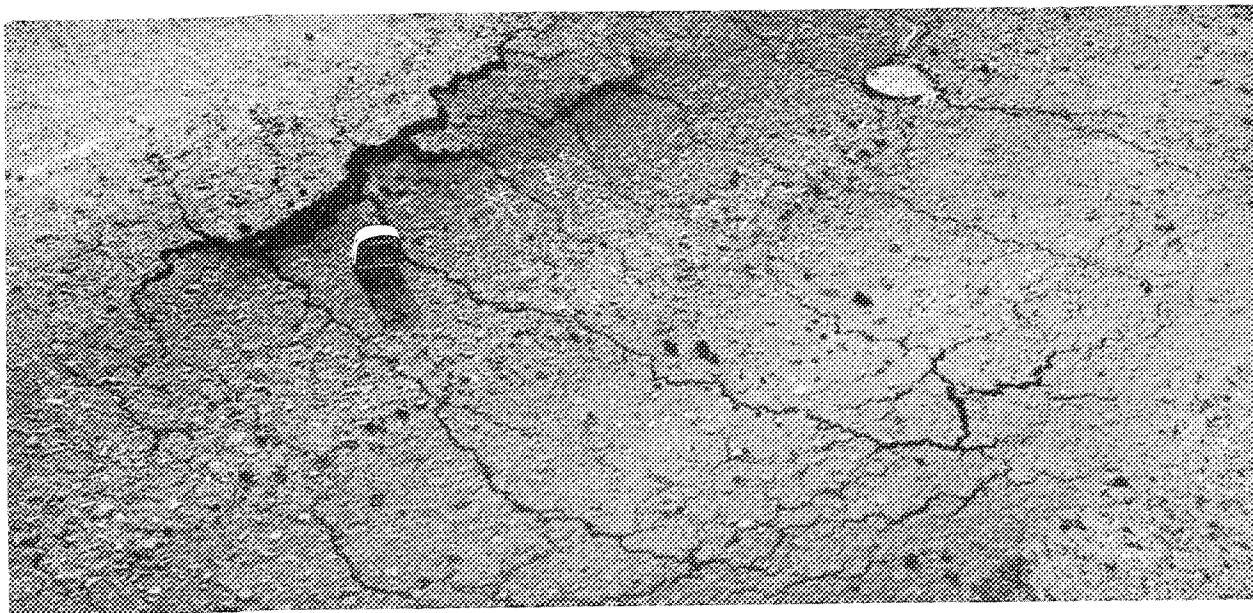


FIGURE 45.--THE APPEARANCE OF SECTION 10 AT ULTIMATE FAILURE AFTER 219,123 WHEEL LOADS.



FIGURE 46.--CONTINUED FAILURE AT 220,377 WHEEL LOADS OF SECTION 10 AFTER AN ASPHALT OVERLAY WAS PUT ON.



FIGURE 47.--OVERALL APPEARANCE OF SECTION 9 (2.0 INCHES OF SPECIAL AGGREGATE ASPHALT-TREATED BASE) AFTER 208,299 WHEEL LOADS.

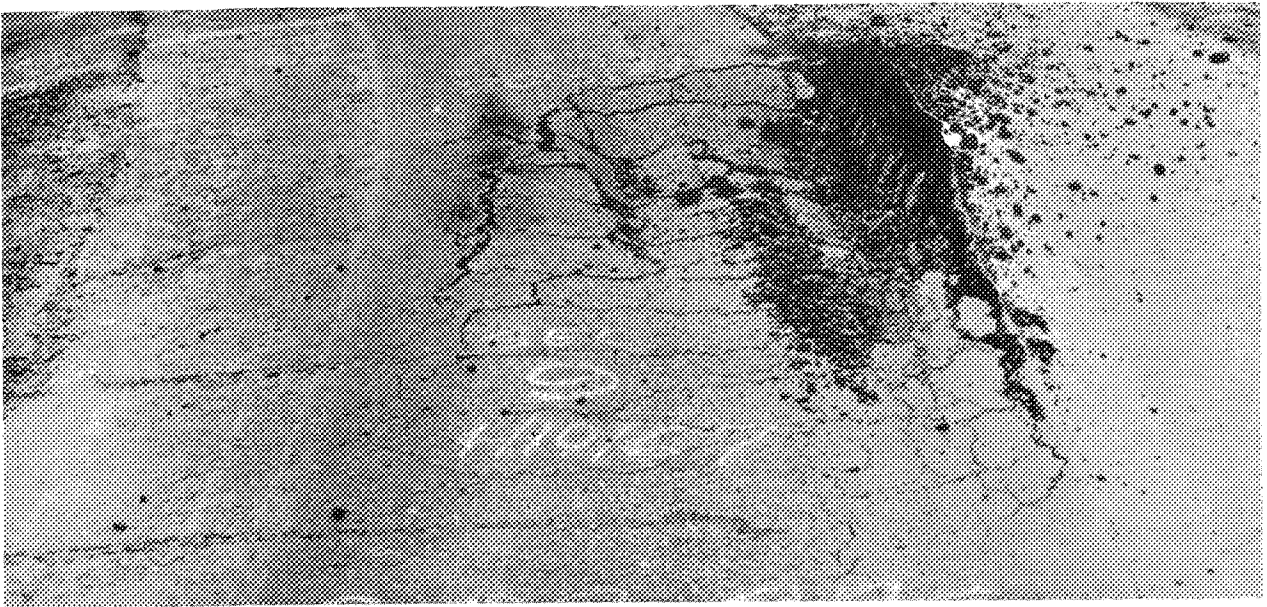


FIGURE 48.--SPECTACULAR FAILURE OF SECTION 9 AFTER 208,876 WHEEL LOADS. NOTE THE UPLIFT OF THE OUTSIDE UNTRAVELLED PART OF THE SECTION.



FIGURE 49.--THE START OF TRANSVERSE CRACKS IN SECTION 11
(5.0 INCHES OF A.T.B.) AT 231,691 WHEEL LOADS.

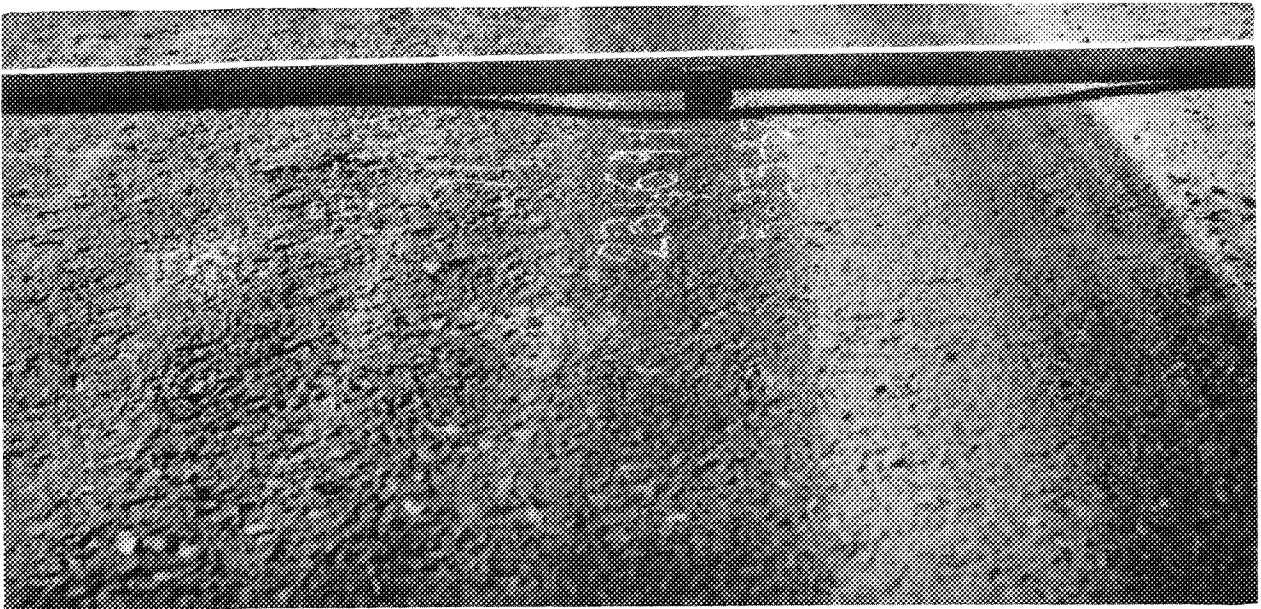


FIGURE 50.--THE PERMANENT DEFORMATION IN SECTION 11
AFTER 231,691 WHEEL LOADS.



FIGURE 51.--ULTIMATE FAILURE OF SECTION 11 AFTER 232,608 WHEEL LOADS. NOTE THE LONGITUDINAL SHEAR FAILURES AND DEPTH OF DEFORMATION.



FIGURE 52.--APPEARANCE OF SECTION 4 (12 INCHES OF UNTREATED BASE) AFTER 232,608 WHEEL LOADS.

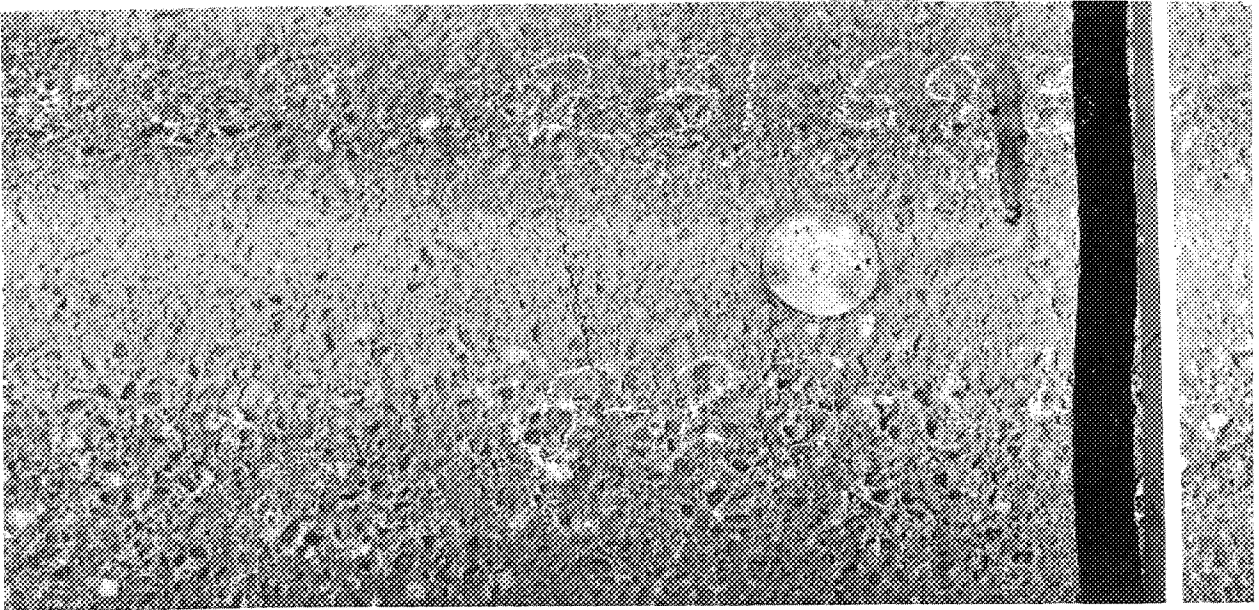


FIGURE 53a--THE APPEARANCE OF SECTION 8 (9.0 INCHES OF E.T.B.) AFTER 231,693 WHEEL LOADS.

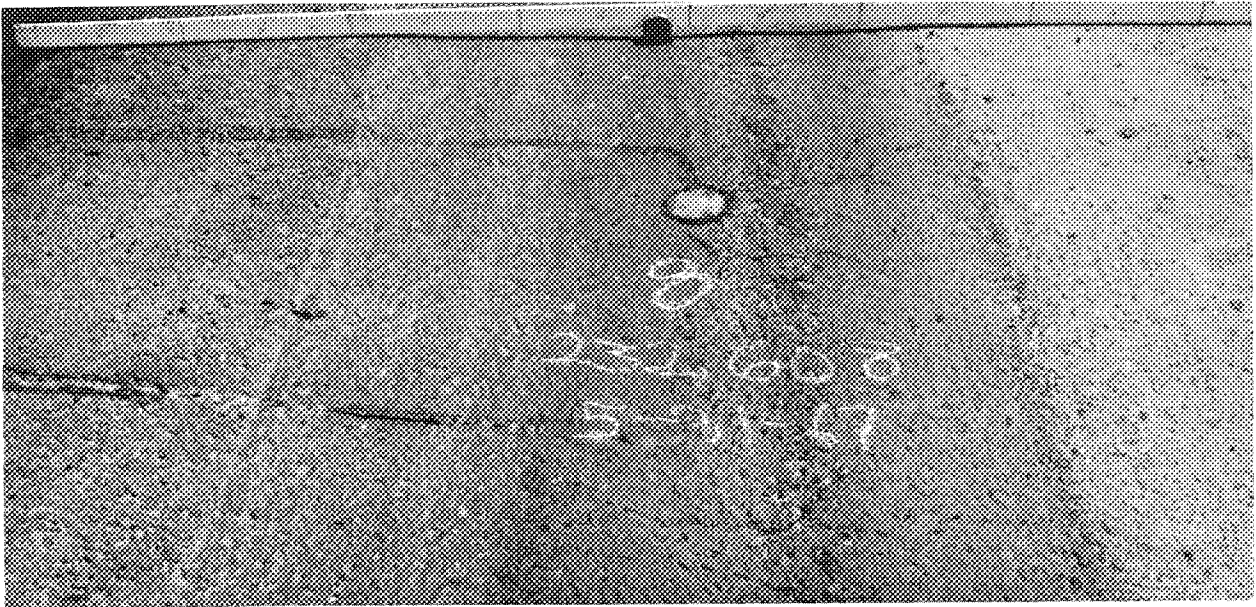


FIGURE 53b--A VIEW OF SECTION 8 SHOWING THE PERMANENT DEFORMATION AND CRACKING AT COMPLETION OF TESTING AT 232,608 WHEEL LOADS.

ment deflections were evident and large with pronounced rutting just before the appearance of cracking.

The difference in modes of failure is probably due to the difference in environmental conditions. A possibility exists that differential recompaction of the saturated subgrade from the traversed part of the pavement to the non-traversed part may have occurred. This differential recompaction could have caused localized stresses at the edge of the wheel track thereby bringing about a punching shear situation. The fact that the special asphalt-treated base is semi-rigid also may have changed the rate of failure. The untreated and emulsion-treated bases seem to be more resilient and their structure enables the base to follow the compaction and contours of the subgrade.

Some interesting figures can be obtained when the wheel load applications at "ultimate" failure are subtracted from wheel load applications at initial cracking (Table XIV). The table shows that for some sections almost as many wheel applications were needed to obtain "ultimate" failure as to cause initial cracking. The table also shows that the more rigid pavement sections (9-12) did not have large pavement failure spans. A pavement failure span (PFS) rating in percentage was developed. The difference in wheel loads at failure and initial cracking divided by the wheel loads at initial cracking and multiplied by 100 gives the Pavement Failure Span. This PFS can be used for maintenance as this figure shows the relative number of wheel loads to failure once initial distress appears. The numbers shown in Table XIV are only valid for this experiment and the conditions of this test and are subject to modification once the series of tests is completed.

The information in Table XIV is plotted in Fig. 54 to see if there are any trends. No trends seem to be evident when the wheel load applications at initial cracking are plotted against base thickness. However, when wheel load

TABLE XIV: PAVEMENT FAILURE SPAN (PFS)²

Base Type	Section	Base Thickness Inches	Wheel Load Applications			PFS	Time Period
			Initial Cracks WL _I	At Failure WL _F	Initial To Failure WL _F -WL _I		
Crushed Stone Untreated	1	4.5	157,203	210,270	53,067	33.8	Fall
	2	7.0	99,000	205,425	106,425	107.8	Fall
	3	9.5	100,000	206,748	106,748	106.7 ¹	Fall
	4	12.0	153,411	232,608	79,197	51.6 ¹	Spring
Emulsion-Treated	5	3.0	99,000	199,233	100,233	101.2	Fall
	6	5.0	99,000	199,233	100,233	101.2	Fall
	7	7.0	175,581	230,856	55,275	31.5	Spring
	8	9.0	197,811	232,608	34,797	17.6 ¹	Spring
Special Aggregate Asphalt-Treated	9	2.0	208,299	208,896	597	0.3	Spring
	10	3.5	211,320	221,451	10,131	4.8	Spring
	11	5.0	216,039	232,608	16,569	7.7	Spring
	12	6.5	231,204	--	--	--	Spring

¹ May be low as these sections were in better condition than section 11.

² P.F.S. = $\frac{\text{Wheel Load Applications (Failure-Initial)}}{\text{Wheel Load Applications to 1st Sign of Cracking}}$

$$= \frac{WL_F - WL_I}{WL_I} \times 100$$

FIGURE 54.--WHEEL LOAD APPLICATIONS (INITIAL & FINAL)
AS A FUNCTION OF BASE THICKNESS

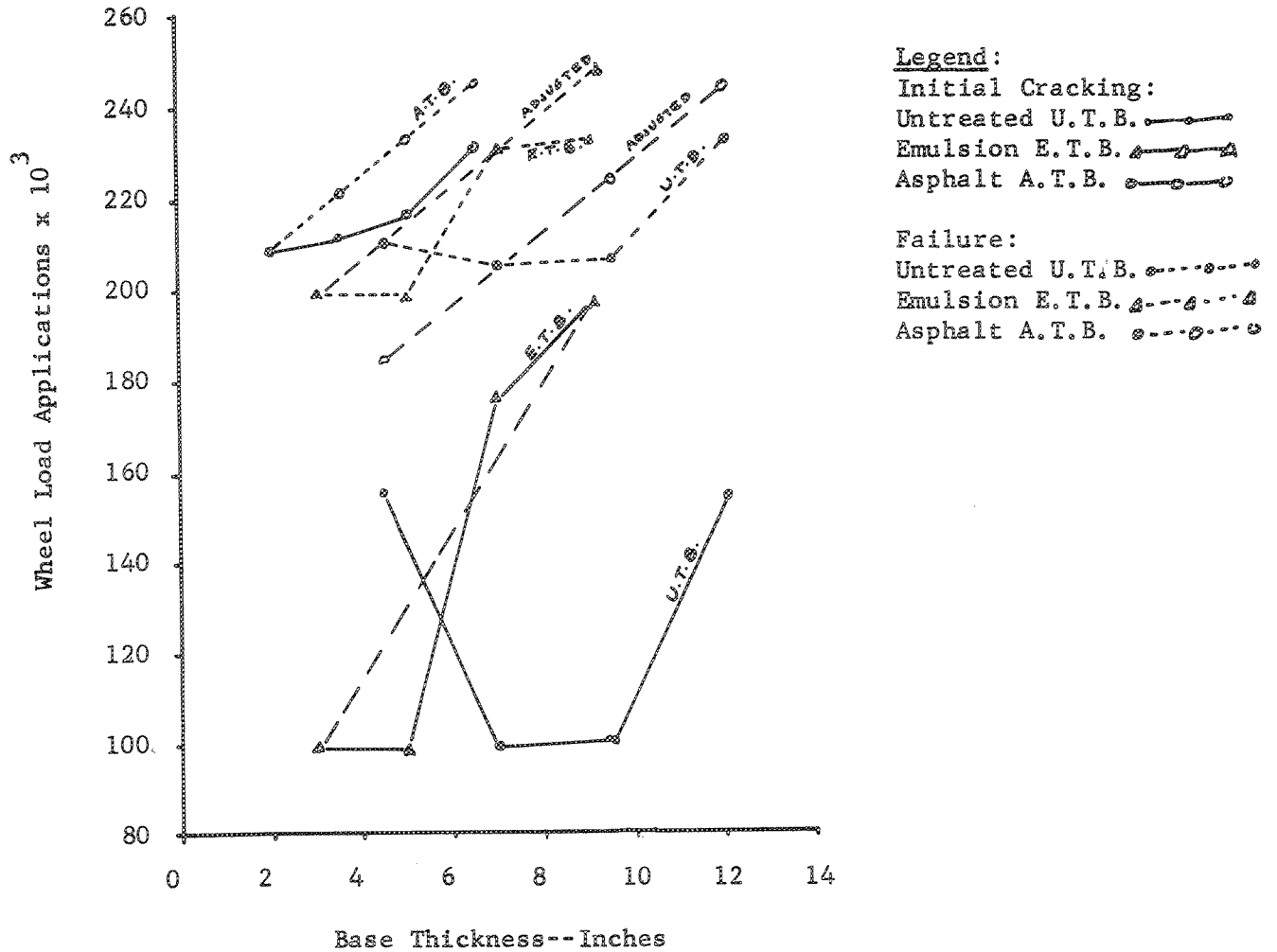


TABLE XV.--EQUIVALENT THICKNESSES
(3.0" of Class "B" A.C. Wearing Course)

Base Type	Fall '66 Period ¹	Spring '67 Period ²	Adjusted ³
Crushed Stone Untreated	9.5 in.	12.0 in.	12.0 in.
Emulsion-Treated Crushed Stone	7.0 in.	9.0 in.	9.0 in.
Special Aggregate Asphalt-Treated	2.0 in.	5.0 in.	6.5 in.

1. The thinnest sections which survived during this period.
2. Thickest sections which failed during this time.
3. Adjusted in the sense that both the untreated and emulsion treated sections were in better condition than A.T.B. one.

applications at "ultimate" failure are plotted against base thickness, some trends are evident. For the special asphalt-treated base the trend is a straight line. However, the line is not as evident for the emulsion-treated base. It is even less evident for the untreated base, but if some adjustments are made, a series of parallel lines can be obtained. These manipulations can be made on the assumptions that "ultimate" failure was not reached for sections 3, 4 and 8. A comparison of Figures 51 (section 11), 52 (section 4) and 53b (section 8) shows that section 11 was in worse condition than sections 4 and 8. If another upward change is made for section 6 and a downward change made for section 1, a series of parallel lines can be drawn (as shown in Fig. 54). These lines will give adjusted equivalencies between the different bases at "ultimate" failures.

The equivalency thickness is shown on Table XV. The equivalencies obtained for the fall period of 1966 are based on the thinnest surviving sections. The 1968 spring equivalencies are based on the thickest sections that failed during this period. The adjusted equivalencies based on "ultimate" failure are also shown. An interesting factor of the adjusted lines is that the thickest sections all fail at the same wheel loads. The adjusted equivalencies are valid if the assumptions are made that (1) the relationship of wheel load applications to base thickness is linear and has the same slope for the three base types tested, and (2) that improvements in performance with increasing thickness of base is the same regardless of base type. If there is no justification for these assumptions, then one must be content with the equivalencies derived from test track testing. It should be mentioned and emphasized that these equivalencies are tentative and are valid only to the testing conditions and are subject to modification upon the completion of the other test rings.

Load Response Characteristics

Temperature Variables

During the 1966 fall period, air, pavement, and soil temperatures were fairly constant until November 20 when the temperatures started to fall and the rain stopped (see Figures 55 to 57). The pavement temperatures seemed to vary as a direct result of varying air temperatures and solar radiation. The 1966 testing period can be divided into two periods--early and late fall, that is prior to and after November 12, when heavy rains began. Any changes in instrument reading results may be attributed to the break in temperatures and the steady rainfall.

During the 1967 spring period, air, pavement, and soil temperatures in April and the early part of May were fairly constant. The temperatures did not start to rise until May 13 (see Figures 58 to 61). High summer temperatures continued up to the end of testing. Temperatures do not seem to be significant variables during the spring period except for a brief period the latter part of May, which may have partly caused high Benkelman beam readings.

Moisture Contents

Moisture contents were measured by moisture tensiometer methods and by regular sampling methods. Samples of bases and subgrade were taken for the measurement of moisture contents after the existing section was removed.

Table XVI shows the range of moisture contents which can be found in the Palouse silt subgrade and untreated bases before the start of testing. The average moisture content after saturation of the Palouse silt in Ring 1 was found to be 21.5%. The moisture contents of the subgrade in Ring 2 were on the dry side. Samples taken from drill borings for the LVDT gages indicated that the top of subgrade was drier than the bottom which rests on basalt bedrock. This acts as a natural drainage floor (11).

FIGURE 55.---
RING #2.

AIR, PAVEMENT, AND SOIL

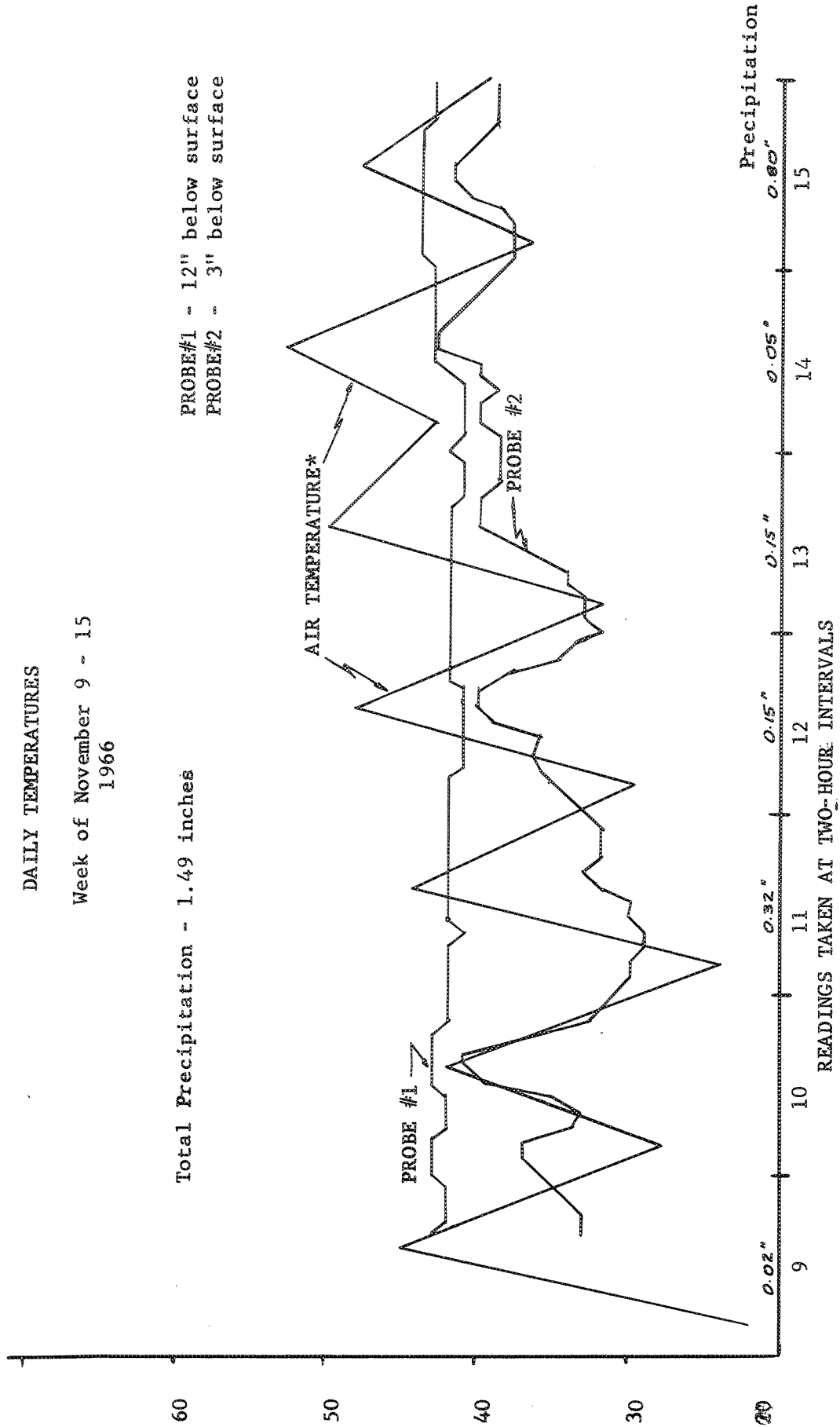
DAILY TEMPERATURES

Week of November 9 - 15
1966

Total Precipitation - 1.49 inches

PROBE #1 - 12" below surface
PROBE #2 - 3" below surface

TEMPERATURE IN DEGREES FAHRENHEIT



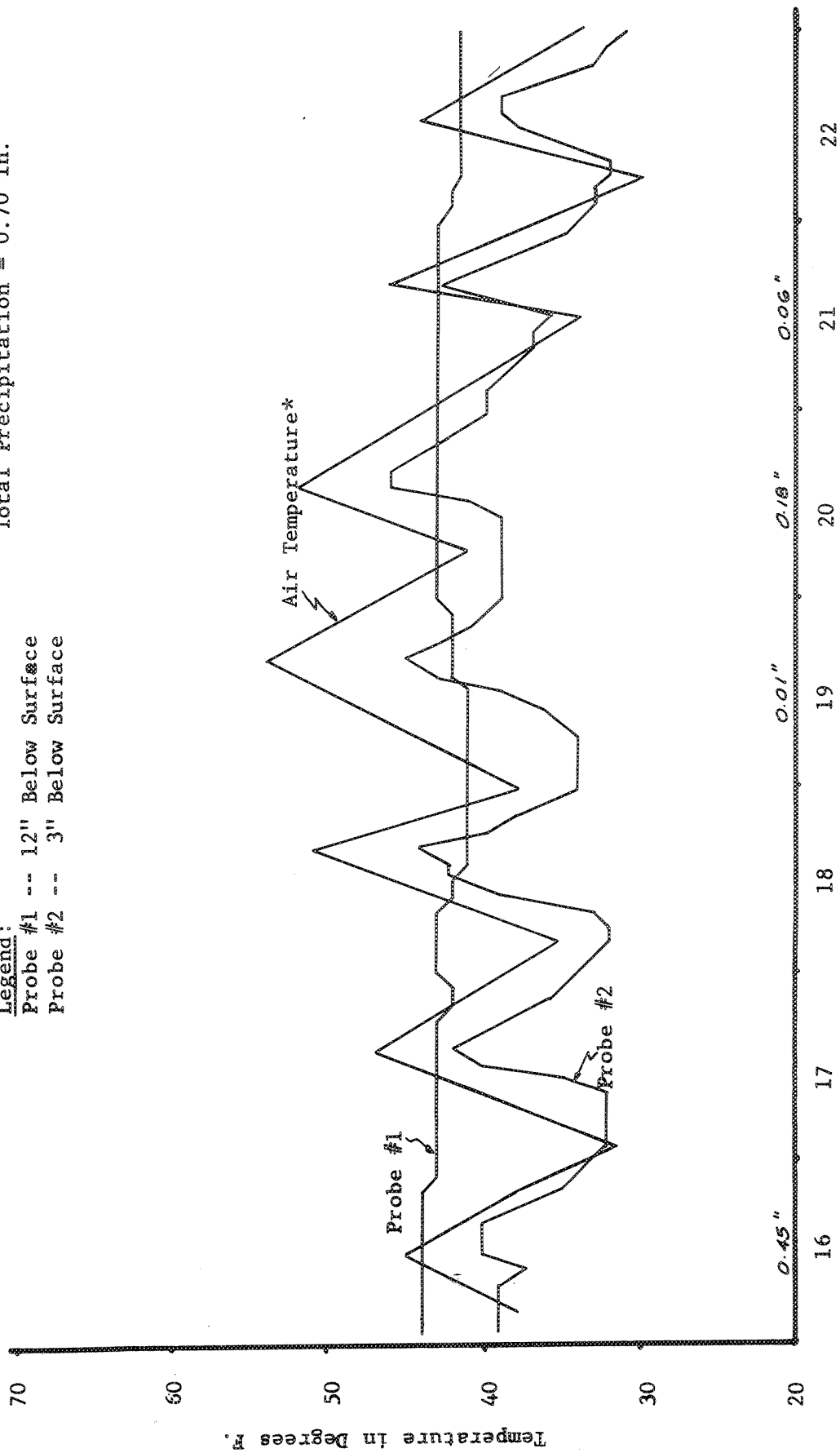
*Climatological Data, U.S. Dept. of Commerce, Environmental Science Service Administration

FIGURE 56.--AIR, PAVEMENT, AND SOIL DAILY TEMPERATURES
Week of November 16-22, 1966

Total Precipitation = 0.70 in.

Legend:

- Probe #1 -- 12" Below Surface
- Probe #2 -- 3" Below Surface



Readings Taken at 2-Hour Intervals

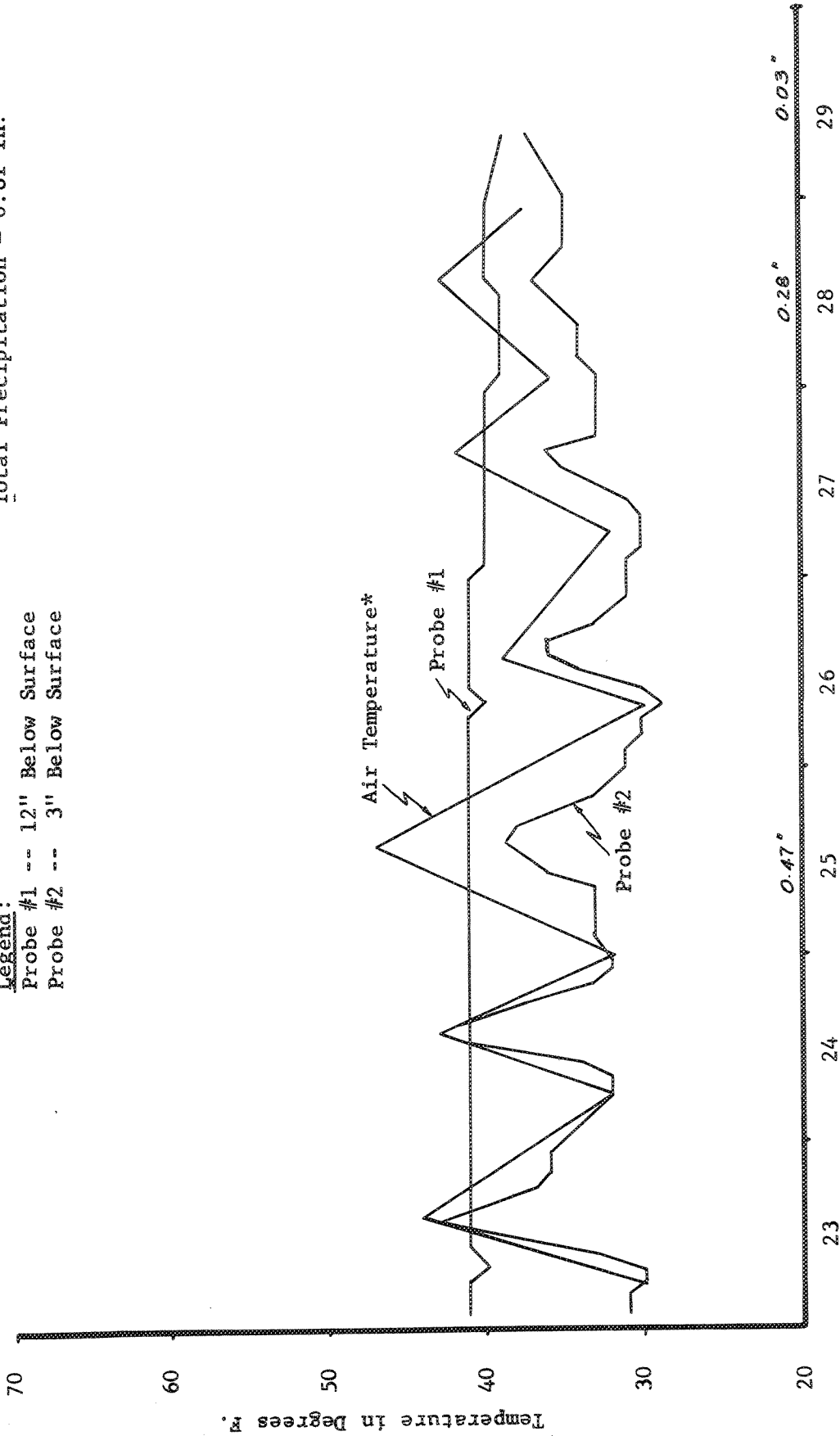
*Climatological Data, U.S. Dept. of Commerce, Environmental Science Service Administration

FIGURE 57.--AIR, PAVEMENT, AND SOIL DAILY TEMPERATURE
Week of November 23-29, 1966

Total Precipitation = 0.81 in.

Legend:

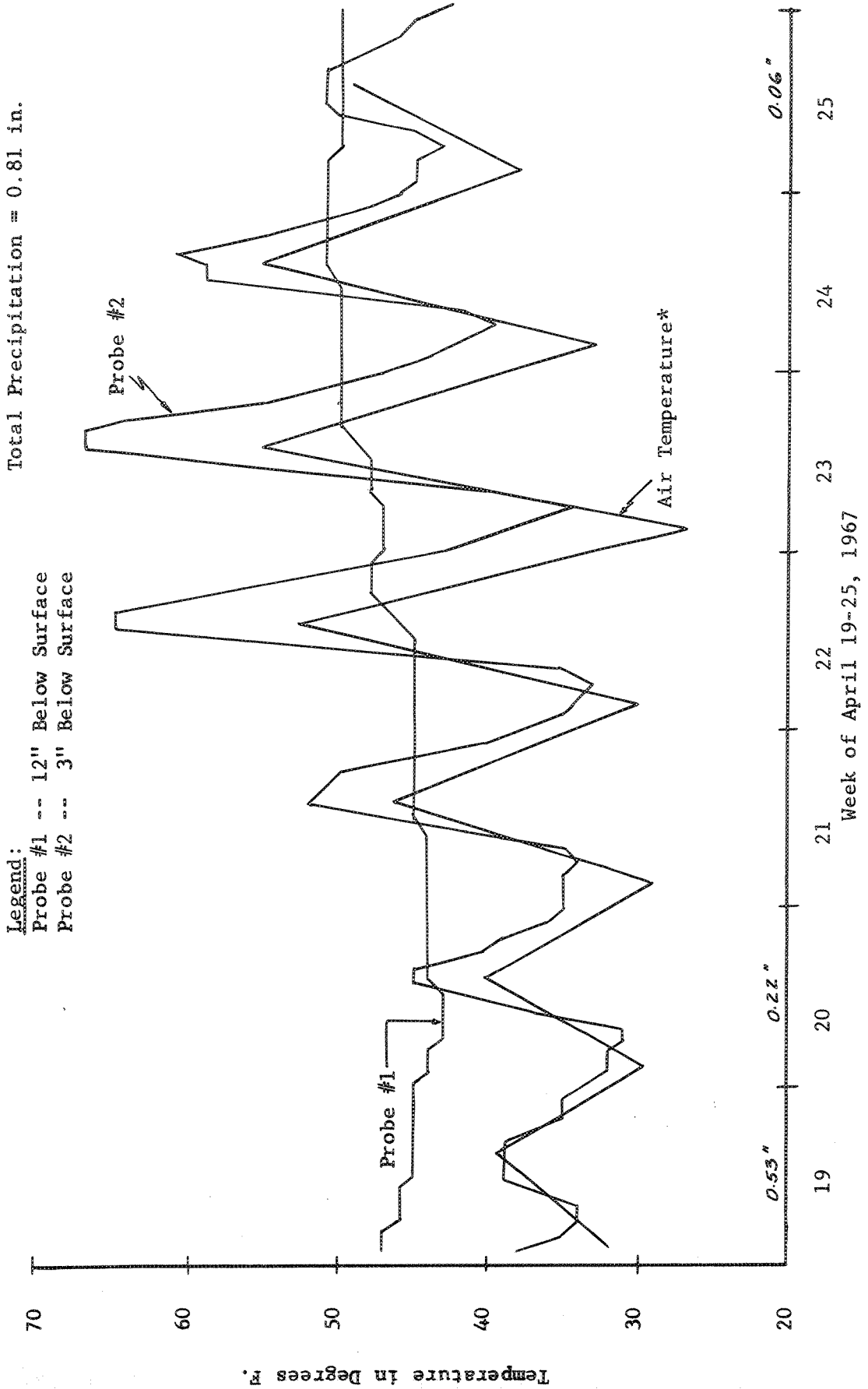
- Probe #1 -- 12" Below Surface
- Probe #2 -- 3" Below Surface



Readings Taken at 2-Hour Intervals

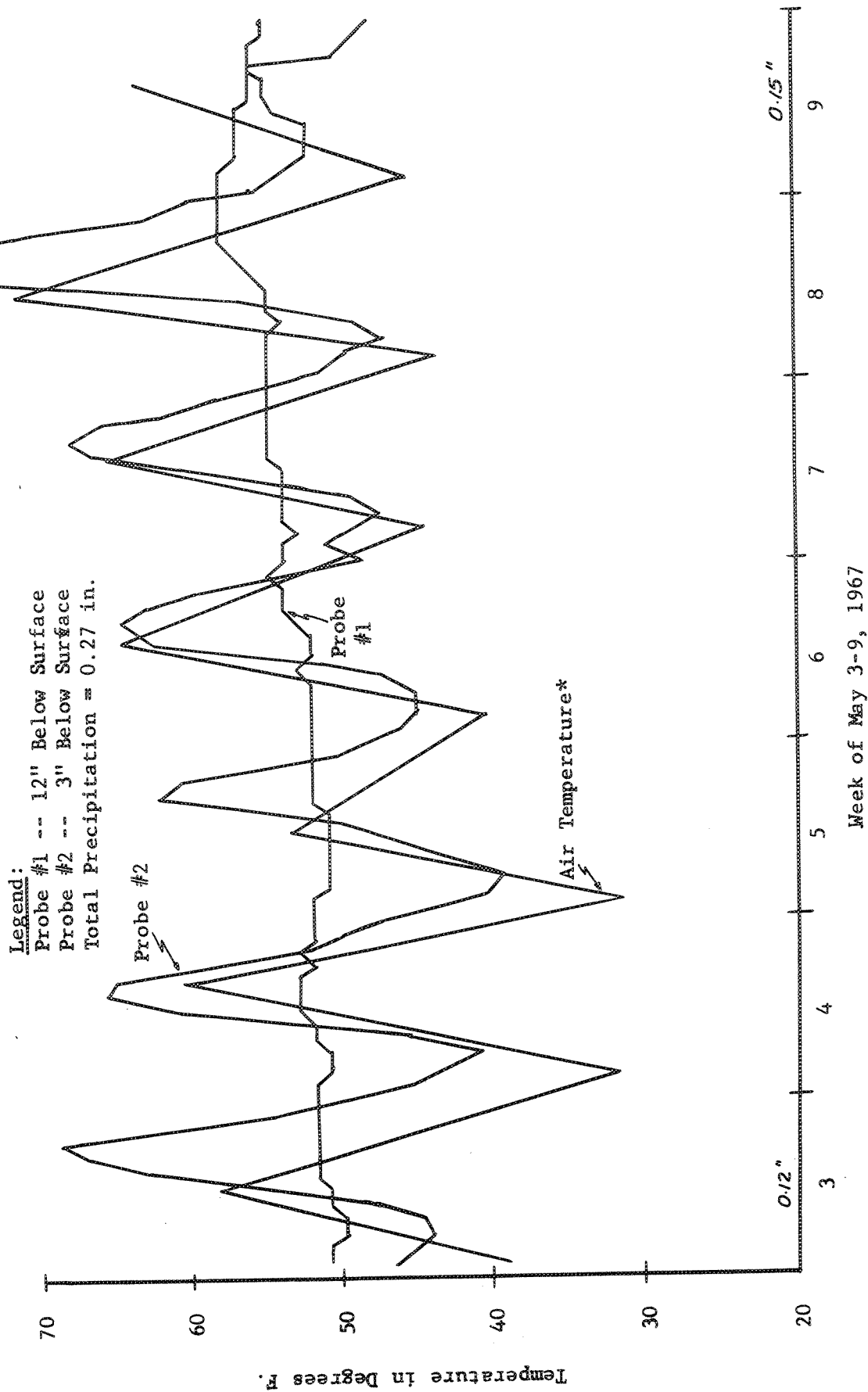
*Climatological Data, U.S. Dept. of Commerce, Environmental Science Service Administration

FIGURE 58. --AIR, PAVEMENT, AND SOIL DAILY TEMPERATURES
Week of April 19-25, 1967



*Climatological Data, U.S. Dept. of Commerce, Environmental Science Service Administration

FIGURE 59.--AIR, PAVEMENT, AND SOIL DAILY TEMPERATURES
Week of May 3-9, 1967



*Climatological Data, U.S. Dept. of Commerce, Environmental Science Service Administration

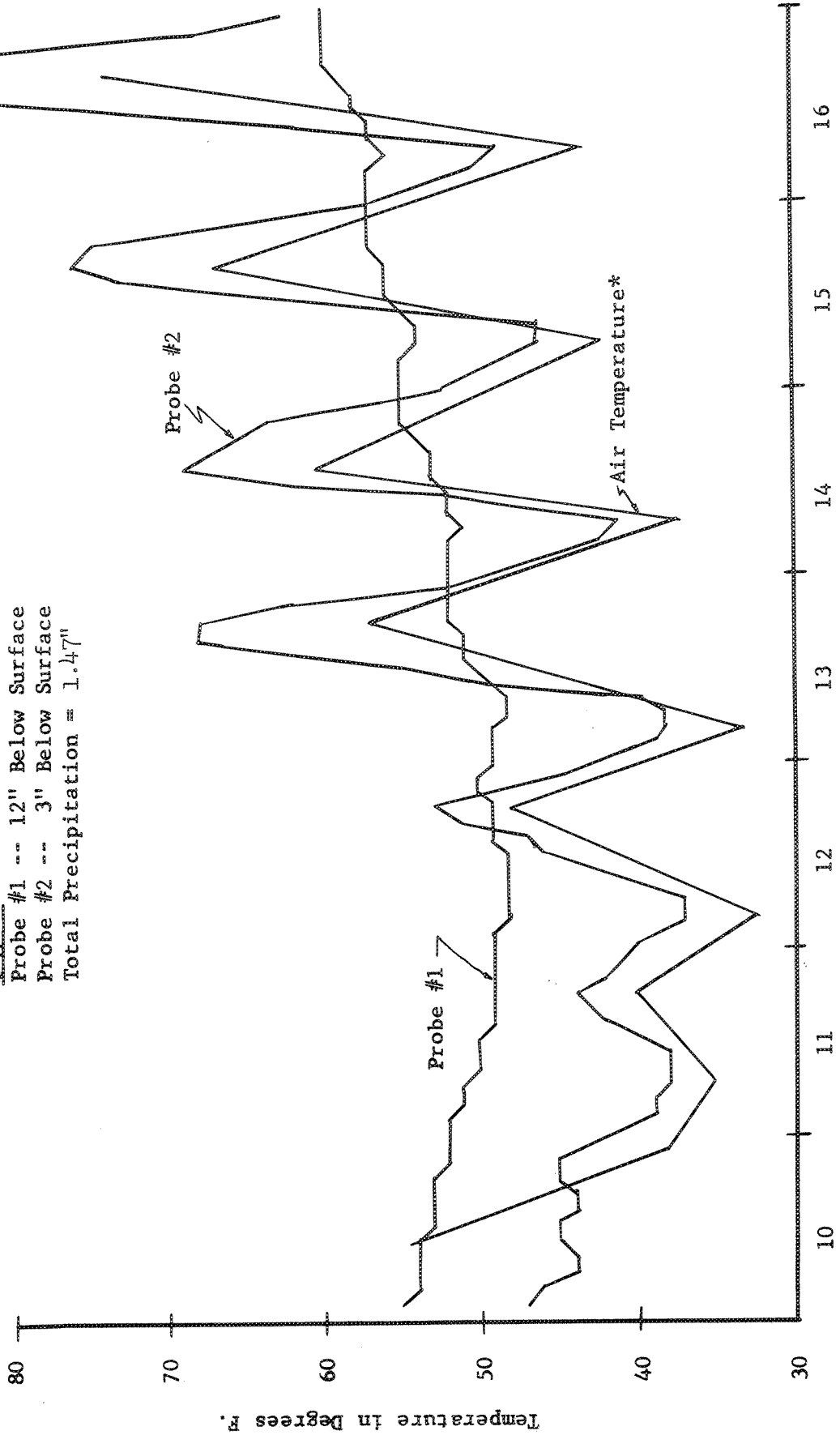
FIGURE 60. --AIR, PAVEMENT, AND SOIL DAILY TEMPERATURES
Week of May 10-16, 1967

Legend:

Probe #1 -- 12" Below Surface

Probe #2 -- 3" Below Surface

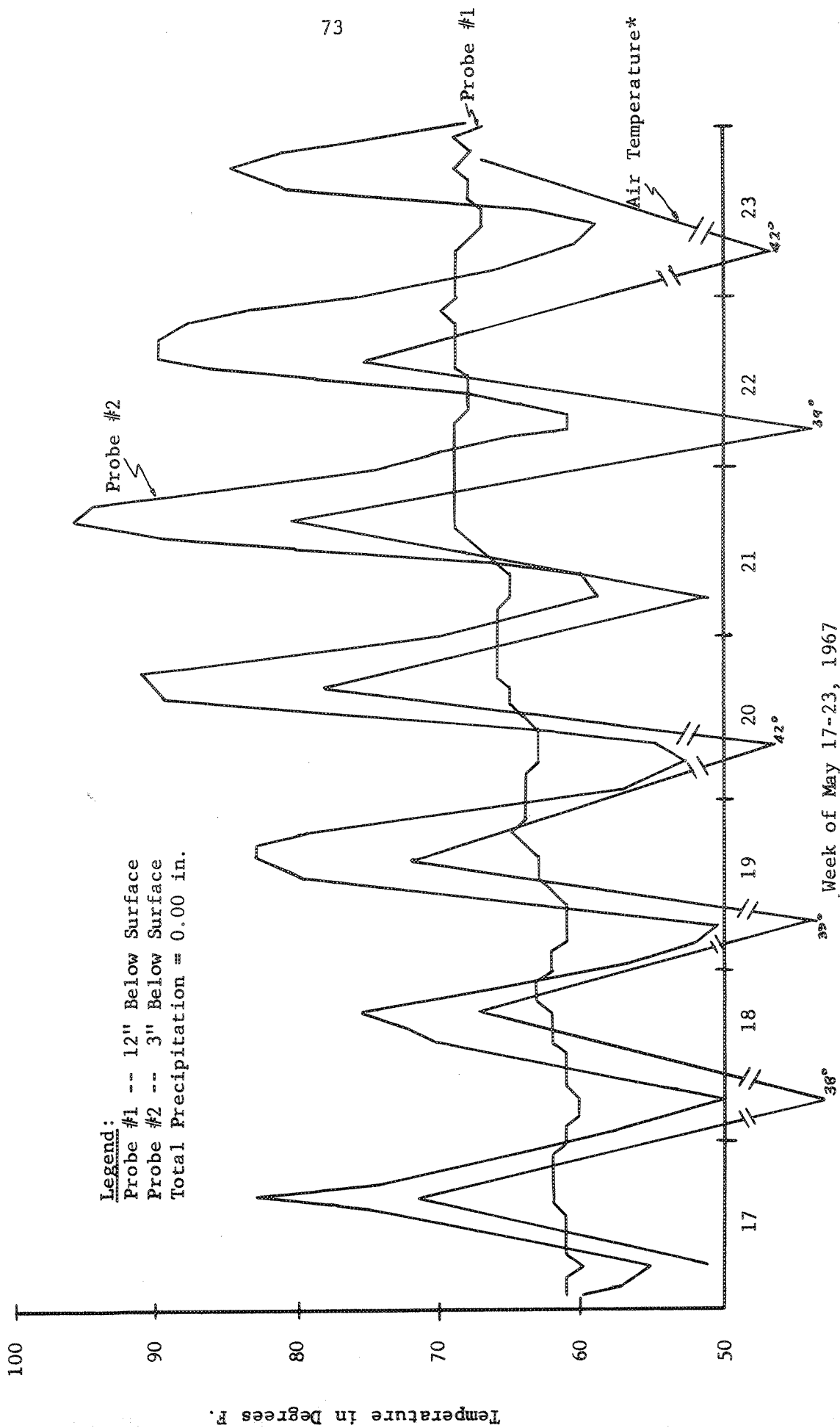
Total Precipitation = 1.47"



Week of May 10-16, 1968

*Climatological Data, U.S. Dept. of Commerce, Environmental Science Service Administration

FIGURE 61. --AIR, PAVEMENT, AND SOIL DAILY TEMPERATURES
Week of May 17-23, 1967



*Climatological Data, U.S. Dept. of Commerce, Environmental Science Service Administration

Nuclear methods indicated that moisture contents in the untreated crushed surfacing top course base (shown in Table XVI) ranged from 6.9% to 7.8% with an average of 7.4%. The moisture content of the sample was 9.4%, which is high and may have been due to the fact that the sample contained more fines (Table XVI). The untreated base was wet when it was laid and had to be dried.

Moisture tensiometers, despite operating problems, indicated some interesting moisture contents (Fig. 63). All tensiometers indicated that the contents were high at the start of testing and that the moisture contents started to drop except for probes #2, 8, and 10 in sections 2 and 6, respectively. These probes indicated that moisture contents started to rise after the heavy rains and after transverse cracks appeared--an indication that rainfall seeped through these cracks and saturated the top of subgrade. This is further verified by the results shown in Fig. 62 which were obtained by digging a deep trench in sections 5 and 6 and checking moisture contents and densities. Figure 62 shows the moisture content appears to decrease with depth. The moisture content appears to increase at the 1- to 2-foot depth then decreases.

The other tensiometer probes showed that moisture contents remained fairly constant then started to rise at the end of January--the beginning of the wet season. All moisture probes showed that the subgrade was above optimum moisture content (18-19%) throughout the testing period. An examination of the subgrade moistures after the tests were completed (Table XVIII) show that moistures were above optimum and varied in different sections. This was borne out by the moisture probes. Figures 64 and 65 show the appearance of the subgrade after testing was completed.

Samples taken from the various bases indicate that moisture contents were high (see Table XVII). The high moisture content of the untreated crushed surfacing top course base may have been a partial cause of subgrade saturation. The emulsion-treated base moisture content was high which might be due

TABLE XVI
MOISTURE CONTENTS IN UNTREATED MATERIALS (11)

Material	Ring No. 2		LVDT Holes		Ring No. 1	
	High	Low	High	Low	High	Low
Subgrade Palouse Silt	14.4	11.6	23.6 ^a	16.0 ^b	24.4	17.9
Untreated Base C.S.T.C	9.4 ^c	7.4 ^d	6.9 ^e	7.8 ^e	6.4	3.6

- a. Taken from the bottom of deep holes - 14 to 16 feet, sections 2 & 10.
- b. Taken 2 feet below the surface of deep hole, sections 2 & 10.
- c. Obtained from a sample taken from C.S.T.C. Base Course after it was laid down.
- d. Average moisture content obtained by nuclear method.
- e. Range of moisture contents obtained by nuclear methods.

TABLE XVII
MOISTURE CONTENTS IN BASES^a

Base Type	Sections	Moisture Content
Untreated C.S.T.C.	1 - 4	7.76
Emulsion-Treated C.S.T.C.	5 - 8	8.48 ^b
Special Aggregate Asphalt-Treated	9 - 12	1 - 2 ^c

- a. Obtained at completion of tests.
- b. From section 5 (3.0 inches of ETB). In section 6, on Nov. 22, average water content was 8.38%; and on Nov 29, ranged from 10.64 to 8.34 % . Probable residual moisture content was about 3 - 4%.
- c. Estimated.

TABLE XVIII
 SUBGRADE MOISTURES AT TEST COMPLETION^a
 RING TWO

Section	Base Type	Average Moisture Content - %	Remarks
1	UTB	20.2	
2	UTB	23.2	
3	UTB	20.0	
4	UTB	20.4	
5	ETB	22.4 ^b 38.36	Just below base (Approx. 1" thick)
6	ETB	19.9 ^b	
9	ETB	21.2	
10	ATB	23.8	
11	ATB	23.5	
12	ATB	22.4	
Average		22.14	

a. Obtained June 16, 1967

b. Obtained December 5, 1966 after these sections were removed.

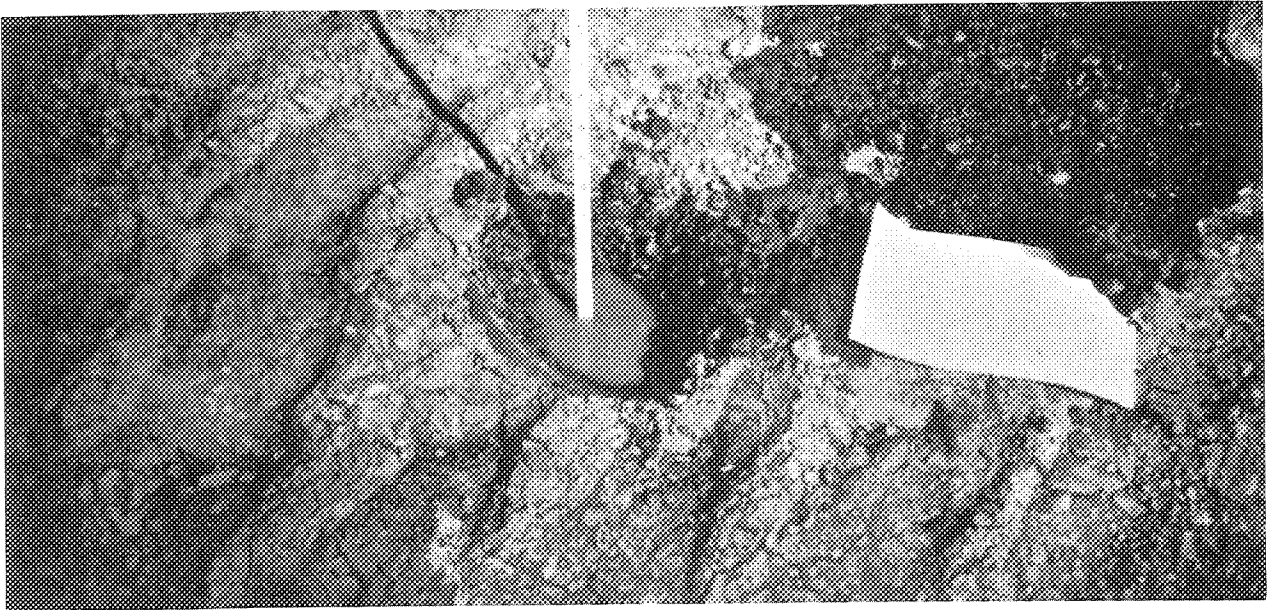


FIGURE 64.--A VIEW OF THE SUBGRADE IN SECTION 1
AFTER THE PAVEMENT WAS REMOVED.

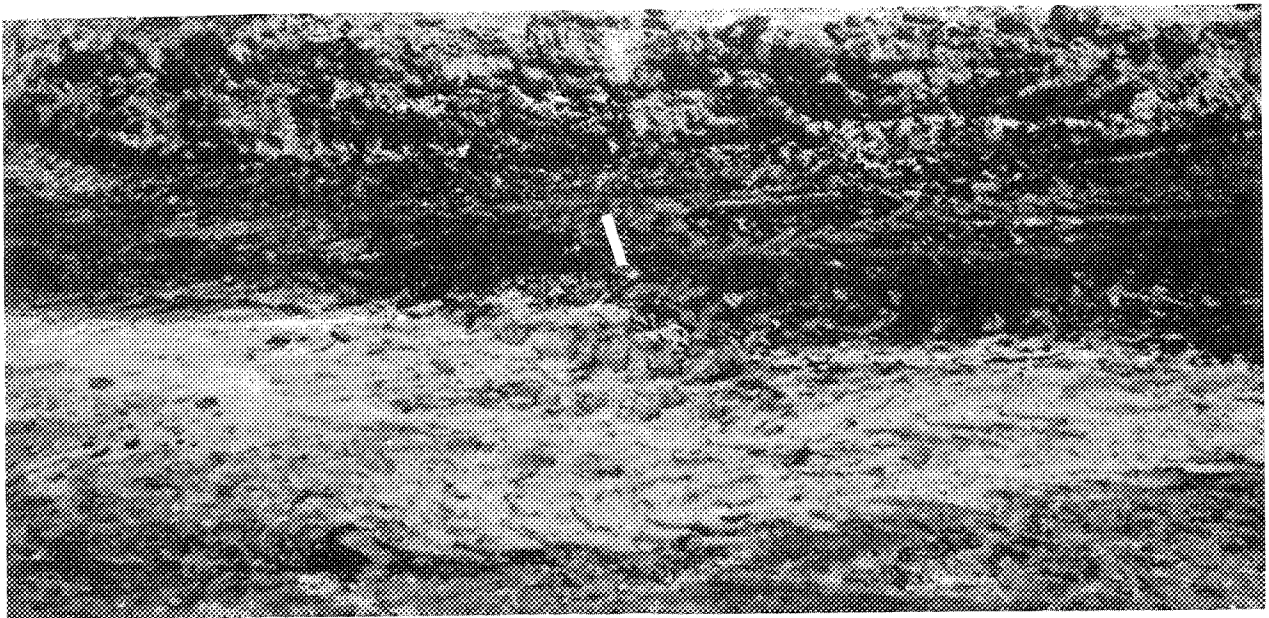


FIGURE 65.--THE APPEARANCE OF SUBGRADE IN SECTION 10
AND 11 AFTER THE EXISTING TEST SECTION HAD BEEN REMOVED.
NOTE THE DIFFERENT COLORING INDICATING VARIATIONS IN
MOISTURE CONTENTS.

to seepage of rain through cracks into the base. The residual moisture content of the emulsion-treated and special aggregate asphalt-treated bases was estimated to range from 3-4% and 1-2%, respectively.

High moisture contents in the subgrade and the bases indicate moisture played an important role in the failures of the sections. The fact that moisture contents were above optimum during the two testing periods implies the subgrade bearing strength was weakened which could have led to the rapid failures during the spring testing period.

Static Deflections

Benkelman beam rebound measurements using the Canadian Good Roads Association procedure were taken at selected intervals (12). Initially only one reading per section was taken. In the spring this was changed to five readings per section which were then averaged. This was done to check the homogeneity of the test pavement sections and to obtain a better rebound average for that test section.

Rebound measurements were started the latter part of November, which limited valuable data to the latter half of the test. Table XIX shows the Benkelman beam deflection measurements. Pavement temperatures were extrapolated from temperature probes. Because of the late date in starting recording, most of these measurements obtained relate to cracked pavements. Benkelman beam rebound measurements in the spring were two to four times greater than those obtained in the fall (see Table XIX).

A comparison of deflections with wheel load applications in Fig. 66 shows that, in general, deflections increase with wheel load applications. This is true only for undamaged pavements; once a pavement starts to crack deflections gradually decrease. A comparison of temperature with deflections in Fig. 67 show that generally as temperatures increase deflections increase. This is not as

TABLE XIX: SUMMARY OF BENKELMAN BEAM DEFLECTION MEASUREMENTS
RING TWO

Section	Date: Wheel Loads: Base	11-29-66 192,753		4-7-67 207,420		4-25-67 211,320		5-15-67 230,800		6-1-67 232,600	
		Temp.	Defl.	Temp.	Defl.	Temp.	Defl.	Temp.	Defl.	Temp.	Defl.
1	4.5" UTB	38	0.055	54	0.181						
2	7.0" UTB	38	0.140	55	0.159						
3	9.5" UTB	38	0.076	55	0.120						
4	12.0" UTB	38	0.057	56	0.078	50	0.087*	75	0.079*	78	0.050*
5	3.0" ETB	37	0.121								
6	5.0" ETB	37	0.131								
7	7.0" ETB	37	0.051	48	0.169	51	0.115	66	0.195		
8	9.0" ETB	38	0.047	48	0.082	50	0.064	65	0.106*	74	0.104*
9	2.0" ATB	38	0.041	54	0.246						
10	3.5" ATB	37	0.043	52	0.084	51	0.166*	70	0.110*		
11	5.0" ATB	37	0.015	51	0.069	51	0.108	70	0.186*		
12	6.5" ATB	37	0.004	50	0.064	51	0.054	68	0.89*	74	0.092*

* Values are averages for 5 measurements, all other values are for one test.

FIGURE 66.--DEFLECTIONS VS WHEEL LOADS
Fall 1966 Spring 1967

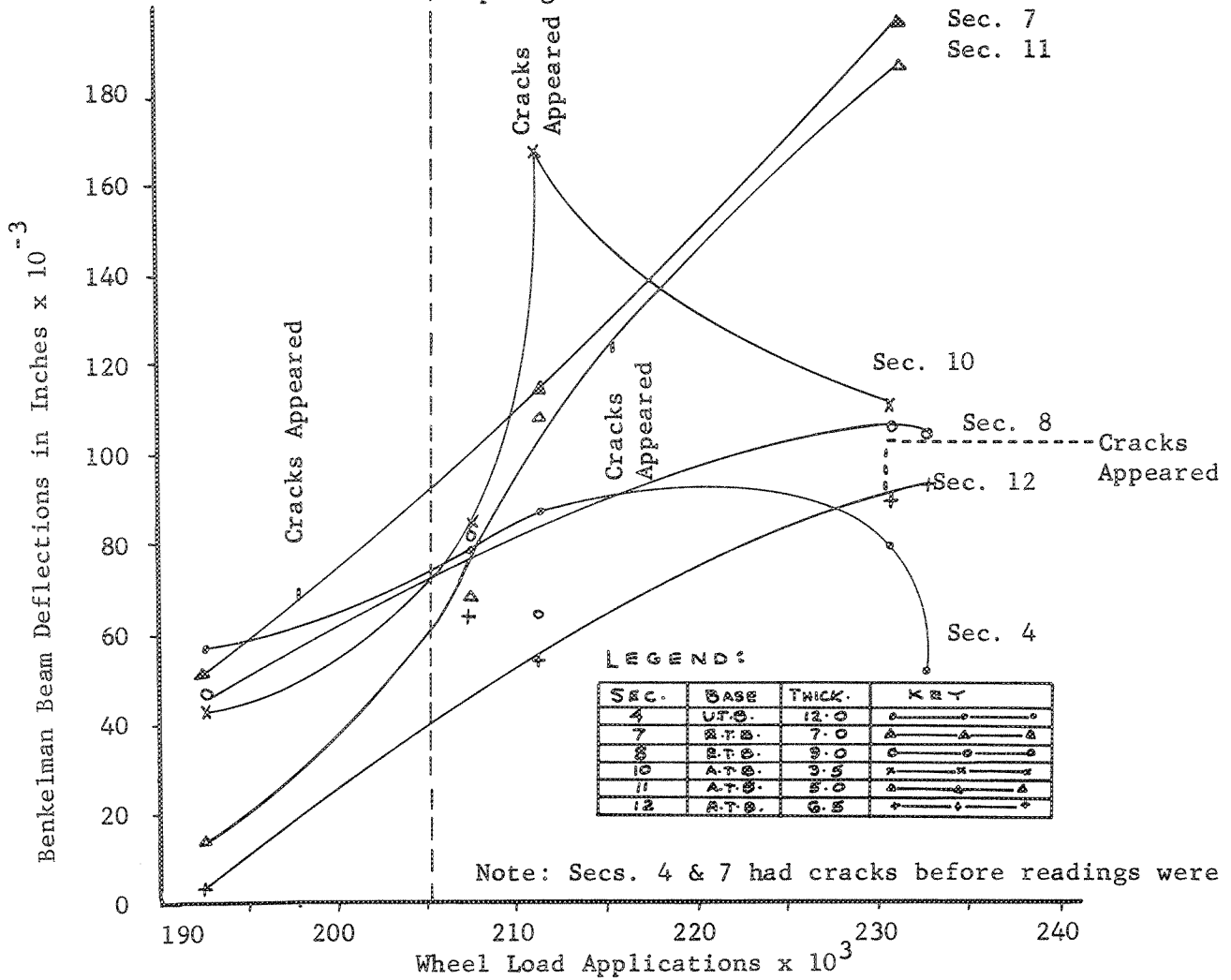
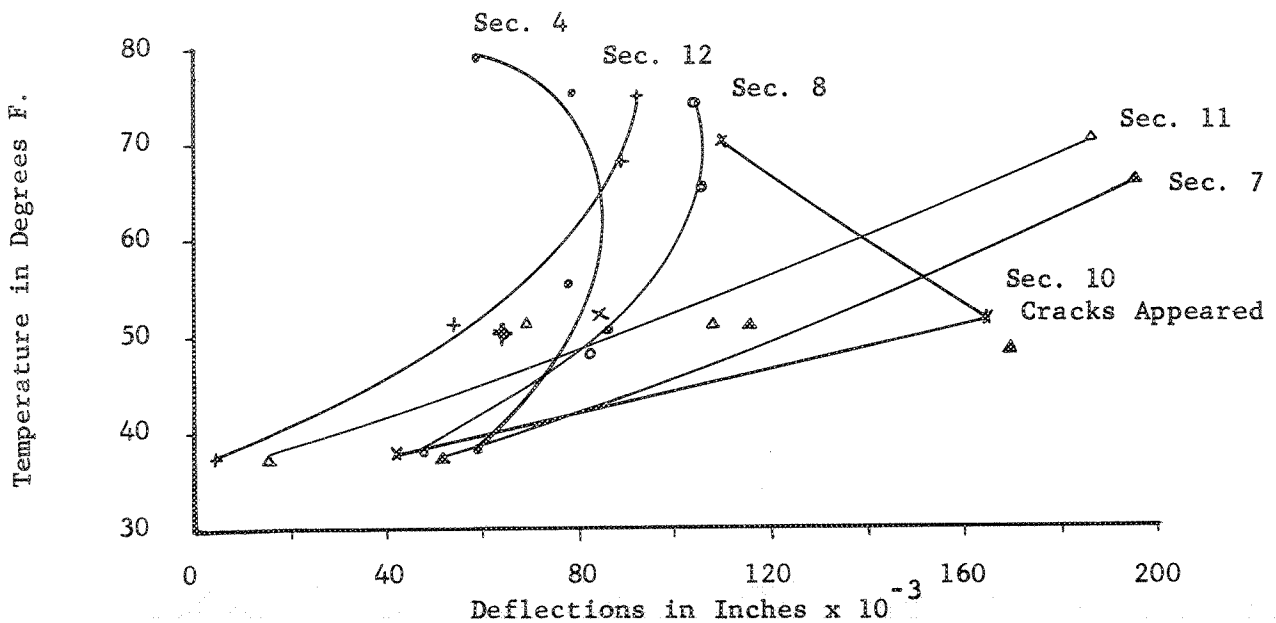


FIGURE 67.--TEMPERATURE VS DEFLECTIONS (BENKELMAN BEAM)



valid for cracked pavements as for uncracked pavements. This may be due to the fact that the subgrade has deformed to such an extent that further deformation is almost nil. Drying out of the subgrade through the cracks with a resulting in density possibly may have occurred. Thus overall deflections may have decreased, and the cracked portions of the pavement may start acting as separate entities rather than a unified slab. Sections 4, 10 and 12 in Figures 66 and 67 seem to show this effect.

Dynamic Deflections

Dynamic deflections were measured by Sanborn LVDT transducers in sections 2, 6, 8 and 10 (7.0 inches of untreated base, 5.0 inches and 12 inches of emulsion-treated base, and 3.5 inches of special aggregate asphalt-treated base, respectively) during the period when strain gage readings were taken. Some dynamic deflections were also taken in conjunction with Benkelman beam measurements. Again the fall testing period was divided into early and late fall periods on the basis of rainfall and temperature. This was done on the basis of wheel load applications--100,000 wheel loads being taken as the division between early and late fall periods to determine variations in the readings. Readings after 205,425 wheel loads were obtained during the spring (1967).

Plotting the deflection data obtained from LVDT gages #1 and #2 located in section 2 (7.0 inches untreated crushed surfacing top course) against transverse distance (Fig. 68) shows that generally deflections were lower for both LVDT gages during the early fall then increased during late fall. It appears that the whole pavement structure became more flexible under wheel load application in a wet environment indicating a possible weakening of the subgrade. Temperature effects on dynamic deflections for LVDT gages seem to be minimal under the conditions of testing. The deflections for the deep gages appear to be two to four times greater than for the shallow gage. Apparently, 25-50% of the deflections occur within the pavement and untreated base.

Figure 69 shows the variation in dynamic deflections of the deep gage in section 2 recorded during a 5-hour period at a constant speed of 20 mph. Deflections drop from a peak at center and continue to fall about 1.1 foot from the track centerline to the outside. As the dual tires move toward the inside and center of the section, deflections increase but do not reach their initial peak. This difference may be due to the fact that section 2 was cracked, and the pavement was not acting as a homogeneous slab, but as independent entities. Deflections appeared to end about 1 foot inside the track's centerline.

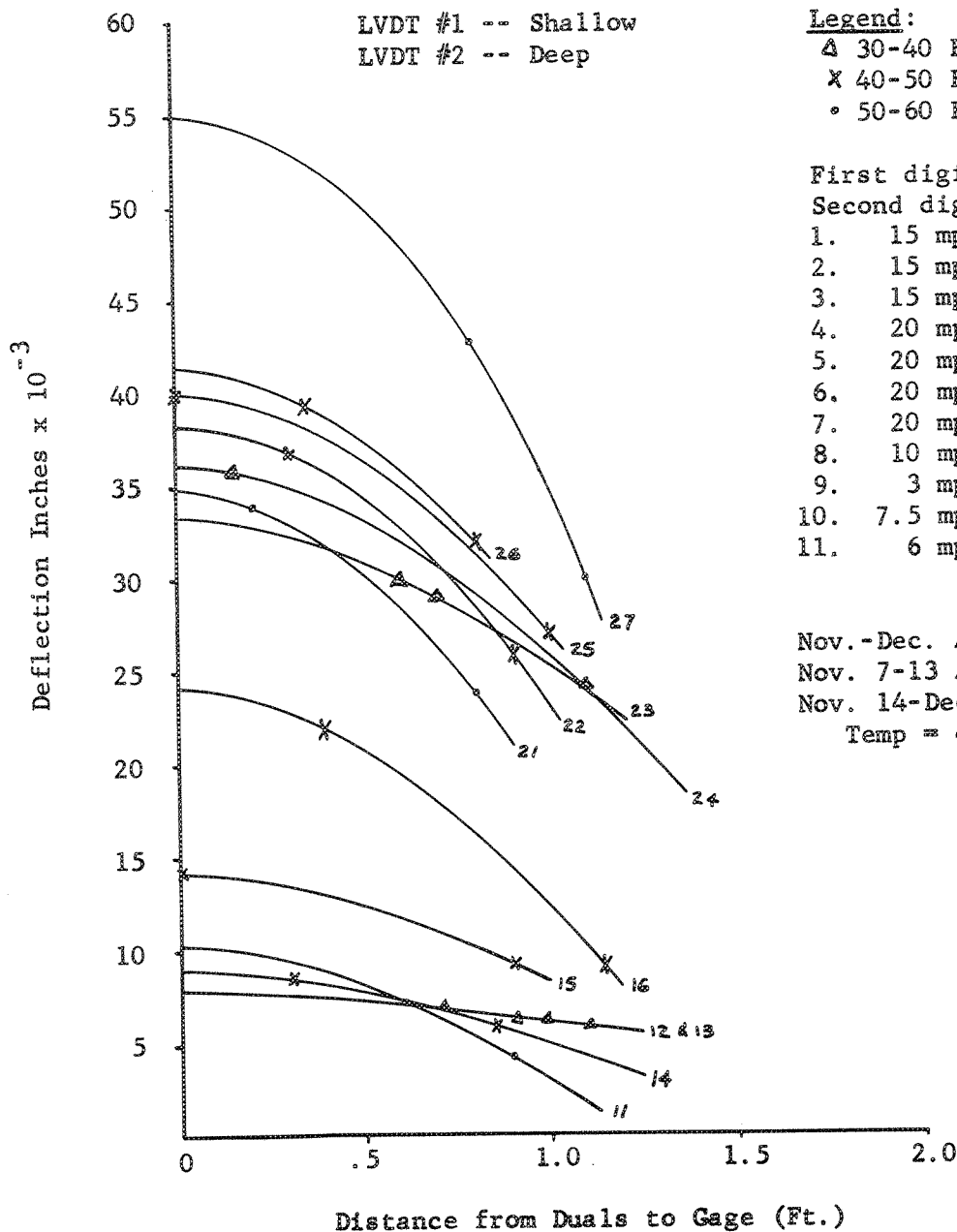
The variation in dynamic deflections against transverse distance for LVDT gages #3 and #4 in section 6 (5.0 inches emulsion-treated base) are shown in Fig. 70. The trends are similar to those found from LVDT gages #1 and #2. In general, the deflections are lower during the early fall and increase later in the season. The deep deflections seem to be three to ten times higher than those recorded by the shallow gage. About 10-30% of the deflections are within the pavement and emulsion-treated base indicating a more rigid structure.

Similar trends were obtained in section 8 (9.0 inches ETB) with LVDT gages #5 and #6 (see Fig. 71). Total or deep deflections are less than those found in sections 2 and 6. Shallow deflections are also lower. A general statement can be made to the effect that the deeper the pavement structure is constructed of the same materials, the lower the shallow and total deflections.

Deflections measured by LVDT gage #7 and #8 in section 10 (3.5 inches special ATB) exhibit the same trends (shown in Fig. 72). Deflections are lower during early November then increased. Total deflections were high as compared to the shallow deflections. Very little total deflection occurred within the pavement structure itself indicating that most of the deflections occurred within the subgrade which denotes a fairly rigid pavement structure.

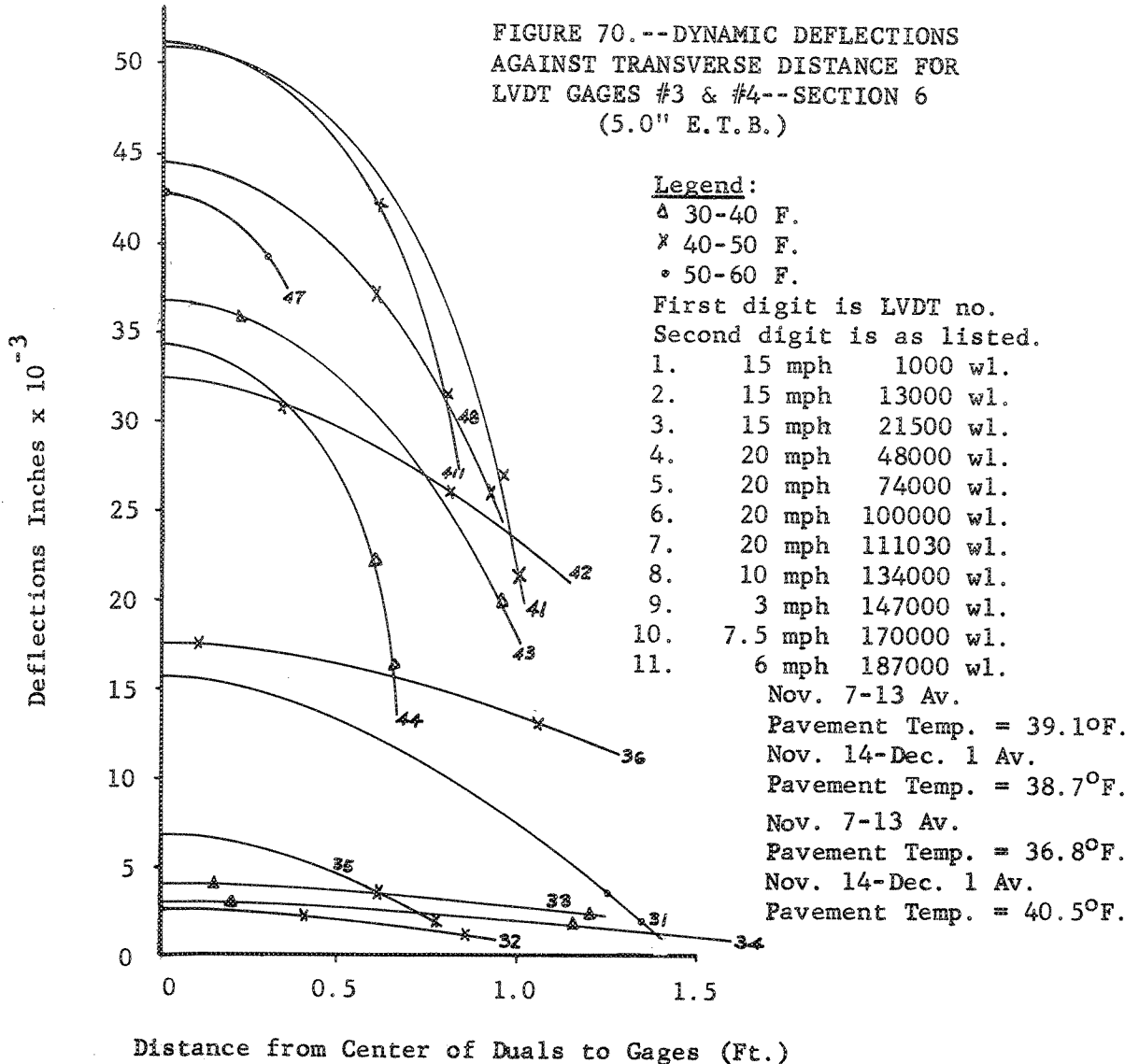
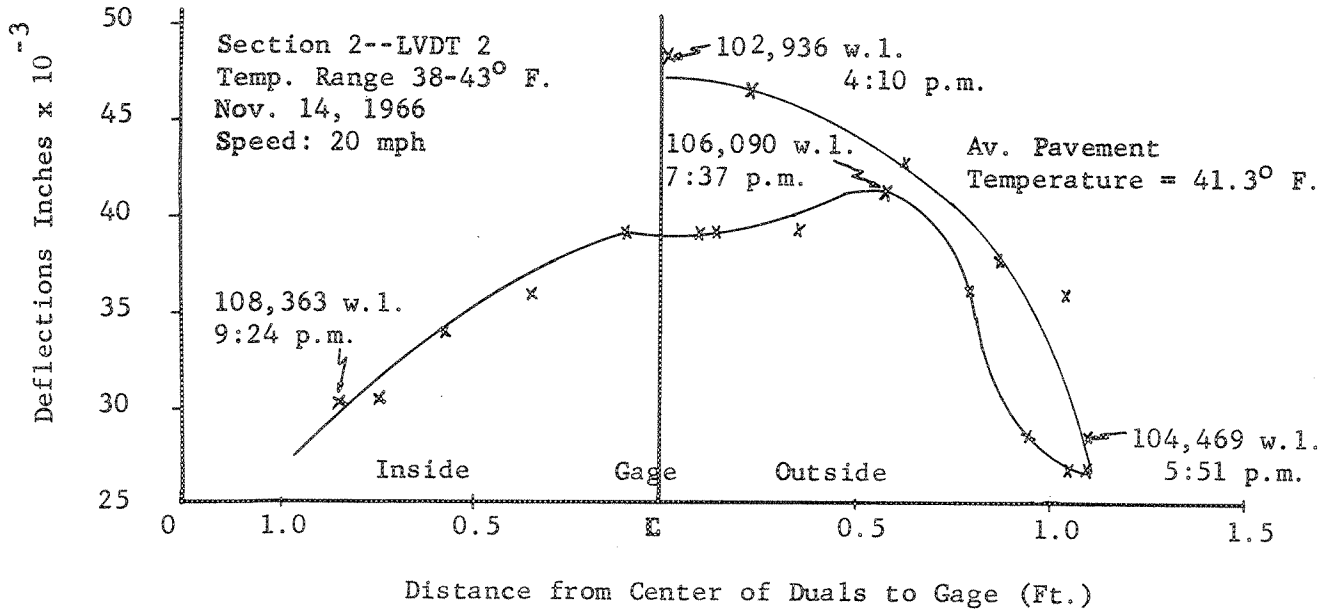
Deflection data is summarized in Table XX, done by Kingham (14) of the Asphalt Institute, which shows that, in general, deflections were lower in early

FIGURE 68.--DYNAMIC DEFLECTIONS AGAINST
TRANSVERSE DISTANCE FOR LVDT #1 & 2 IN
SECTION 2 (7.0" of Untreated Crushed Stone)



Note: Results from the Shell Avenue Test Road (15) show that maximum deflection values obtained from LVDT were not found in the center of the duals, but rather under the tires. Figure 69 seems to bear this out. Unfortunately, not enough values were obtained to show these curves in Figures 68, 70, 71 and 72. It is hoped that LVDT results from the next ring will show more definite trends.

FIGURE 69.--DYNAMIC DEFLECTION VARIATIONS WITH TRANSVERSE DISTANCE



November and higher later on. Deflections during the spring period were three times higher than those measured in the fall which would point up a different environmental condition. This also is borne out by the difference of failures associated with the different time periods.

Plotting the LVDT deflections against wheel load repetitions on a log scale (Fig. 73) reveals that deflections decreased up to 21,500 to 30,000 wheel loads, then began to increase. In the range of 21,500 to 30,000 wheel loads the testing environment was fairly dry and pavement temperatures ranged from 35 to 45° F. Thus the pavements and subgrade may have been at their greatest strength and maximum stability. As soon as the environment changed, the deflections started to increase indicating a decrease in pavement and subgrade modulus and strength.

The speed of the testing apparatus also affected deflection readings. In general, the lower the speed the higher the deflection readings. Only one study was made using LVDT gage #2 in section 2. Deflection readings were clearly affected by the speed (Fig. 74). Unfortunately readings were only taken between speeds of 15 to 35 mph. Dynamic deflections at low speeds, 0-5 mph, approach those of static conditions and will decrease as the speed increases; these dynamic deflections will continue to decrease until a certain speed is reached, +35 mph, after which dynamic deflection will be constant. These trends are shown by the dotted line in Fig. 74, and seem to confirm the findings of the AASHO Road Test on deflection versus speed (13). The reason that deflections decrease within a certain range of speed is that the entire wheel load does not have time to develop its effect throughout the pavement structure. This has been borne out by static load measurements which are usually higher than dynamic loads.

The dynamic deflection ratio of shallow deflections (deflections above subgrade) and total deflections are tabulated in Table XXI and plotted in Fig. 75. In general, the ratio increases with wheel load repetitions.

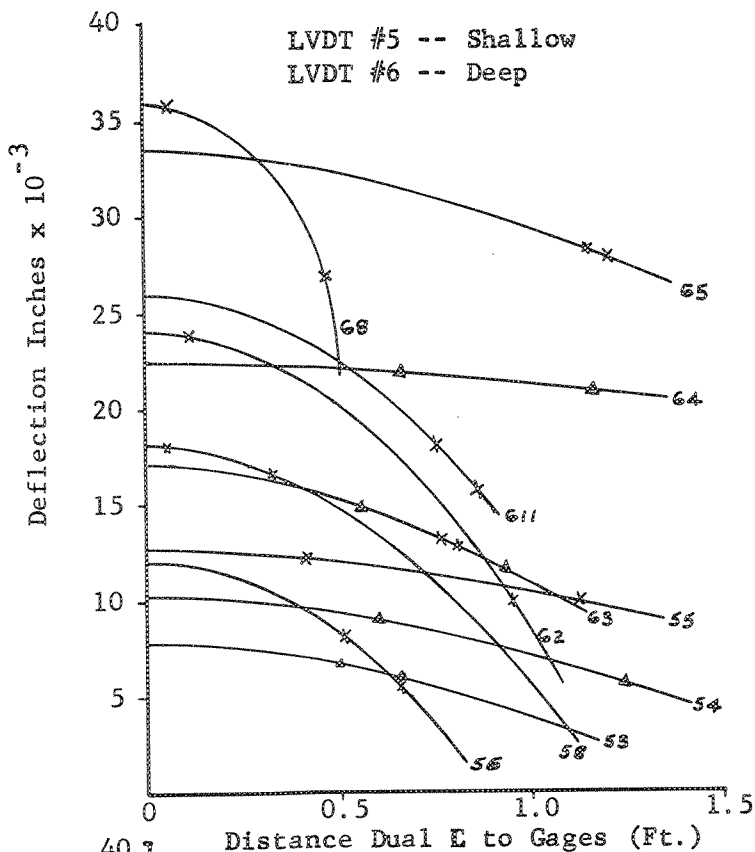
TABLE XX
SUMMARY OF LVDT DEFLECTION MAXIMUM MEASUREMENTS
RING TWO

Section	LVDT	Position*	Period**	Deflection Under Tire Inches	Deflection & Duals Inches	Average Pavement Temp. -°F
2	1	Shallow	Early Nov.	0.009	0.014	37
	1	Shallow	Late Nov.	0.020	0.025	41
	2	Deep	November	0.042	0.038	39
6	3	Shallow	Early Nov.	0.004	0.003	37
	3	Shallow	Late Nov.	0.017	0.016	41
	4	Deep	Early Nov.	0.040	0.033	39
	4	Deep	Late Nov.	0.057	0.043	39
8	5	Shallow	November	0.012	0.012	39
	5	Shallow	Spring	0.039	0.035	53
	6	Deep	November	0.030	0.026	45
	6	Deep	Spring	0.068	0.061	53
10	7	Shallow	November	0.017	0.009	39
	8	Deep	November	0.034	0.030	46

**Early November is the period prior to the rain - around November 13 and at about 100,000 wheel loads.

*Shallow LVDT's measure deflection occurring above the subgrade soil. Deep LVDT's measure total deflection.

FIGURE 71.--DYNAMIC DEFLECTIONS
SECTION 8



Legend:

- △ 30-40 F.
- × 40-50 F.
- 50-60 F.

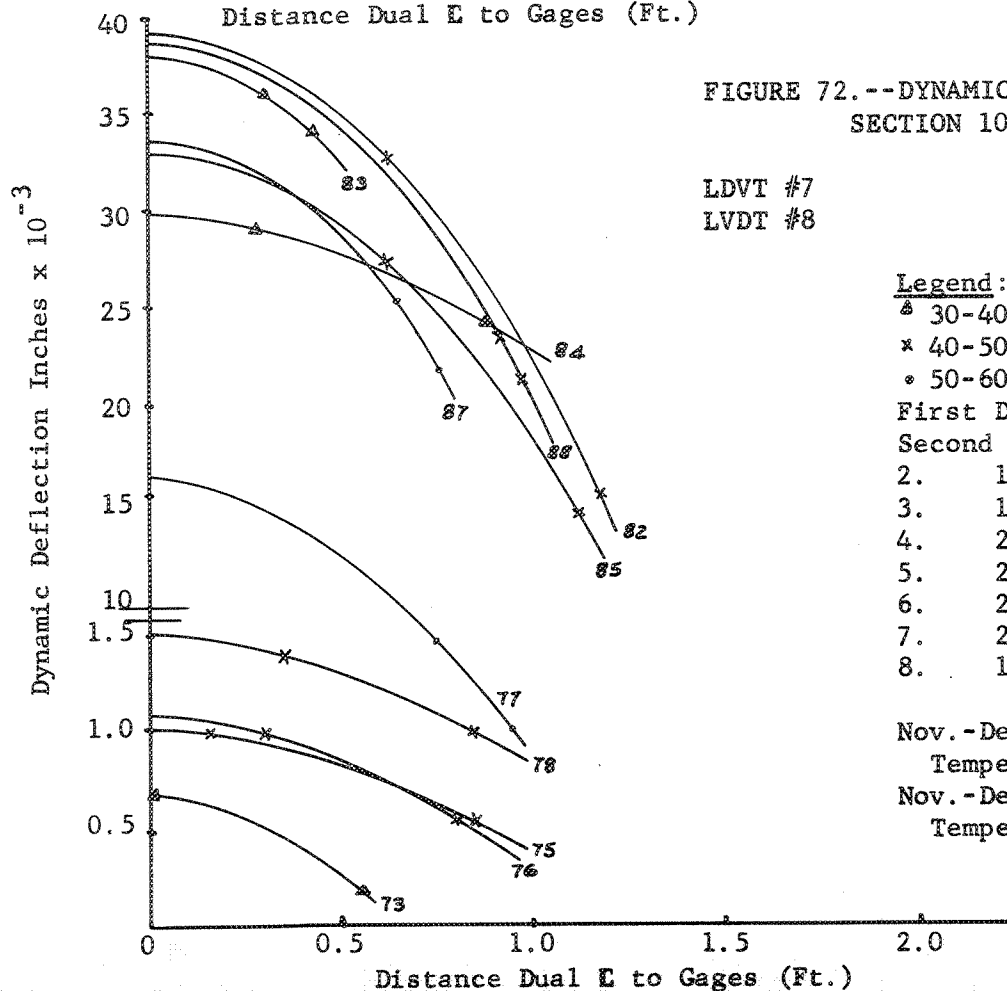
First digit is LVDT no.
Second digit is as listed.

- | | | |
|-----|---------|------------|
| 1. | 15 mph | 1000 wl. |
| 2. | 15 mph | 13000 wl. |
| 3. | 15 mph | 21500 wl. |
| 4. | 20 mph | 48000 wl. |
| 5. | 20 mph | 74000 wl. |
| 6. | 20 mph | 100000 wl. |
| 7. | 20 mph | 111030 wl. |
| 8. | 10 mph | 134000 wl. |
| 9. | 3 mph | 147000 wl. |
| 10. | 7.5 mph | 170000 wl. |
| 11. | 6 mph | 187000 wl. |

Nov.-Dec. Av. Pavement
Temperature = 45.1°F.
April-May Av. Pavement
Temperature = 52.7°F.

Note: 1, 7, 9, and 10 are
omitted as there were not
enough points for plotting.

FIGURE 72.--DYNAMIC DEFLECTIONS
SECTION 10



Legend:

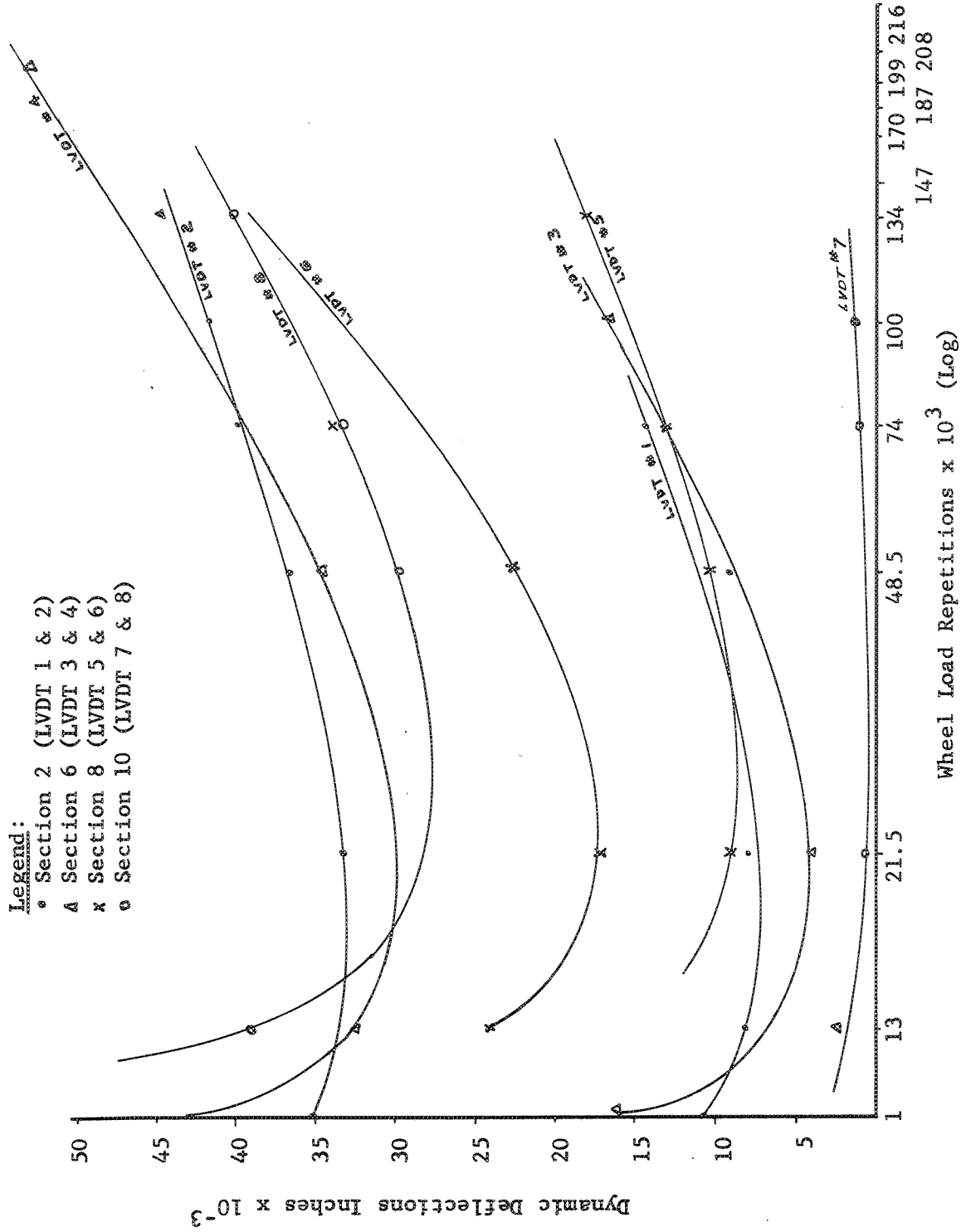
- △ 30-40 F.
- × 40-50 F.
- 50-60 F.

First Digit is LVDT no.
Second digit is as listed.

- | | | |
|----|--------|------------|
| 2. | 15 mph | 13000 wl. |
| 3. | 15 mph | 21500 wl. |
| 4. | 20 mph | 48000 wl. |
| 5. | 20 mph | 74000 wl. |
| 6. | 20 mph | 100000 wl. |
| 7. | 20 mph | 111030 wl. |
| 8. | 10 mph | 134000 wl. |

Nov.-Dec. Av. Pavement
Temperature = 46.3°F (deep)
Nov.-Dec. Av. Pavement
Temperature = 39.3°F (shallow)

FIGURE 73. DYNAMIC DEFLECTIONS WITH RESPECT TO WHEEL LOAD REPETITIONS



The increase in the ratios shows that the increase in shallow deflections is greater than for the deep deflections; that is, the proportion of deflection occurring within the pavement structure increases.

Examination of the dynamic deflections shows that deflections occurring in the subgrade were larger than in the pavement structure (wearing course plus base), but as the wheel load repetitions accumulate deflections within the pavement system increase and eventually become greater. This is shown in Figure 75A and Table XXI A. This was especially true for the untreated and emulsion-treated bases. This is also borne out by the dynamic deflection ratios shown in Figure 75 and Table XXI. Figures 75 and 75A also show that most of the deflections in the asphalt-treated base occurred within the subgrade.

The explanation is that as wheel load repetitions are increased, more of the deflection is taken up by the pavement and bases. The ratio will continue to increase until some point is reached where distress occurs. At this point the pavement structure is under a heavy flexible strain and distress will occur due to extreme flexibility and fatigue. The dynamic deflection ratio is a function of thickness and of the pavement material. The asphalt-treated bases had the smaller ratio indicating high rigidity. More study is needed before definite conclusions can be made. These views may be modified as more information is available from other rings.

No meaningful comparison could be made between deflections obtained by LVDT transducers and the Benkelman beam because of the late start in taking Benkelman beam measurements. When the Benkelman beam recordings were started most of the LVDT gages had been removed.

FIGURE 74.--EFFECT OF DIFFERENT SPEEDS ON DEFLECTION
Section 2--LVDT #2, November 4, 1966

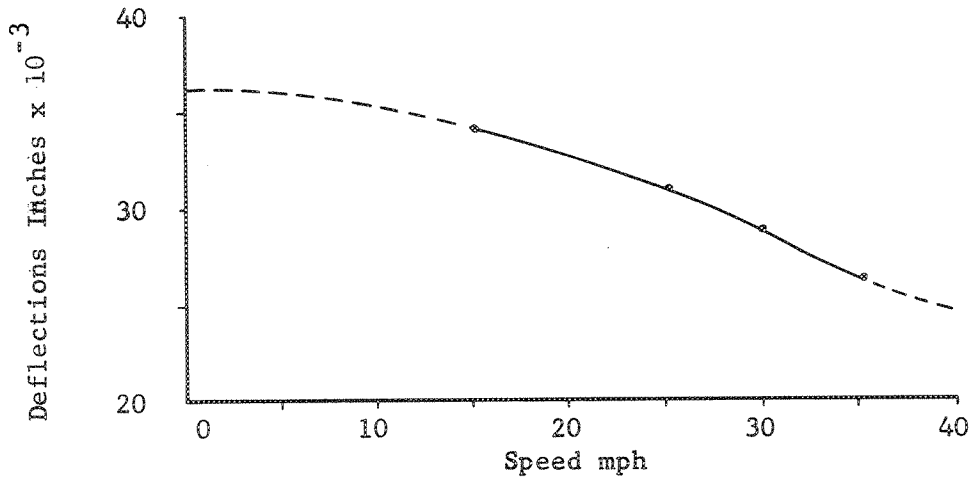


FIGURE 75.--DYNAMIC DEFLECTION RATIO ($\frac{\text{Shallow}}{\text{Deep}}$)
RING 2

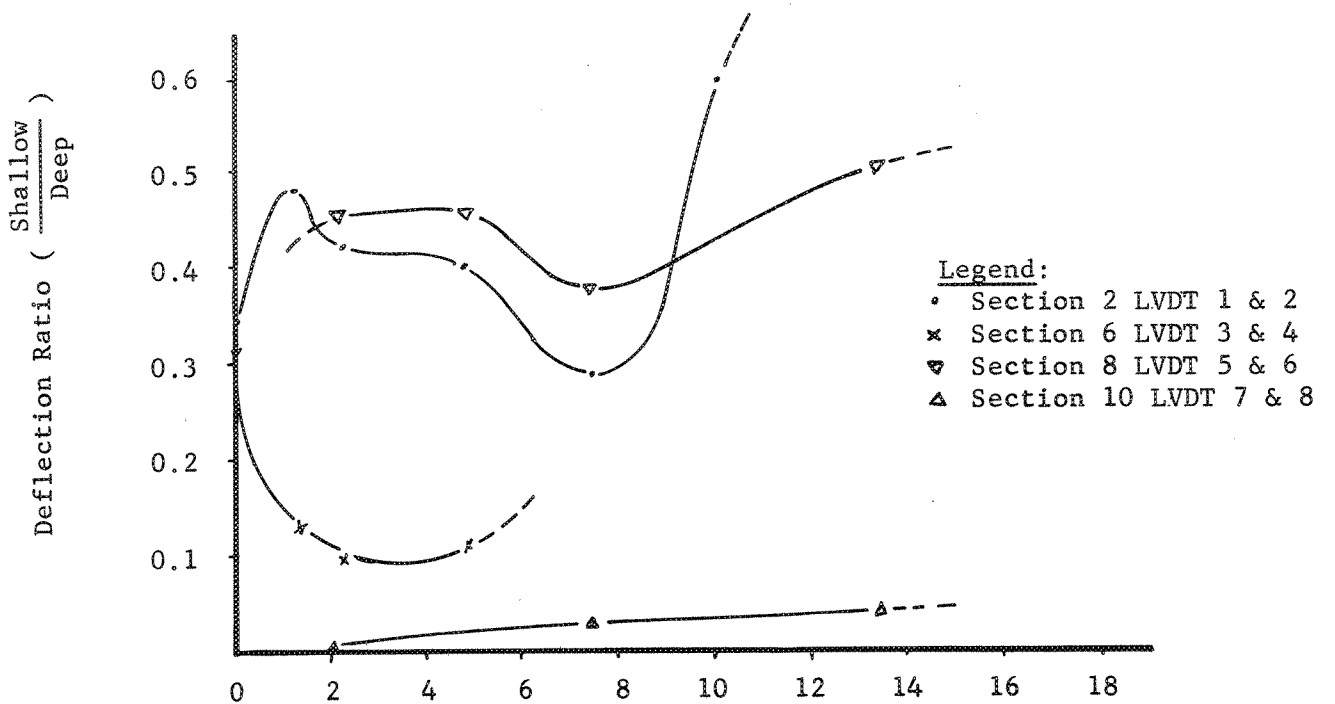


TABLE XXI: RATIO OF SHALLOW TO DEEP DYNAMIC DEFLECTIONS

Section:	#2 (7.0" U.T.B.)				#6 (5.0" E.T.B.)				#8 (9.0" E.T.B.)				#10 (3.5" A.T.B.)			
	LVDT	Deflection in. x10 ⁻³	Ratio Shallow/Deep		LVDT	Deflection in. x10 ⁻³	Ratio Shallow/Deep		LVDT	Deflection in. x10 ⁻³	Ratio Shallow/Deep		LVDT	Deflection in. x10 ⁻³	Ratio Shallow/Deep	
1,000	1	10.5	0.333	3	15.7	0.325	5	11.6	7	0.4	0.339	7	0.4	0.012	8	32.0
	2	35.0		4	51.0		6	34.2		8		32.0				
13,000	1	8.0	0.482	3	2.5	0.126	5	10.2	7	0.19	0.425	7	0.19	0.012	8	15
	2	38.5		4	32.5		6	24.0		8		15				
21,500	1	8.0	0.418	3	4.0	0.111	5	7.7	7	0.7	0.453	7	0.7	0.018	8	38.0
	2	33.5		4	36.6		6	17.1		8		38.0				
48,000	1	9.0	0.403	3	3.0	0.089	5	10.2	7	0.72	0.453	7	0.72	0.030	8	24.0
	2	36.2		4	34.0		6	22.5		8		24.0				
74,000	1	14.0	0.350	3	3.4	0.113	5	12.7	7	1.0	0.379	7	1.0	0.032	8	33.0
	2	40.0		4	30.0		6	33.5		8		33.0				
100,000	1	24.0	0.586	3	16.7	0.468	5	8.3	7	0.56	0.638	7	0.56	0.026	8	21.0
	2	41.5		4	35.6		6	13.0		8		21.0				
134,000	1	27.9	0.612				5	18.2	7	1.6	0.506	7	1.6	0.040	8	38.7
	2	45.6		6	36.0	6	36.0	8		38.7						
198,000							5	22.0	7	0.9	0.474	7	0.9	0.026	8	34.0
							6	46.4		8		34.0				
216,000							5	40.9			0.637					
							6	64.2		6		64.2				
222,125							5	22.3			0.787					
							6	28.3		6		28.3				
MEAN			0.455			0.205					0.509					0.025

FIGURE 75(A).--DEFLECTIONS - PAVEMENT SYSTEM (PS)
VERSUS SUBGRADE (S)

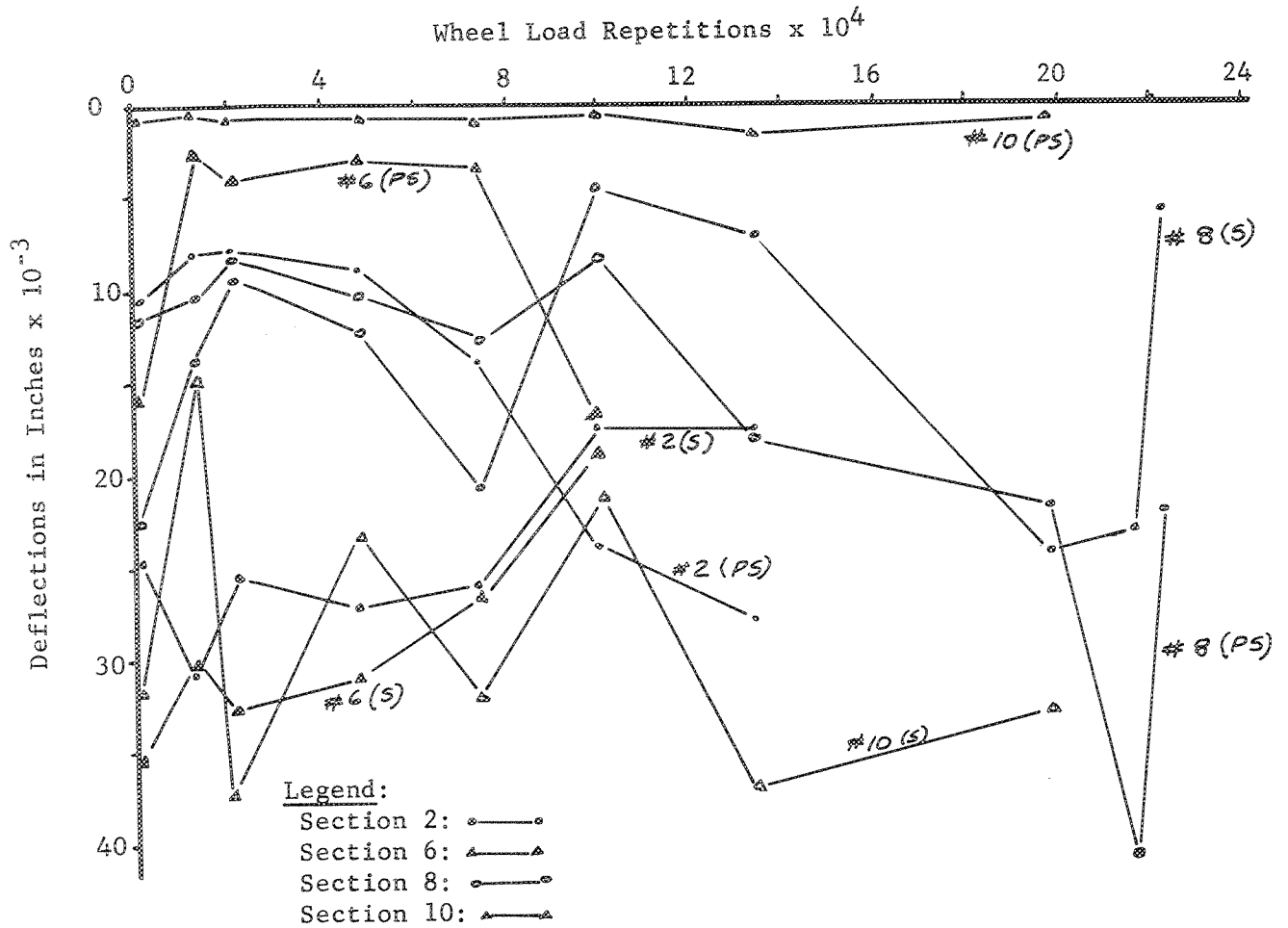


TABLE XXI(A): PAVEMENT SYSTEM (PS) VS SUBGRADE (S) DEFLECTIONS

Section	#2 (U.T.B.)		#6 (E.T.B.)		#8 (E.T.B.)		#10 (A.T.B.)	
	Deflections - Inches x 10 ⁻³							
Wheel Loads	PS	S	PS	S	PS	S	PS	S
1,000	10.5	24.5	15.7	35.3	11.6	22.6	0.4	31.6
13,000	8.0	30.5	2.5	30.0	10.2	13.8	0.2	14.8
21,500	8.0	25.5	4.0	32.6	7.7	9.4	0.7	37.3
48,000	9.0	27.2	3.0	31.0	10.2	12.3	0.7	23.3
74,000	14.0	26.0	3.4	26.6	12.7	20.8	1.0	32.0
100,000	24.0	17.5	16.7	18.9	8.3	4.7	0.6	20.5
134,000	27.9	17.7			18.2	7.2	1.6	37.1
198,000					22.0	24.4	0.9	33.1
216,000					40.9	23.3		
222,125					22.3	6.0		

Strain Gage Data

Examination of the strain gage data showed that it was necessary to plot all the data against wheel placement by fall and spring periods. Although there was much data, there was not enough or sufficient data to establish definite clear-cut relationships. The test track findings confirm strain gage studies made elsewhere that the lateral displacement of the wheel relative to the gage greatly influences the measured values of strain, deflection and stress. The data also indicates that the temperature effects were negligible as the temperature range was rather narrow. Trend lines were established for each strain gage based on the test road experiences referred to above. Maximum values from these trend lines were then inferred and are shown in Table XXII.

The majority of maximum values occurred when one of the tires was over the gage. Strain values were two to four times higher in the spring than in the fall. This seems to correlate with the different modes of failure which occurred in the fall and the spring. An attempt was made to try to match strains with first appearance of cracking and to try to establish failure criteria. This will have to await the completion of the next two rings before the full significance of the values can be realized. The strain values shown are maximum values measured as the wheels were moving longitudinally at some lateral wheel motion, hence both tensile and compressive strains were measured.

Inclusion of all the strain curves would be too voluminous. Only plots of strains obtained from section 8 (9.0 inches of emulsion-treated base) and section 10 (3.5 inches of special asphalt-treated base) have been included in this report, because much data was available, especially for comparison purposes between the different layers. Comparisons between fall and spring strains could also be made. Some continuous strain data was available for section 10 and is included. Some typical strain gage readings reproduced from actual data is included and shown in Fig. 102(g).

Strain gage data for section 8 is shown in Figures 76 to 95. Examination of the plots reveals that strain is usually maximum under the tire rather than under the center of duals. In many of the longitudinal gages there were different modes of strain depending upon the lateral position of the duals. Another interesting development was that tensile strains increased while compression strain decreased with depth. Larger tensile strains occurred at the 3.0-inch depth. Strain reversals with tensile strains larger than compressive strains occurred on the subgrade.

Transverse strain gage data was very complex varying with lateral position of the tires and with depth. Tensile strains seem to increase with depth. Comparison of tensile strains in the transverse and longitudinal directions shows that tensile strains in the longitudinal direction were larger. This may indicate why transverse cracks appeared rather than longitudinal cracks.

Figure 95 shows strain with depth. The plot shows that compressive strain decreases with depth and that the tensile strain also decreases but not as much. This holds true for strains in the transverse direction, except that tensile strains increase slightly with depth. During the spring there was a large increase in strain in both directions. This may be an indication of the changes in subgrade support and changes in flexure strength.

An attempt was made in Figs. 77, 82, 83 and 86 to try to correlate strain with wheel load applications. Not enough data was available, hence only trend lines could be inferred. It appears that strains increase with wheel load applications, and perhaps in future tests, failure criteria can be developed with more data.

Figures 96 to 102 show the strain data plotted for section 10 (3.5 inches of special asphalt-treated base). In an attempt to obtain better curves, it was assumed that the curves were symmetrical around the centerline of the pavement.

Hence a set of points were plotted around the centerline giving one set of graphs, and points were plotted for one-half of the pavement giving another set of graphs. The attempt was partially successful. The plots show almost the same strain trends as found in sections 2, 6 and 8. Tensile strain increased appreciably in the longitudinal direction as compared with strains in the transverse direction. Transverse strains seem to be more complex with reversals of strains occurring depending upon the lateral position of the duals. High tensile strains were found to exist at the 3.0-inch depth (top of the base or bottom of the wearing course).

Continuous strain gage readings are shown in Fig. 102 (a to g). The data was usually obtained during a 24-hour period and are maximum values of strain, compressive and tensile, measured while the tires were traveling in longitudinal direction. The reasons the plots are not as symmetrical as they should be are twofold. One, during the 24-hour period temperature differences existed and may have caused variations in strains and two, as the duals moved laterally the weight distribution may have changed due to transverse load placement. The camber of wheels was set to the slope of the pavement so that weight distribution on each wheel was equal. As the pavement became rougher, the load on each wheel may have shifted due to this camber thus causing some variations in strain, both in longitudinal and transverse direction. More continuous strain gage readings are desirable to study the effects of wheel load applications and temperature on strain patterns. This knowledge would be very useful in the determination of failure criteria.

Stress Data

Only vertical stresses were measured. The maximum values of this stress data are summarized in Table XXIII. This table shows the stress values obtained by the Filpup transducers and the WSU pressure cells. Maximum vertical stresses

were measured in the spring period of testing for the sections which survived the fall period of testing. Temperature effects were negligible due to the small range of temperatures encountered during this period.

Figures 103 (a, b and c) show the general trend lines of stress with respect to the lateral position of the duals. The figures show that maximum stress values were obtained when the duals were directly over the gages. Spring values were about two times higher than the fall values. Although Fig. 103 represents the results obtained for the 9.0-inch emulsion-treated base section, the curves represent similar curves obtained for other sections. Stress values obtained by the Filpips at 3.0 inches seem to be suspect as readings at this level were very erratic. This may be due to overstressing caused by rolling during construction.

Vertical stress varied with speed. As the speed of the apparatus increased, stress declined. This is shown in Figs. 104 (a, b and c) as measured by the WSU pressure cells. The data from both sections 6 and 8 are shown. The WSU pressure cells work better at lower speeds. It is difficult to read the manometer board at speeds over 20 mph as the displacement of fluid becomes very rapid and difficult to read.

Vertical stresses at subgrade level against depth and base material were plotted in Fig. 105. This figure shows that vertical stress at subgrade decreased with increasing thickness of base, and that spring values are higher than during the fall. The stress reduction ratios (Table XXIV) indicate that the ratios increase with thickness of base materials. Table XXIV shows that after a certain thickness is reached, virtually no stress reduction is achieved and, hence, any more increase in thickness will not cause stress reduction. This would, of course, hold true only for certain wheel loads.

Curve #4 in Fig. 105 shows stresses measured just at or before "ultimate" failure for the emulsion-treated bases. Figure 106 shows stresses measured when

no signs of distress were visible, that is for 0 to 100,000 wheel loads and afterwards--after the appearance of cracking to "ultimate" destruction. Stresses measured during the latter stage increased. Part of this increase may have been due to the fact that as the pavement cracked up into individual pieces, the pavement started to act as individual entities rather than a continuous slab causing points of intense high pressure and high vertical stresses.

Both Table XXIV and Fig. 105 show that stresses were high under the untreated bases, followed by the emulsion-treated bases, and finally, the special asphalt-treated bases. For the bases tested, the results suggest that increasing the thickness of the base beyond 8 inches is unnecessary as far as the reduction of stress is concerned. This seems to be valid for the asphalt and emulsion bases, but not valid for the untreated bases. At the AASHO Road Test, pavements which failed in the 18 kip axle load loop had vertical stresses on the top of the subgrade in excess of 8 psi (13). Therefore, greater thickness than 8 inches of untreated base are required to reduce the vertical stress to 8 psi in the spring. This may not be true for reduction of deflection and strain. More data is needed before certain conclusions and recommendations can be drawn. Complete analysis awaits the completion of Rings #3 and #4.

Comparison between the two kinds of cells seems to indicate that neither cell is satisfactory. At high speeds, the fluid displacement in the manometer was difficult to read. The necessity of long tubing for hydraulic fluid limits its use to short distances. The Filpip cells proved to be unreliable. The capacitor structure of the Filpip transducer may be prone to overstressing, especially during construction and hence led to erratic readings. Stray readings were a hazard. The Filpip had to be balanced constantly which led to difficulty in stability. The WSU cell is being used in Ring #3. New strain gage diaphragm cells have been built replacing the Filpip transducers and are now in use in Ring #3.

TABLE XXII: SUMMARY OF MAXIMUM LONGITUDINAL & TRANSVERSE STRAIN GAGE MEASUREMENTS
 (Readings are Maximum Values Taken in Longitudinal Direction)
 RING TWO

Period	Section Number	Position	Average Pavement Temp. °F*	Longitudinal Maximum Values			Transverse Maximum Values				
				Measurements		Lateral Position	Measurements		Lateral Position		
				Compression	Tension	Compression	Tension	Compression	Tension		
Fall	2	Surface	39**	220	40	Not defined	Not def.	240	None	Under tire	---
Fall		Base Top	40**	100	200	Under tire	Und.tire	120	200	Under tire	£ duals
Fall		Subgrade	38**	80	140	Uniform	Uniform				
Fall	4	Surface	39	230	80	Under tire	Uniform	260	None	Under tire	---
Spring		Surface	50	420	120	Under tire	Und.tire	500	60	Under tire	Outside
Fall	6	Surface	39	200	40	Under tire	Uniform	300	20	Under tire	Und.tire
Fall		Subgrade	39	110	---	Not defined	Not def.	55	260	Not defined	Not def.
Fall	8	Surface	39	340	60	Under tire	Uniform	320	100	Under tire	Und.tire
Fall		Base Top ¹	39	60	50	Under tire	Und.tire	120	140	Under tire	£ duals
Fall		Base Top ²	39	50	300	Uniform	£ duals	90	180	Under tire	£ duals
Fall		Subgrade ³	39	50	50	Uniform	Uniform				
Fall		Subgrade ⁴	39	30	20	Not defined	Not def.	160	150	Not defined	Not def.
Spring		Surface	53	420	120	Under tire	Uniform	None	600	---	Under tire
Spring	Base Top ¹	53	100	150	Not defined	Not def.	100	440	Under tire	Und.tire	
Spring	Base Top ²	53	60	500	Uniform	Und.tire	None	240	---	Under tire	Not def.
Spring	Subgrade ⁴	53	50	20	Not defined	Not def.					
Fall	10	Surface	39	250	40	Under tire	Uniform	300	None	Under tire	---
Fall		Base Top ⁵	39	60	210	Uniform	Und.tire	40	200	Under tire	£ duals
Fall		Base Top ⁶	39	40	100	Uniform	Und.tire	40	50	Under tire	£ duals
Fall		Subgrade	39	40	100	Uniform	Uniform	40	80	Not defined	Not def.
Spring		Surface	50	560	250	Under tire	Uniform	440	None	Under tire	---
Spring		Base Top ⁵	50	240	550	Under tire	Und.tire	180	1000?	Not defined	Not def.
Spring	Base Top ⁶	50	180	320	Uniform	Und.tire					

1. S. G. C-7-L, C-8-T
 2. S. G. D-5-L, D-6-T
 3. S. G. E-7-L
 4. S. G. D-9-L, D-10-T
 5. S. G. C-9-L
 6. S. G. D-7-L

* Average of temperatures measured at 3" and 12" depths in asphalt portion of the pavement
 ** Temperature at 3" depth only.

FIGURE 76.--SECTION 8 9.0" EMULSION-TREATED BASE SURFACE LONGITUDINAL STRAIN GAGE B-5-L

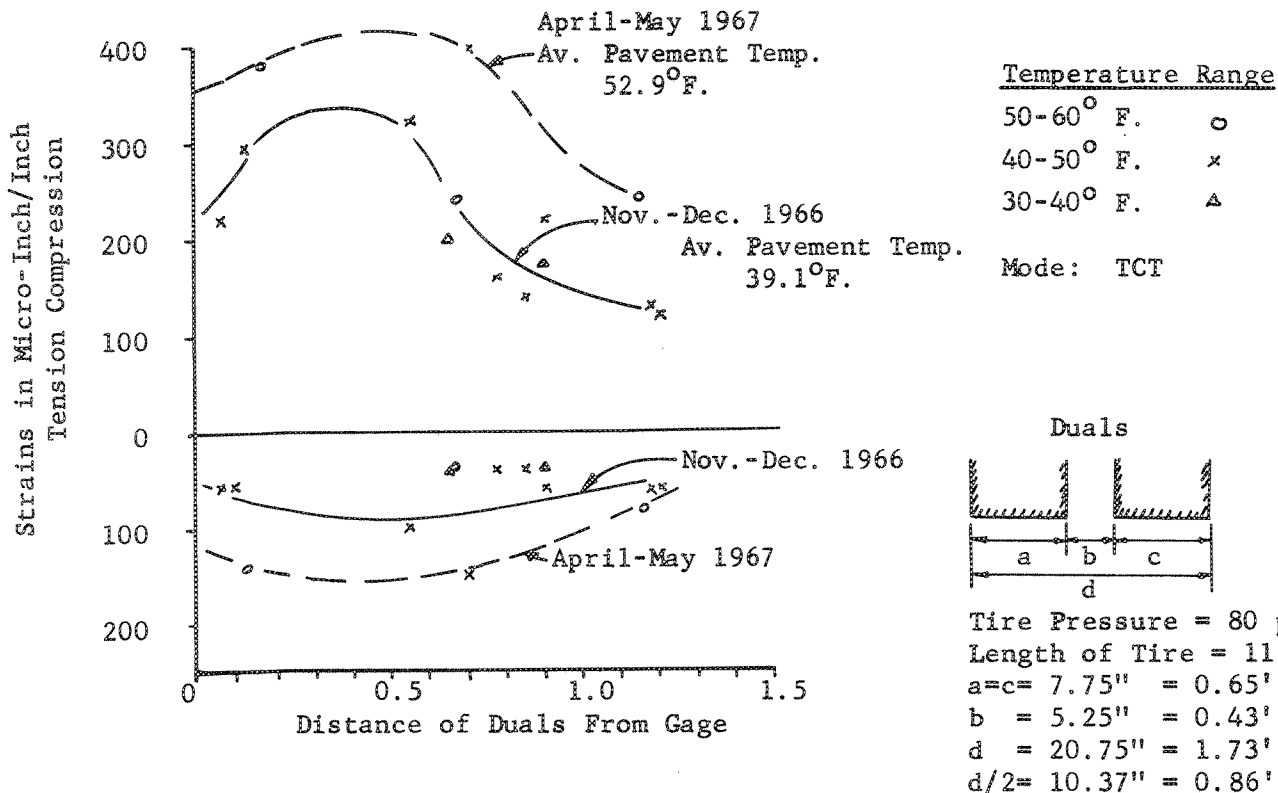


FIGURE 77.--SURFACE LONGITUDINAL STRAIN GAGE B-5-L (Ring 2, Section 8--Emulsion-Treated Base = 9.0")

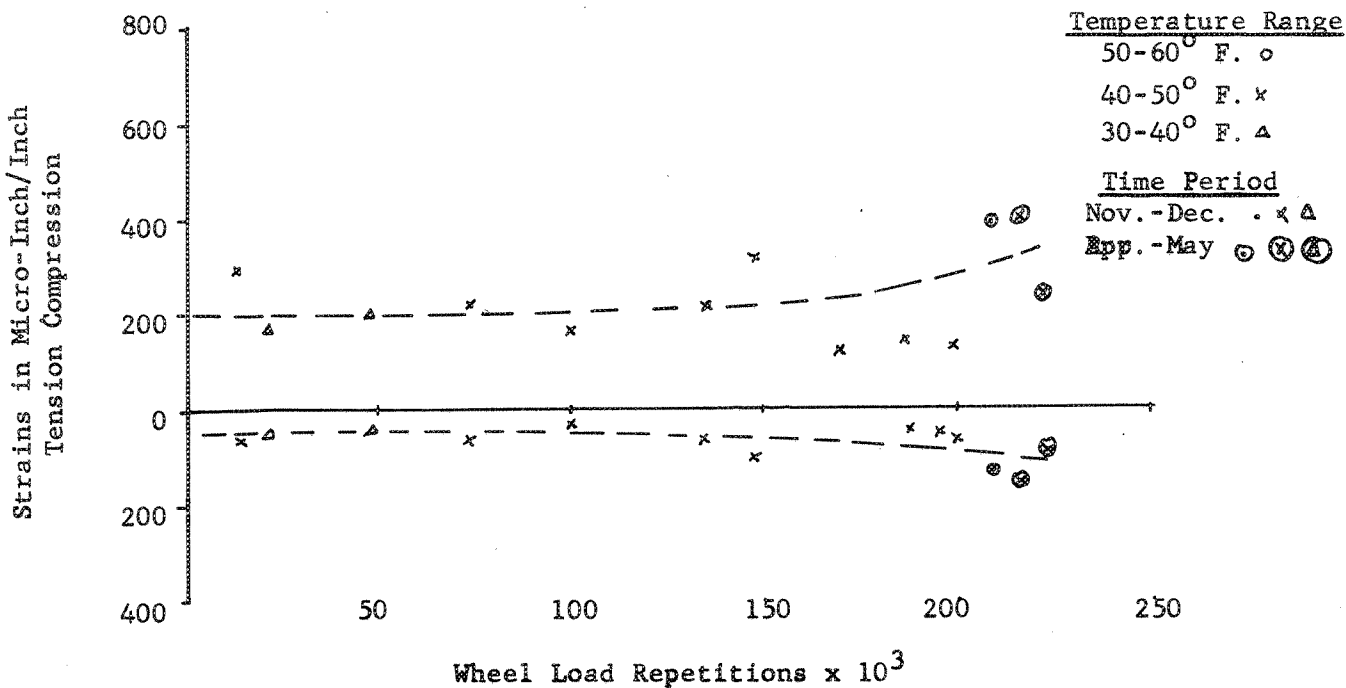


FIGURE 78.--SURFACE TRANSVERSE STRAIN GAGE B-6-T
(Ring 2, Section 8--Emulsion-Treated Base = 9.0")

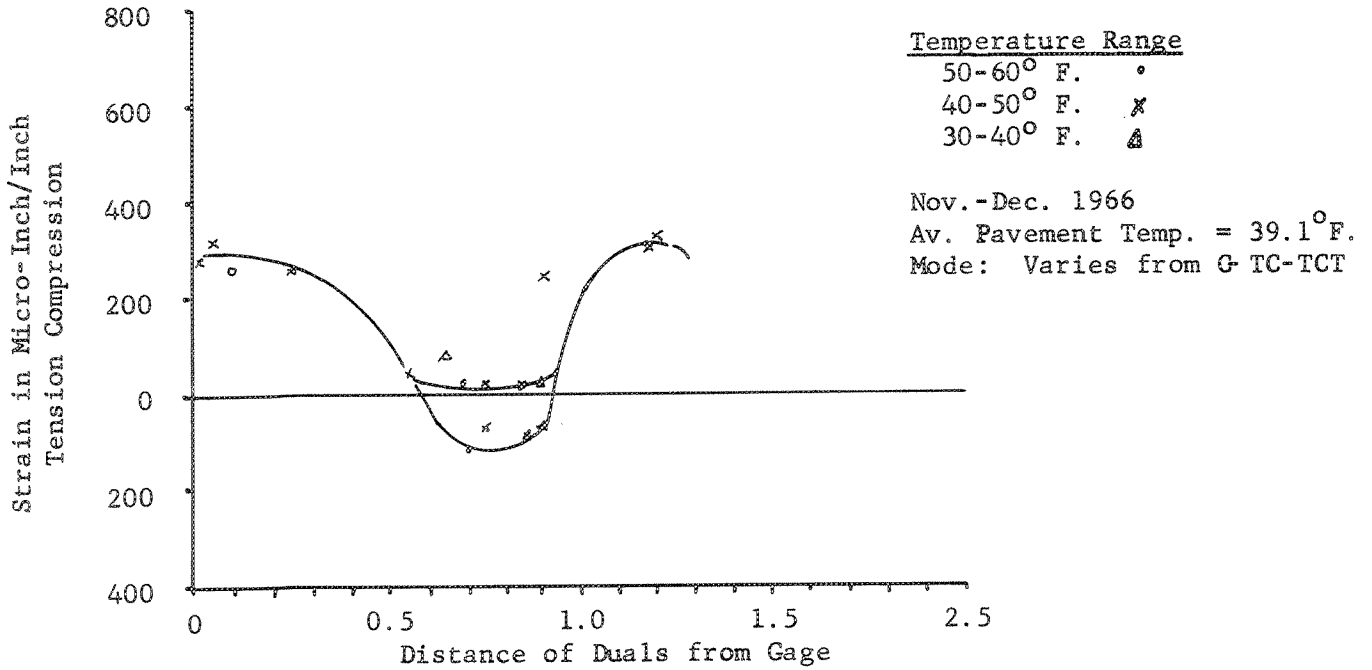


FIGURE 79.--SURFACE TRANSVERSE STRAIN GAGE B-6-T
(Ring 2, Section 8--Surface)

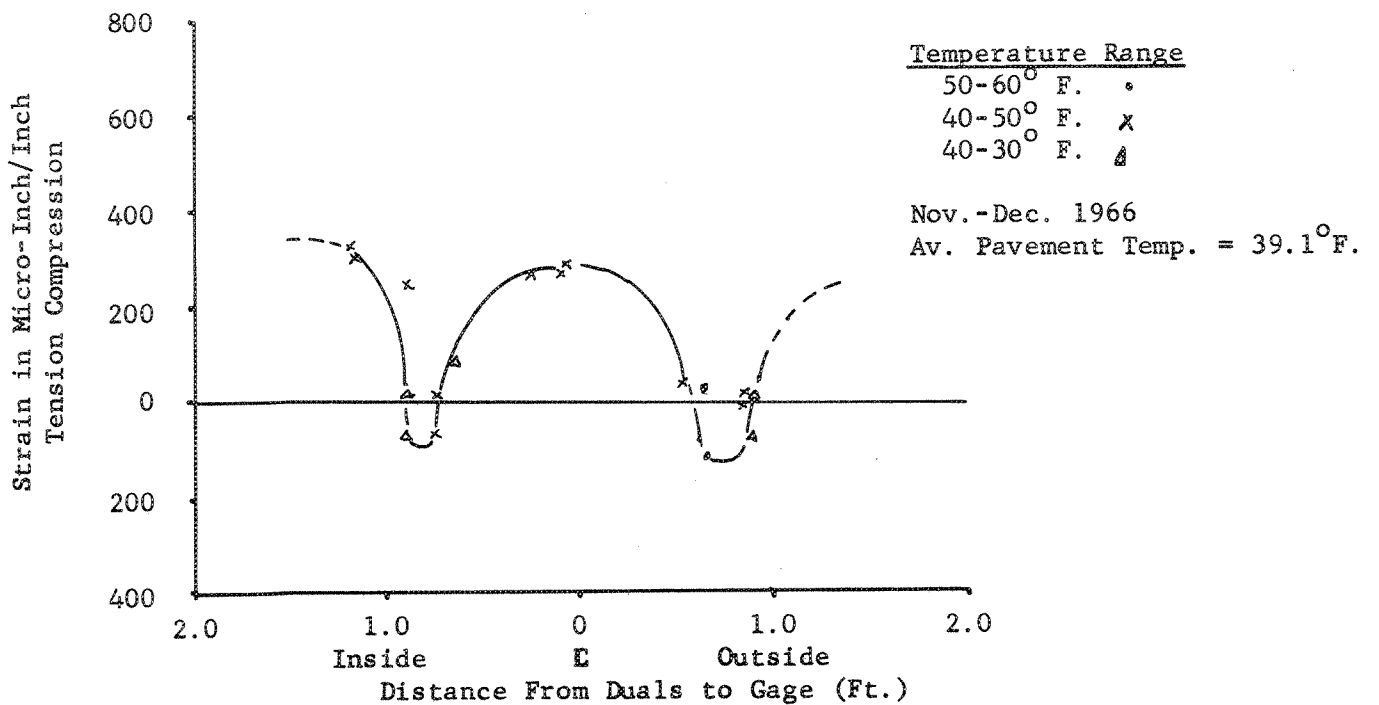


FIGURE 80.--LONGITUDINAL STRAIN GAGE C-7-L
Ring 2, Section 8

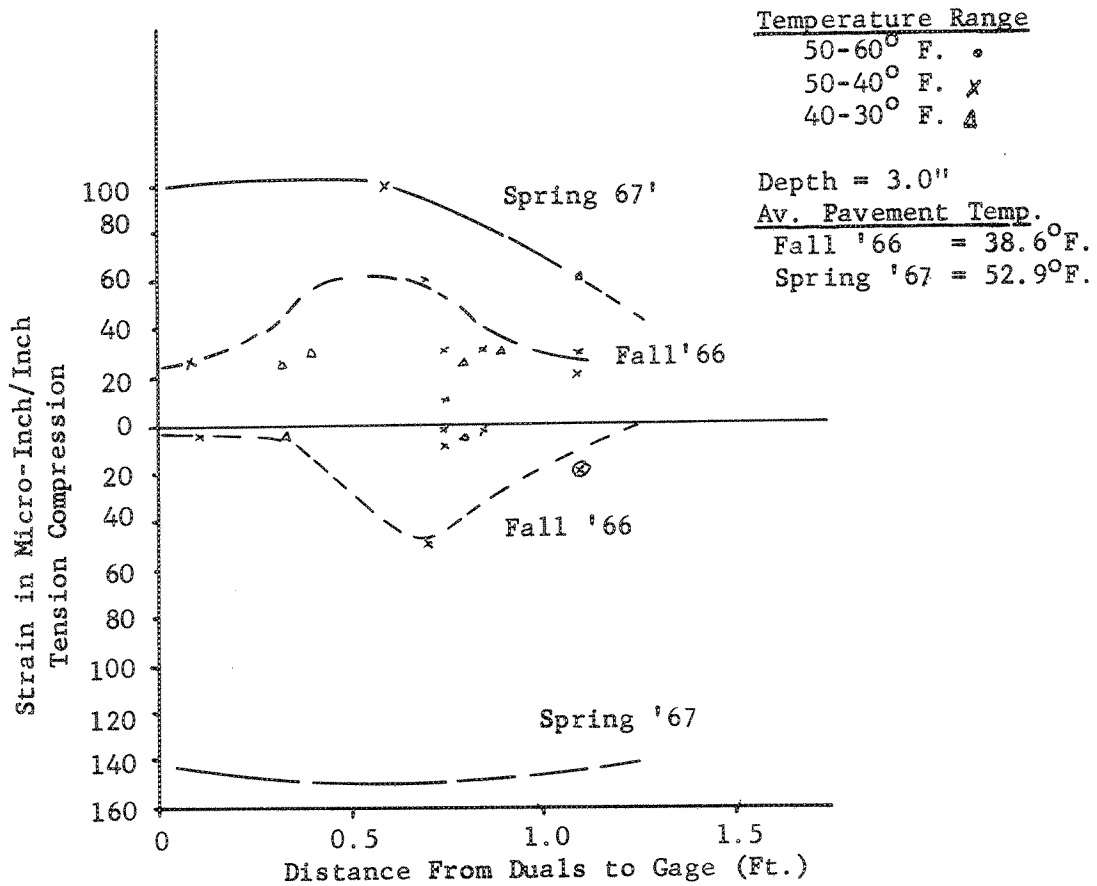


FIGURE 81.--LONGITUDINAL STRAIN GAGE C-7-L
Ring 2, Section 8

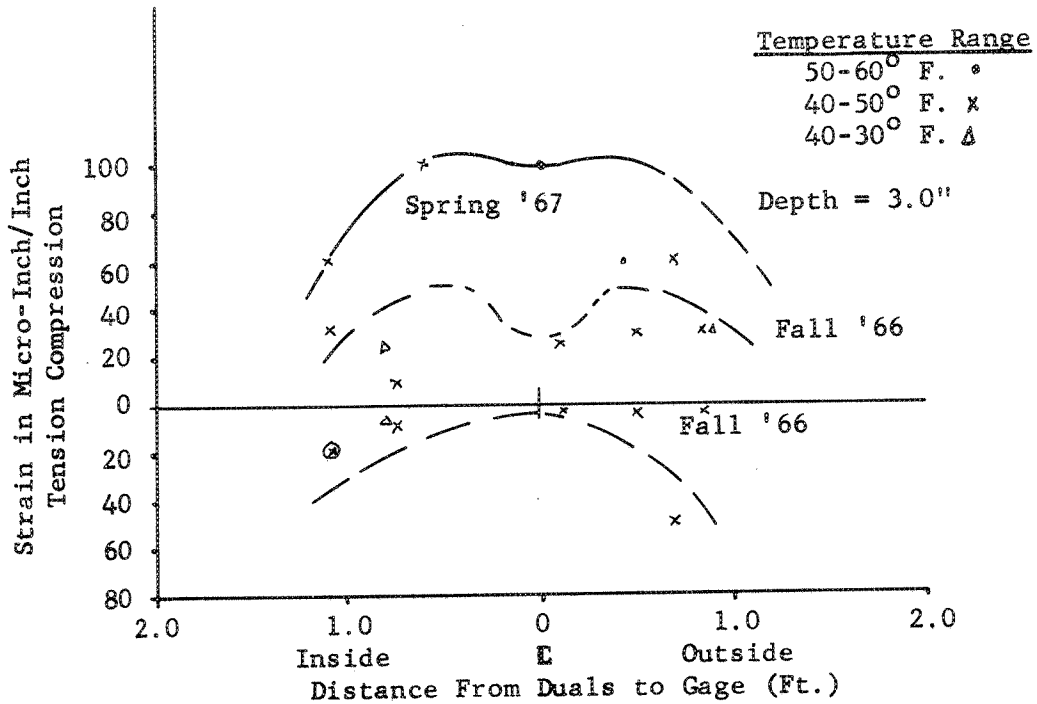


FIGURE 82.--SURFACE TRANSVERSE STRAIN GAGE B-6-T
Ring 2, Section 8

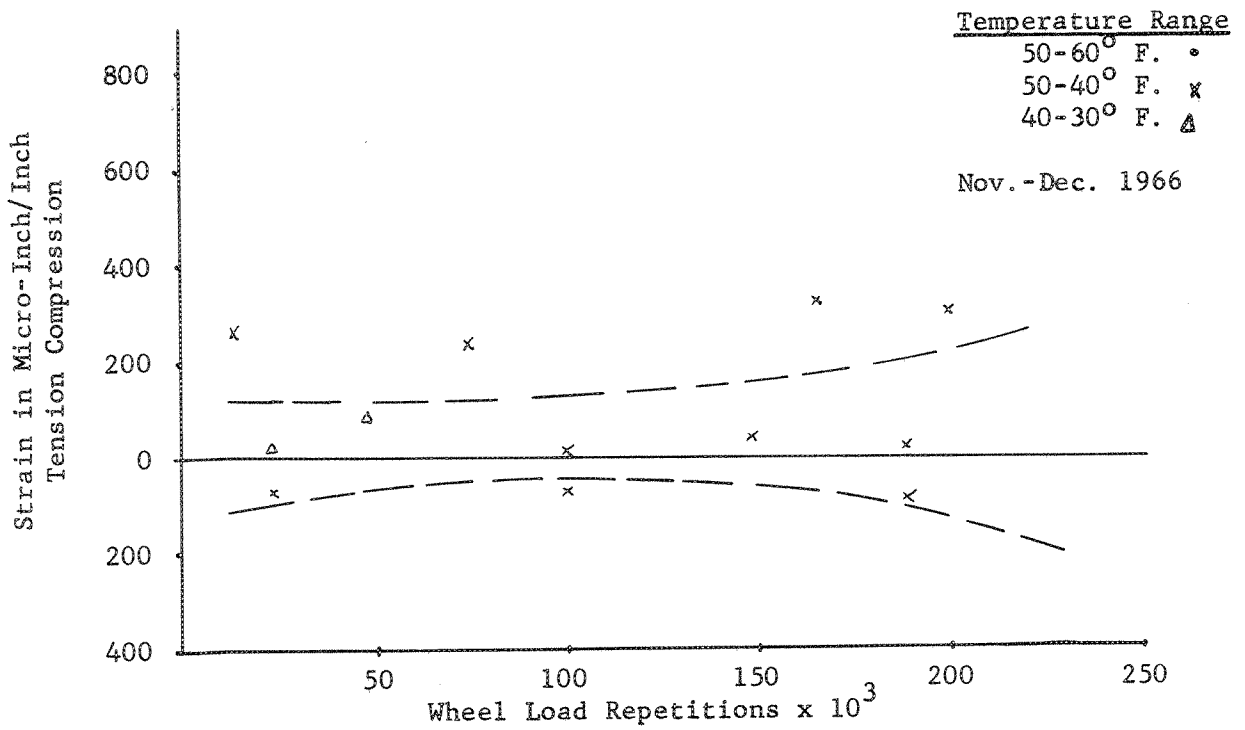


FIGURE 83.--LONGITUDINAL STRAIN GAGE C-7-L
Ring 2, Section 8

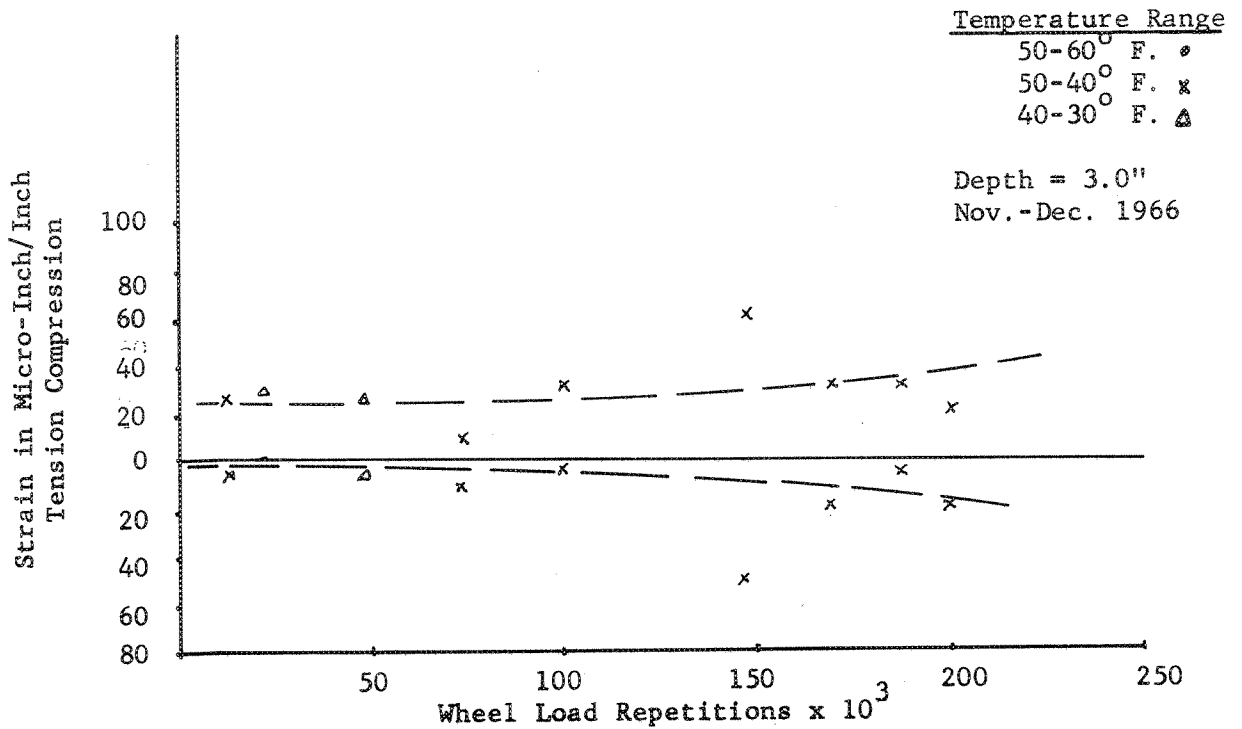


FIGURE 84.--TRANSVERSE STRAIN GAGE C-8-T
Ring 2, Section 8

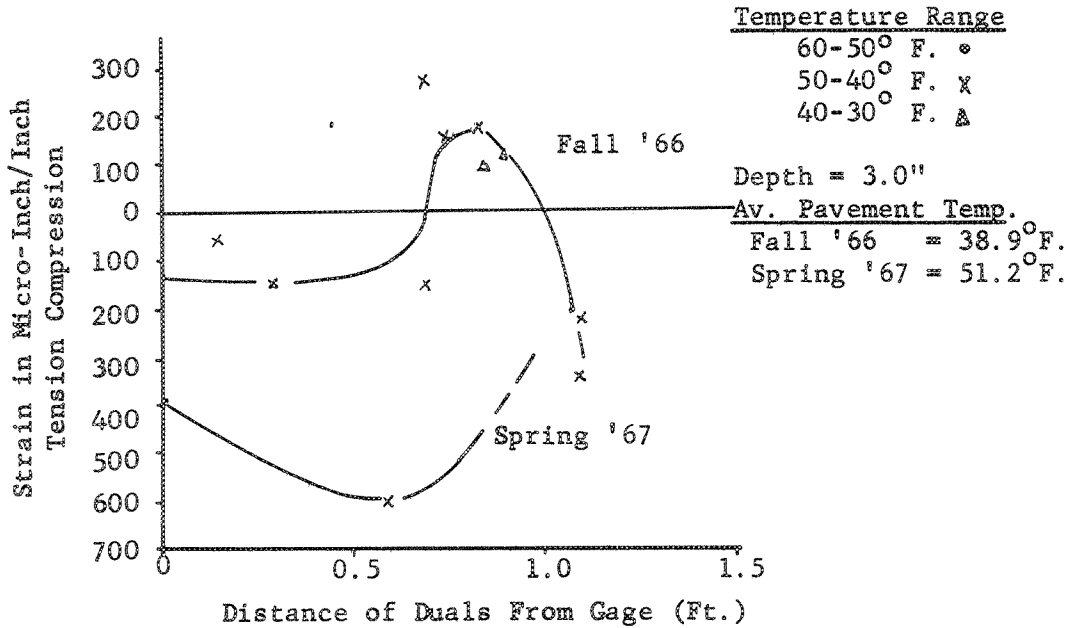
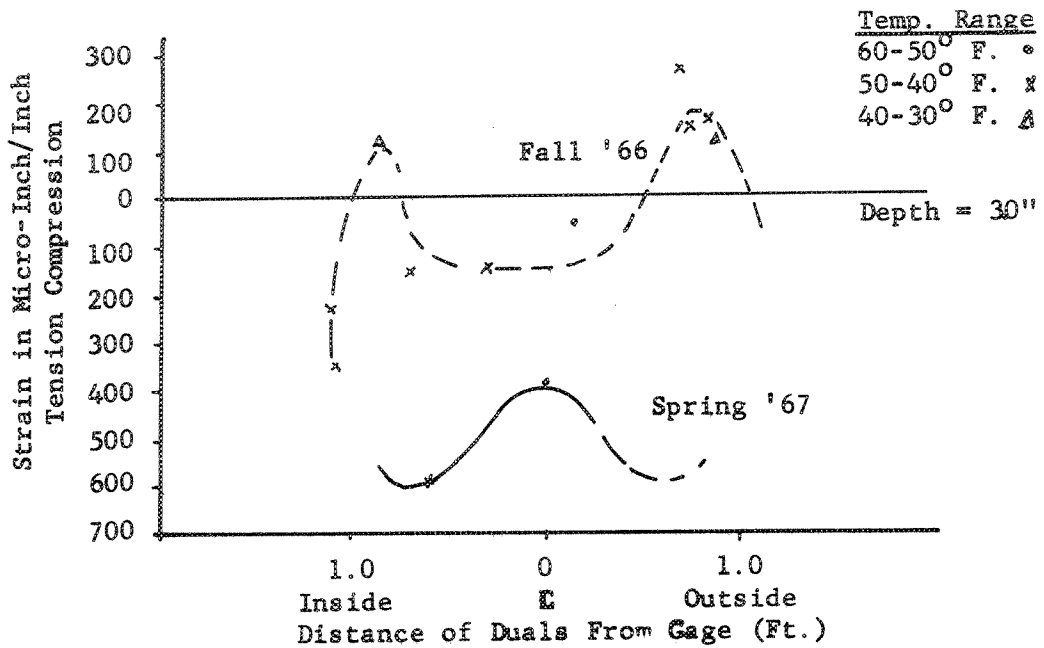


FIGURE 85.--TRANSVERSE STRAIN GAGE C-8-T
Ring 2, Section 8



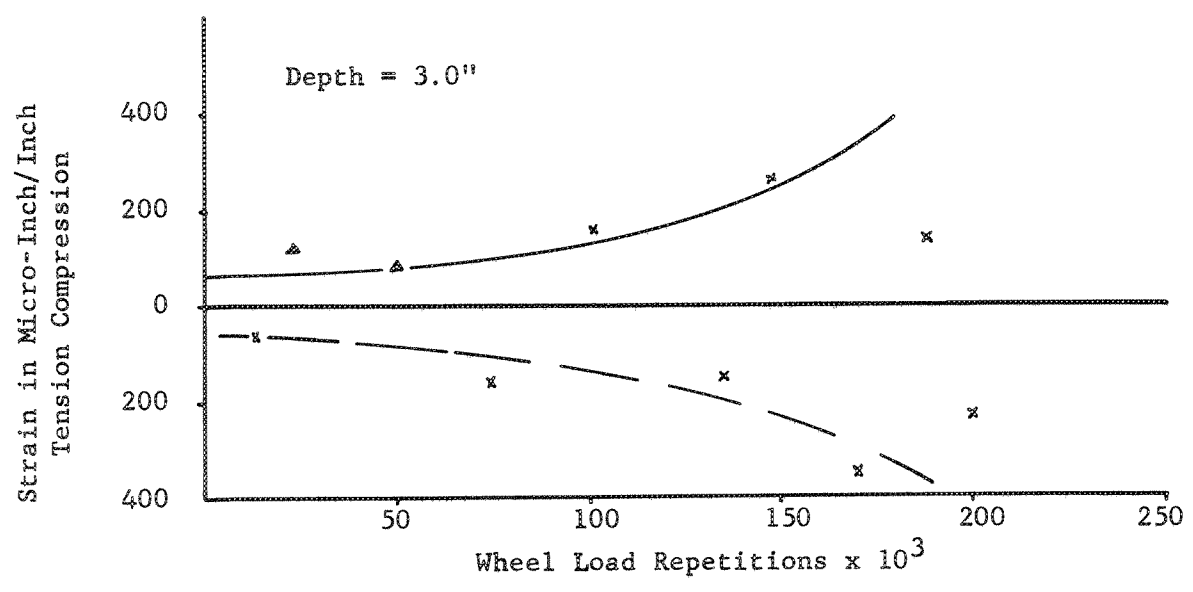


FIGURE 86.--TRANSVERSE STRAIN GAGE C-8-T
Ring 2, Section 8

FIGURE 87.--LONGITUDINAL STRAIN
Ring 2, Section 8, D-5-L

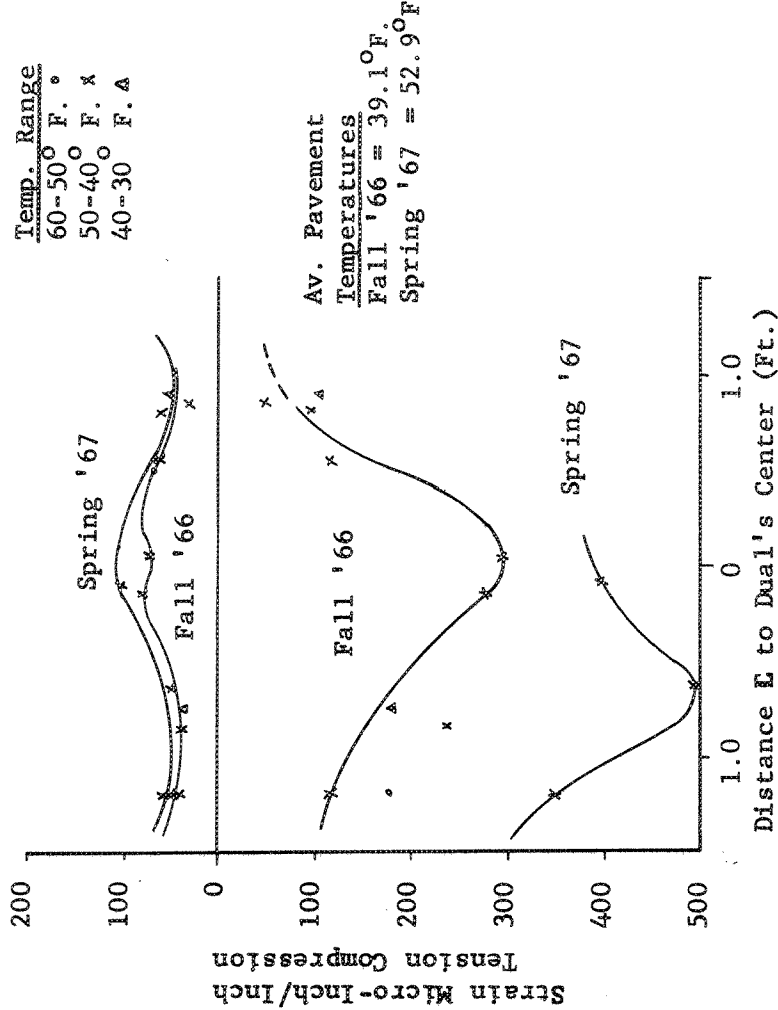


FIGURE 88.--LONGITUDINAL STRAIN
Ring 2, Section 8, D-5-L

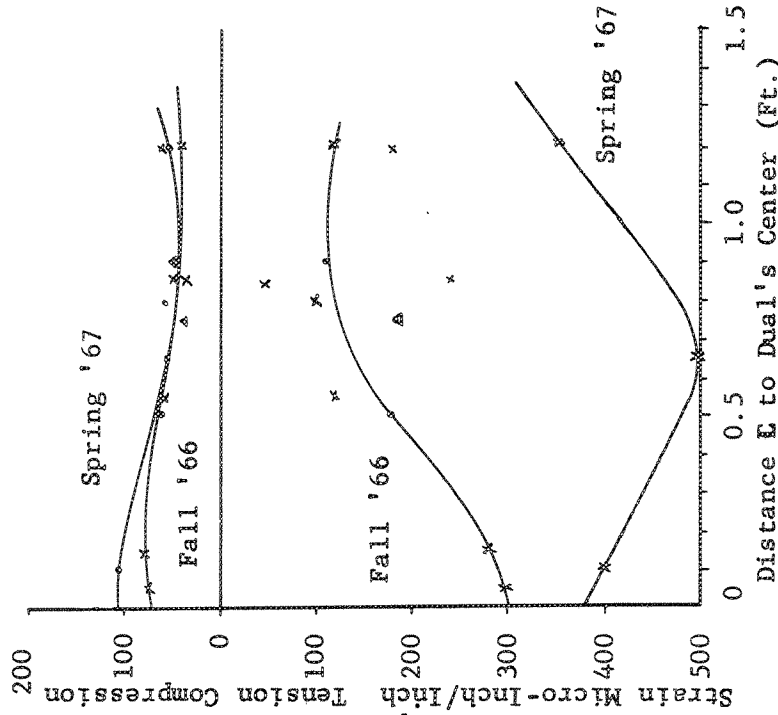


FIGURE 89. --- TRANSVERSE STRAIN
 Ring 2, Section 8, D-6-T
 Depth 3"

Av. Pavement Temperature
 Fall '66 = 34.2°F.
 Spring '67 = 53.3°F.

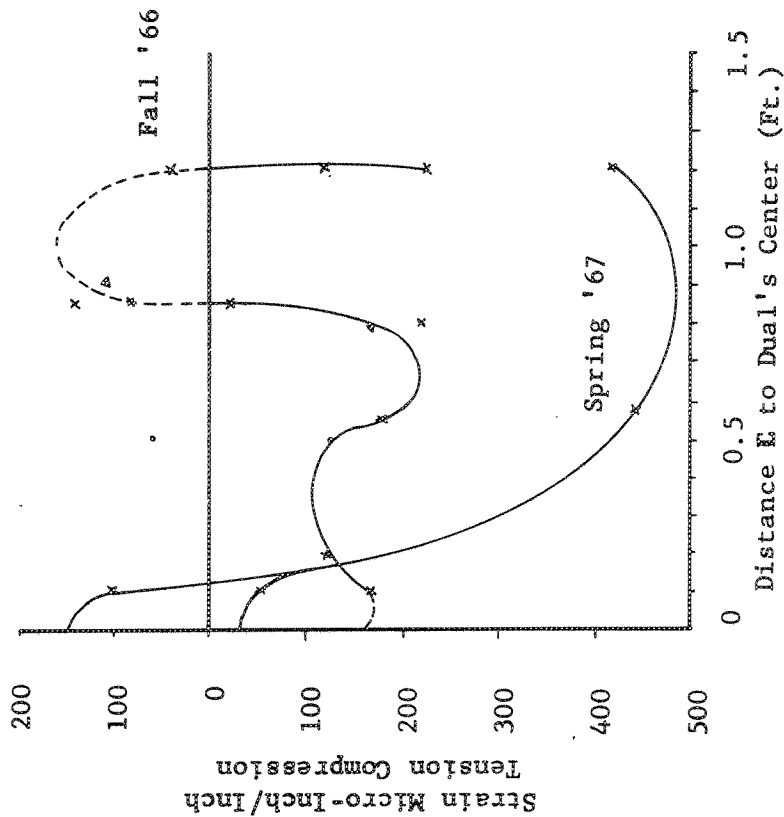


FIGURE 90. --- TRANSVERSE STRAIN
 Ring 2, Section 8, D-6-T
 Depth 3"

Temperature Range
 60-50° F. ◦
 50-40° F. x
 40-30° F. Δ

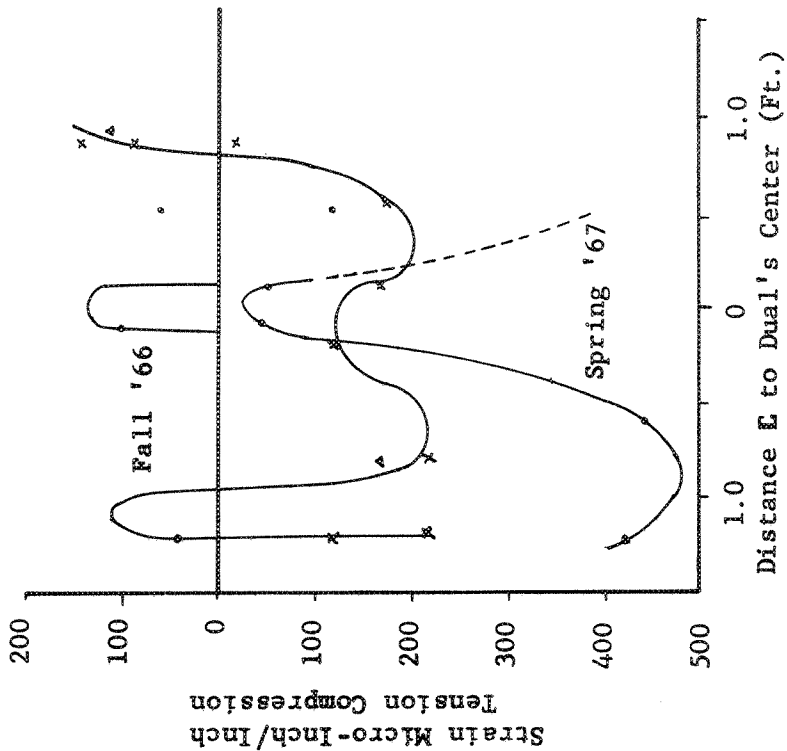


FIGURE 91.--LONGITUDINAL STRAIN GAGE D-9-L
Ring 2, Section 8

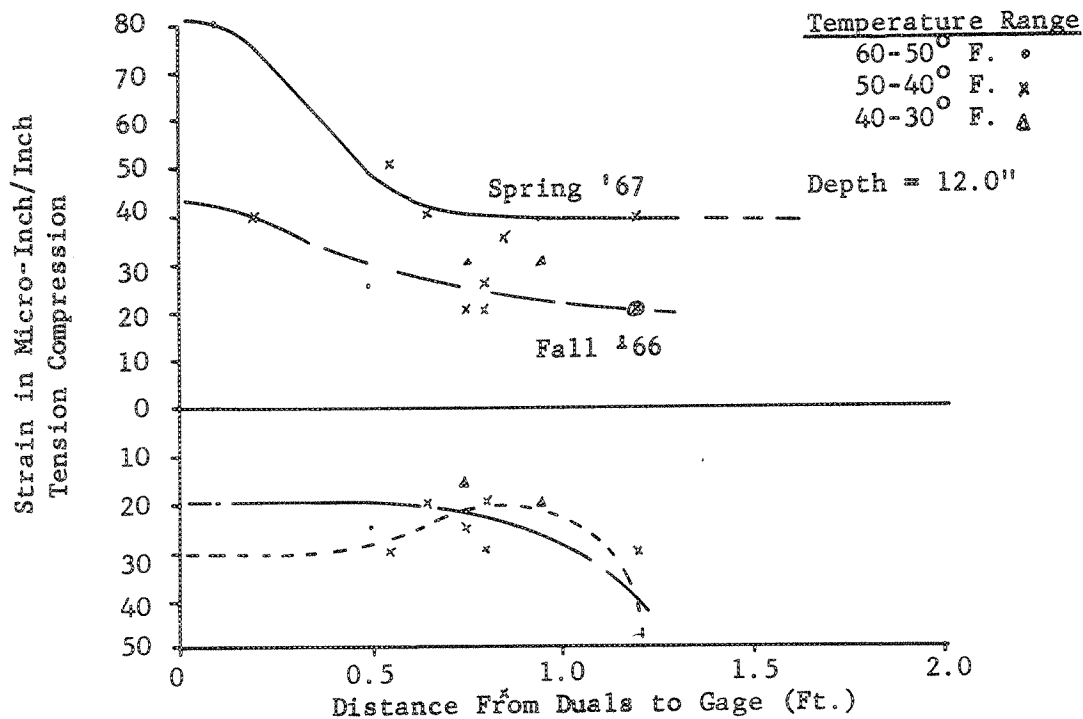


FIGURE 92.--LONGITUDINAL STRAIN GAGE D-9-L
Ring 2, Section 8

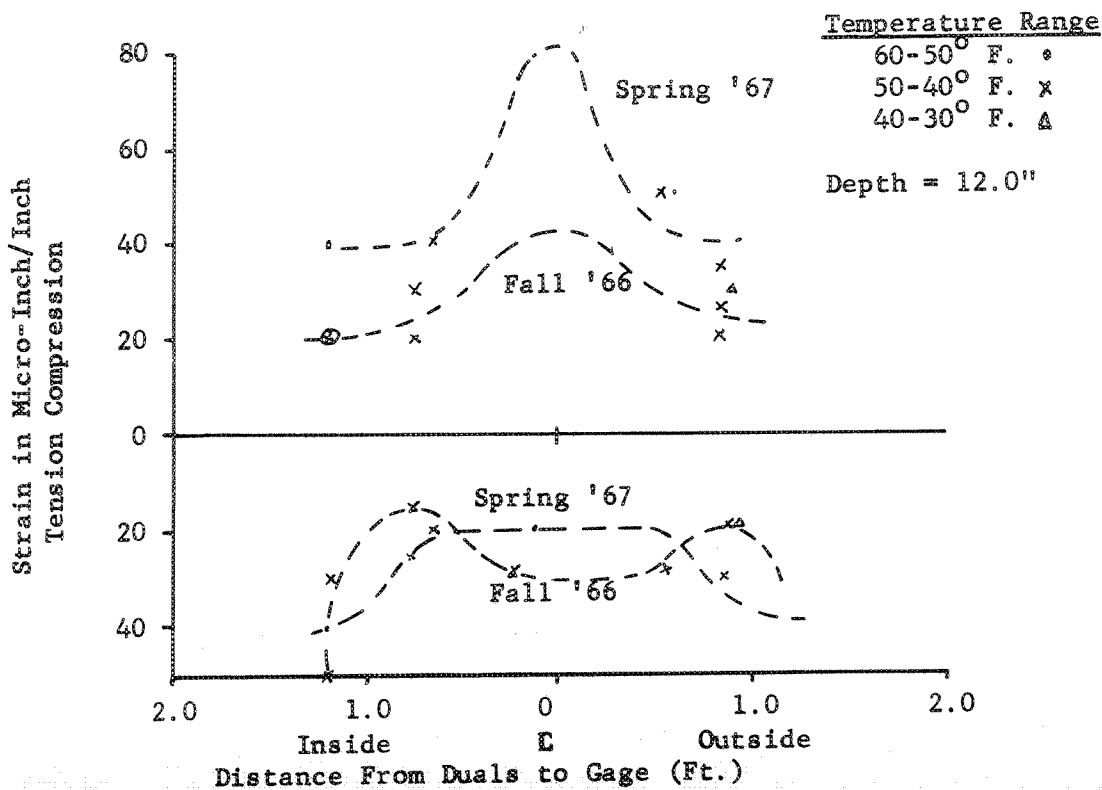


FIGURE 93.--TRANSVERSE STRAIN GAGE D-10-T
Ring 2, Section 8

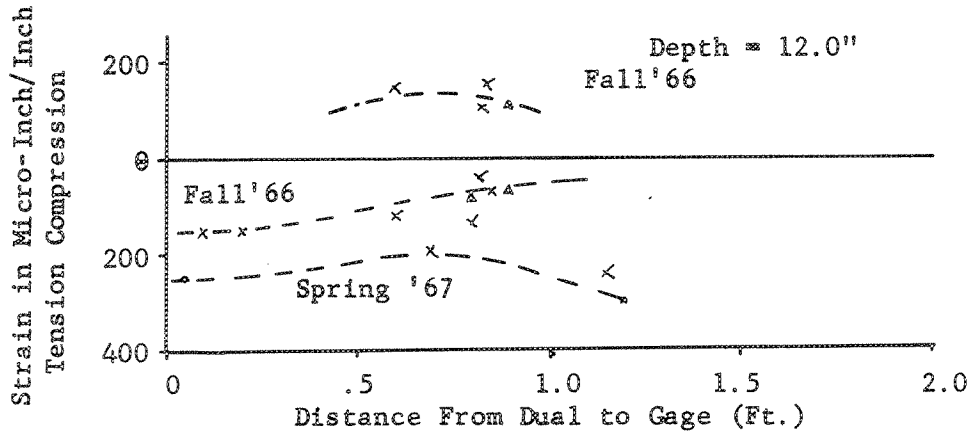


FIGURE 94.--TRANSVERSE STRAIN GAGE D-10-T
Ring 2, Section 8

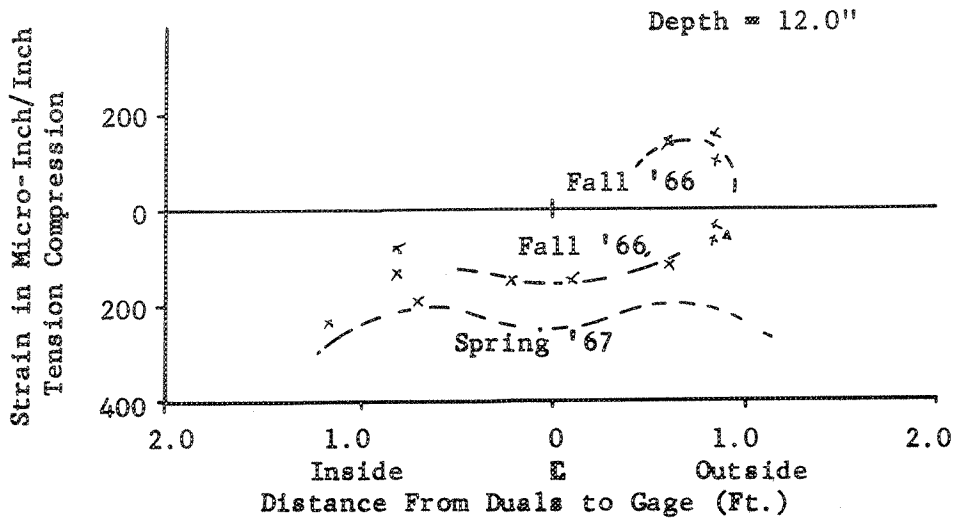
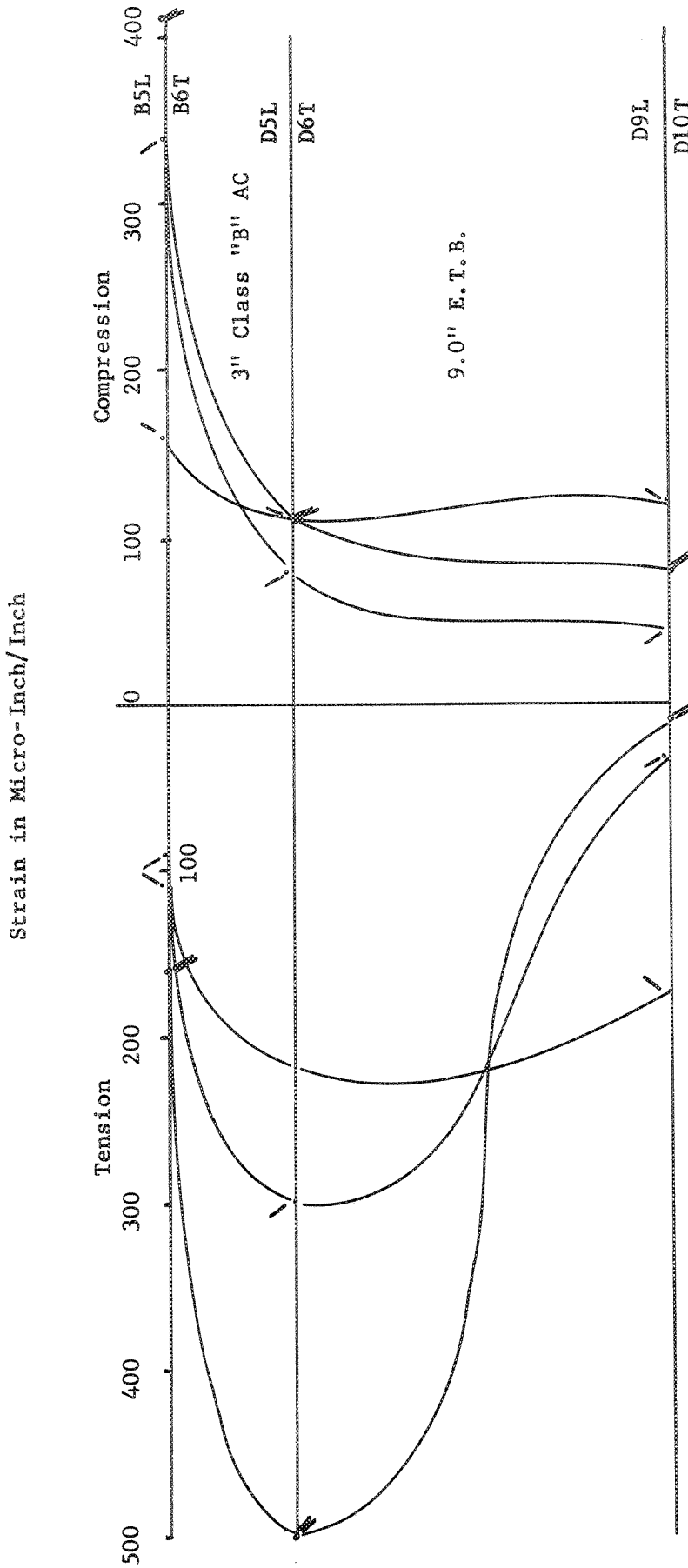


FIGURE 95. --MAXIMUM STRAIN VS DEPTH--SECTION 8 9" EMULSION-TREATED BASE



- Legend:**
- \ Fall '66 Longitudinal Gages (B-5-L, D-5-L, D-9-L)
 - / Fall '66 Transverse Gages (B-6-T, D-6-T, D-10-T)
 - Spring '67 Longitudinal Gages (B-5-L, D-5-L, D-9-L)
 - B-5-L & B-6-T on surface
 - D-5-L & D-6-T 3" deep
 - ◇ D-9-L & D-10-T 12" deep

FIGURE 96.--LONGITUDINAL STRAIN GAGE B-9-L
Section 10, Surface

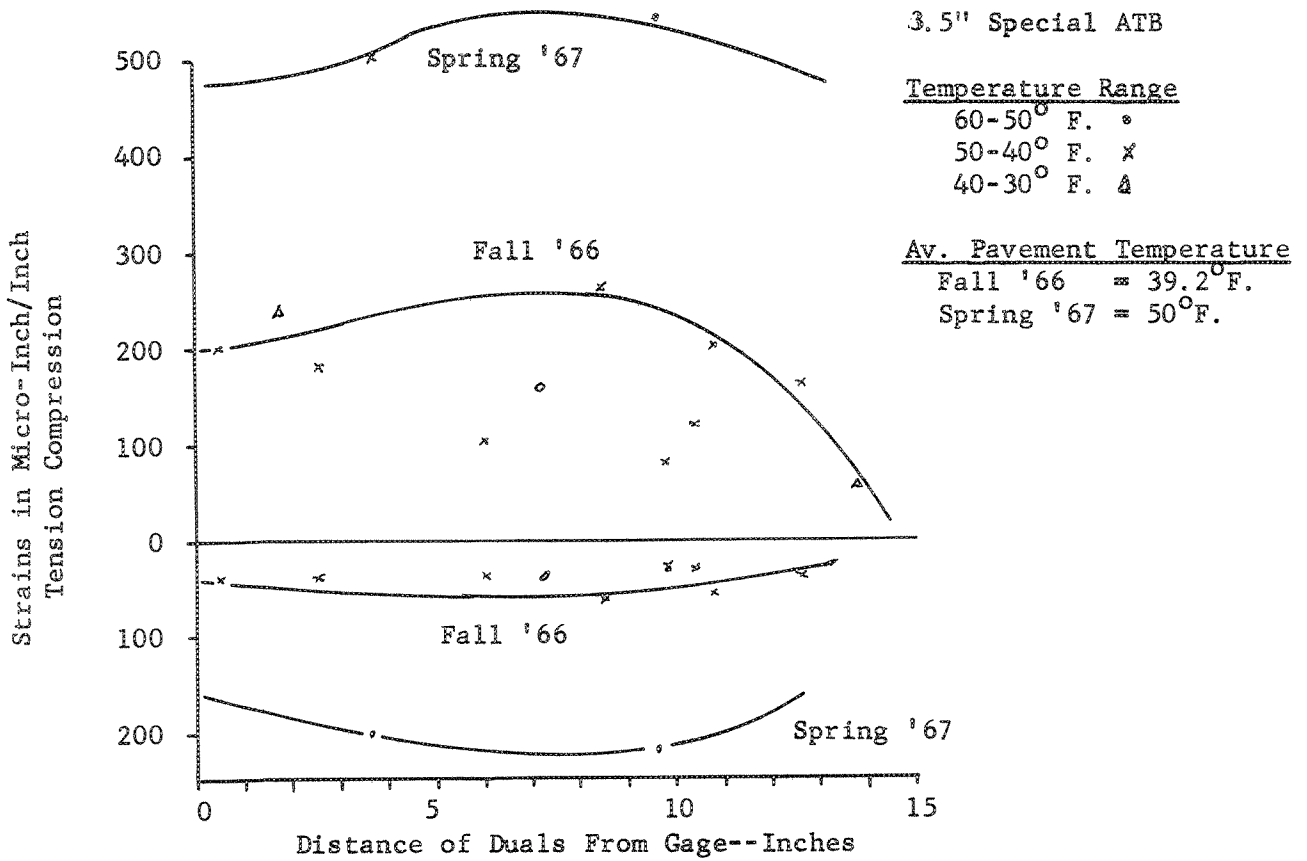


FIGURE 97.--TRANSVERSE STRAIN GAGE B-10-T

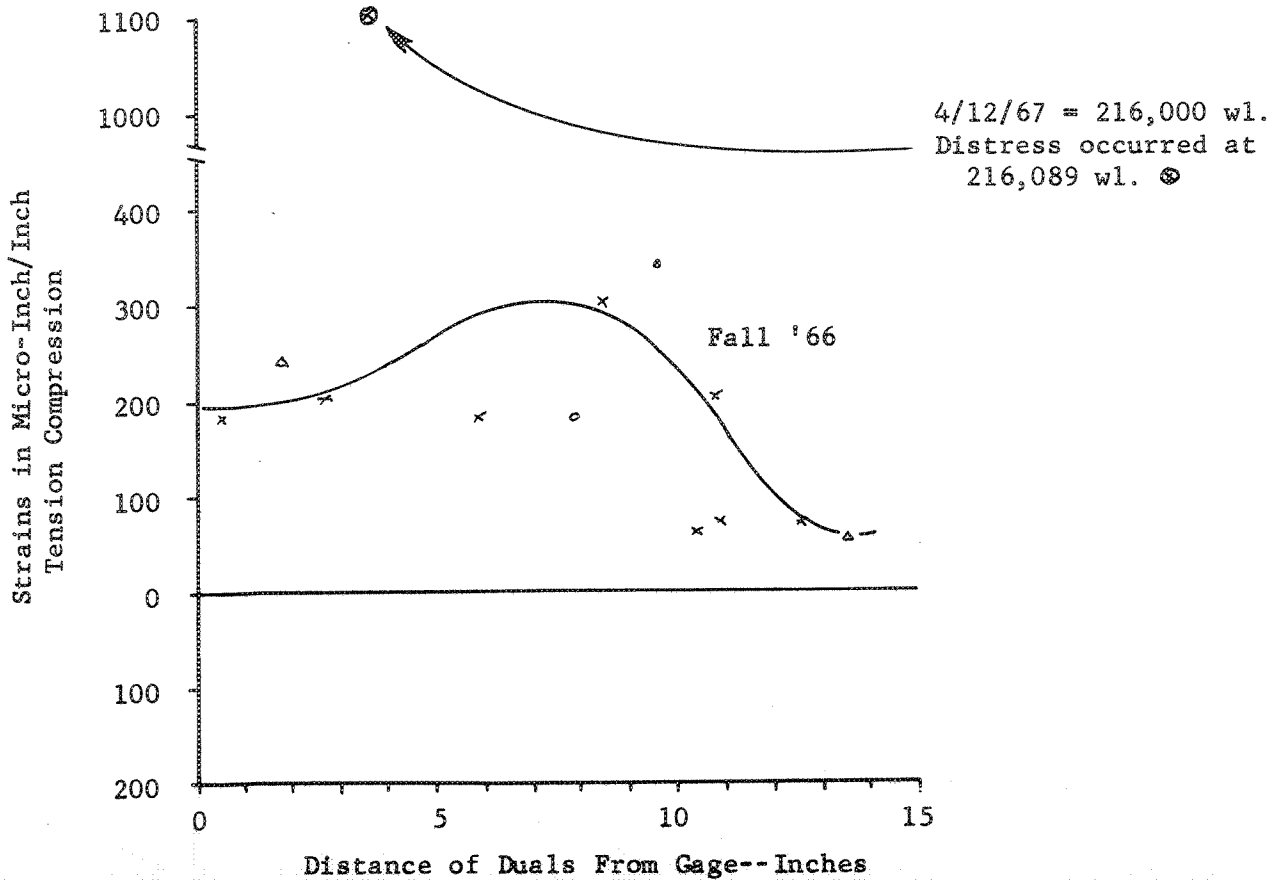


FIGURE 98.--LONGITUDINAL STRAIN GAGE C-9-L
Section 10, 3.0" Depth

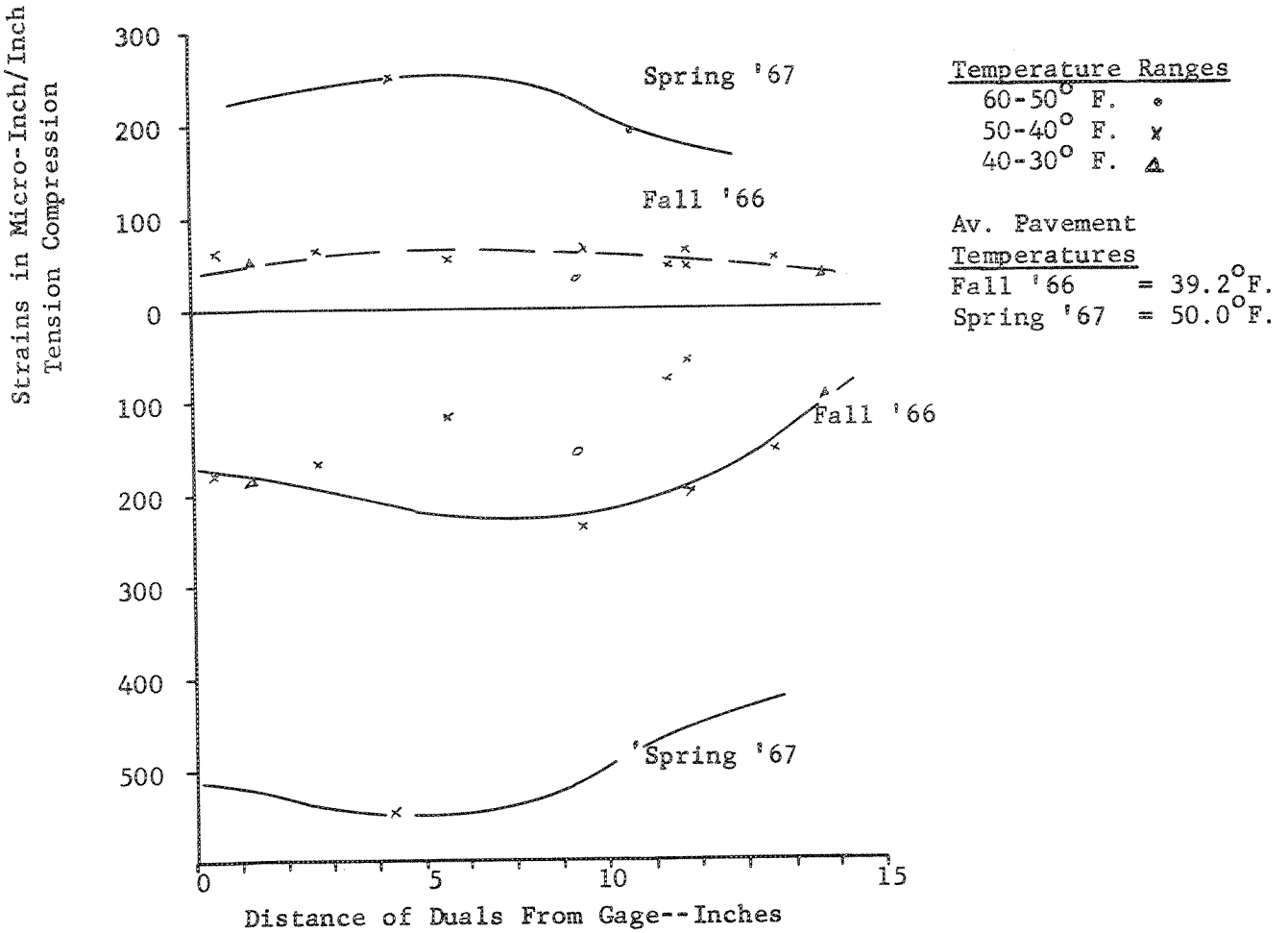


FIGURE 99.--TRANSVERSE STRAIN GAGE C-10-T

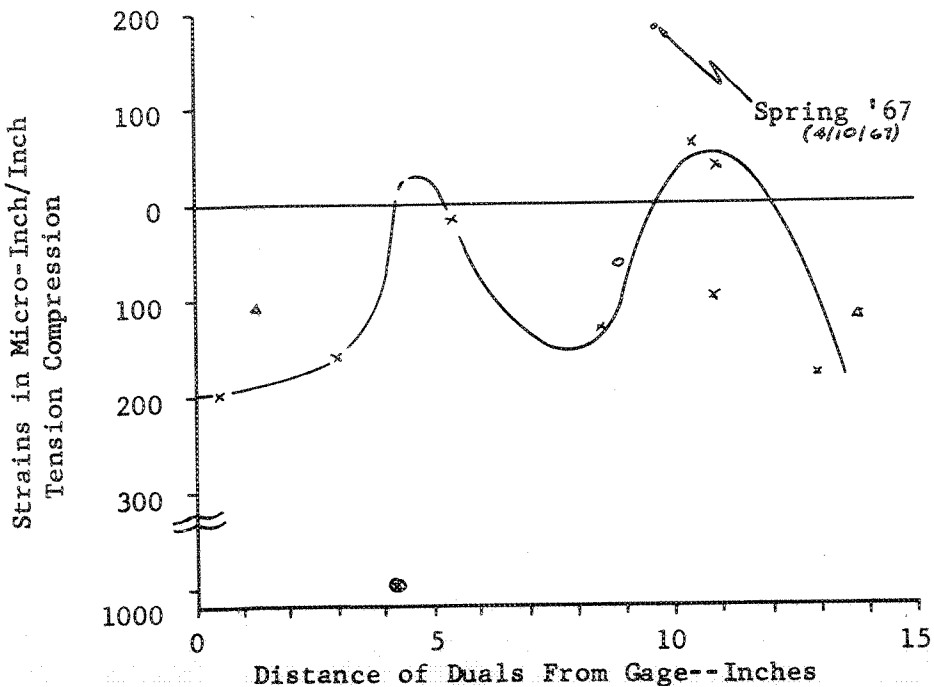
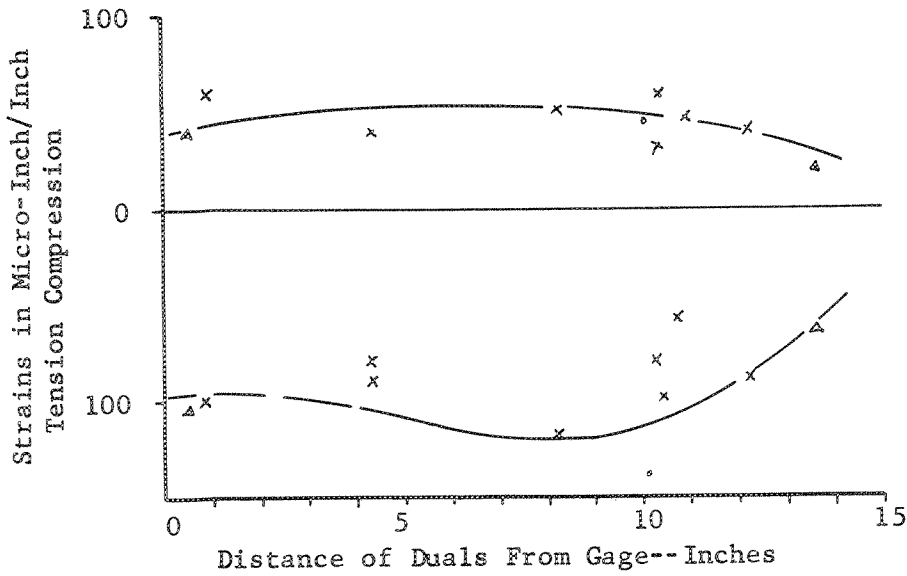


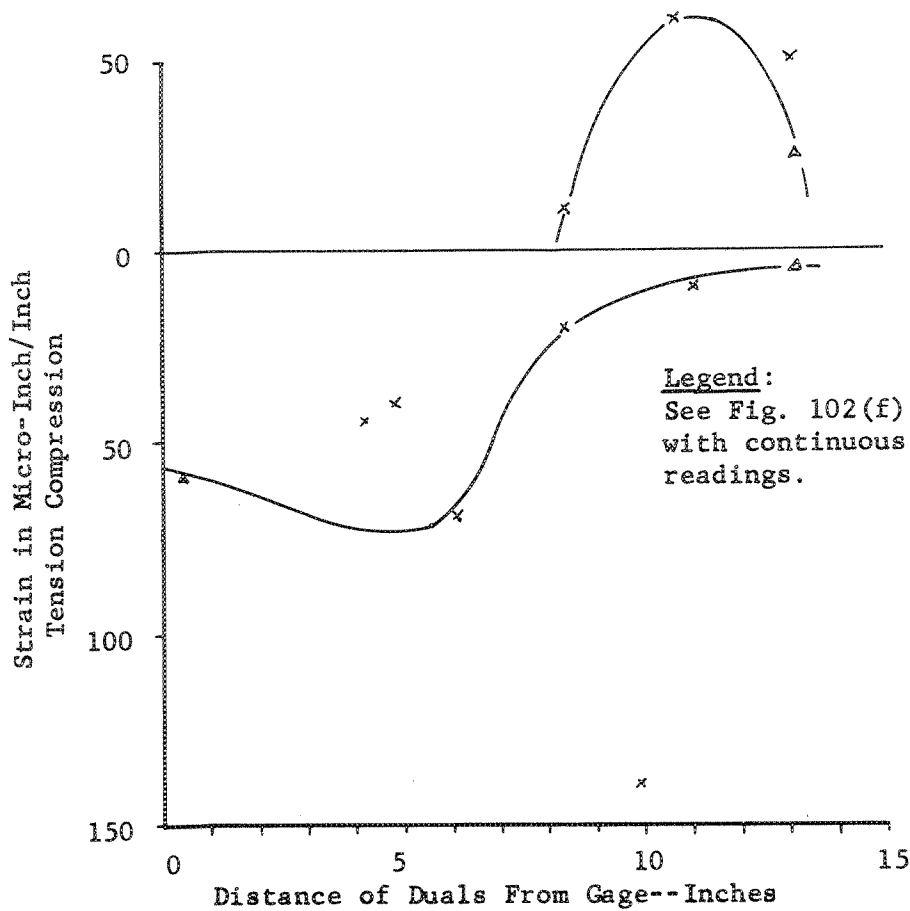
FIGURE 100.--LONGITUDINAL STRAIN GAGE E-1-L
Section 10, 6.5" Depth



Temperature Range
60-50° F. •
50-40° F. x
40-30° F. Δ

Av. Pavement
Temperatures
Fall '66 = 39.1° F.

FIGURE 101.--TRANSVERSE STRAIN GAGE E-2-T



Av. Pavement
Temperatures
Fall '66 = 38.5° F.

Legend:
See Fig. 102(f) for comparison
with continuous strain gage
readings.

FIGURE 102.--MAXIMUM VALUES OF STRAIN MEASURES AS WHEELS WERE MOVING LONGITUDINALLY WITH RESPECT TO LATERAL WHEEL POSITION--SECTION 10
3" Special A.T.B.

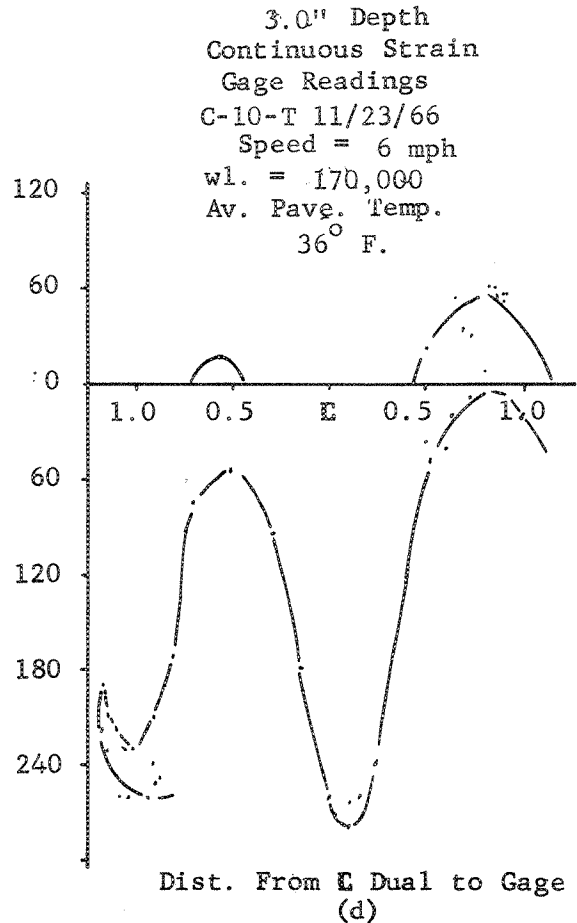
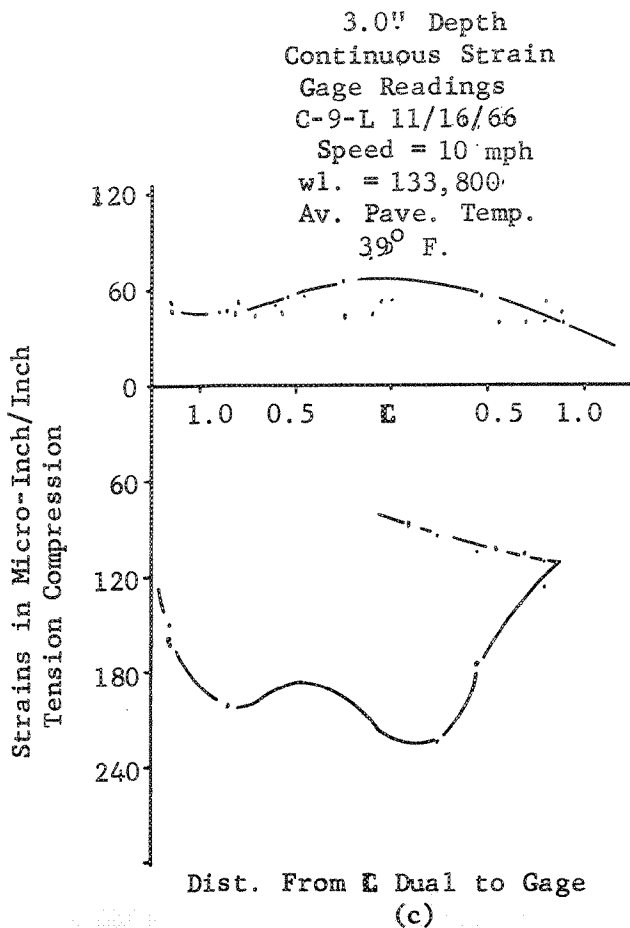
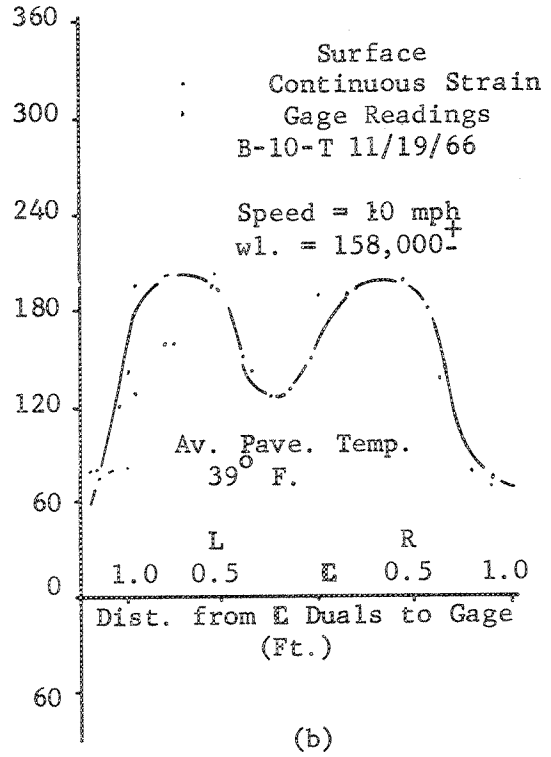
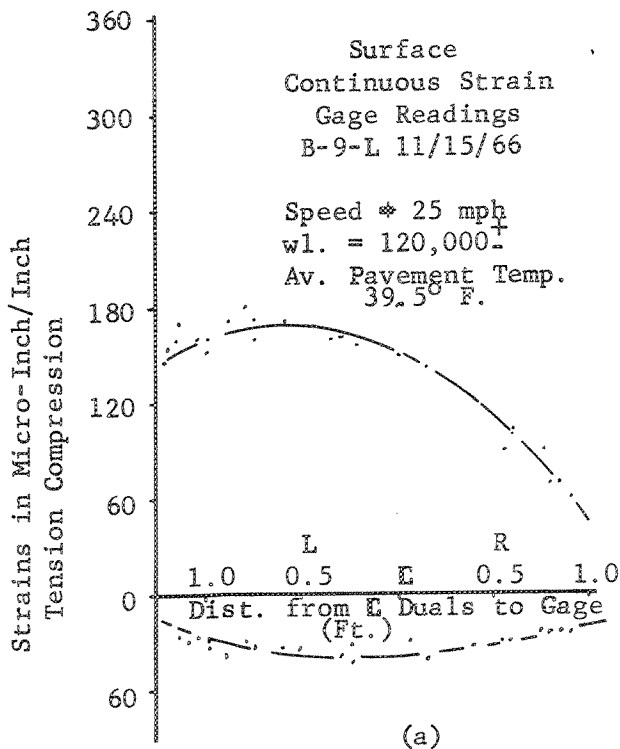
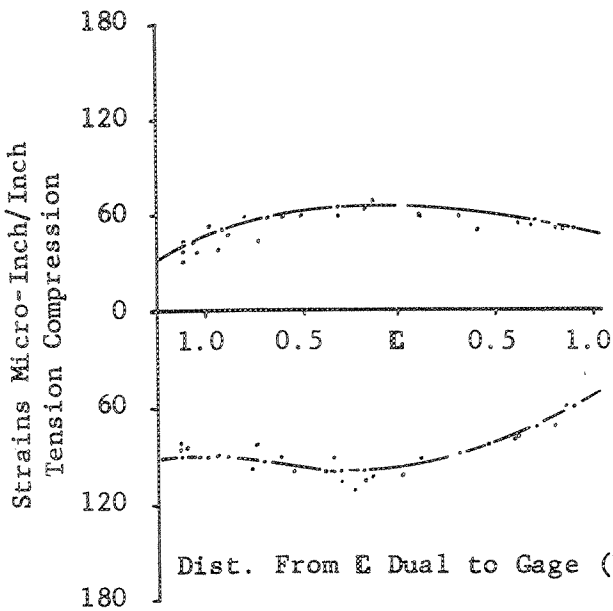
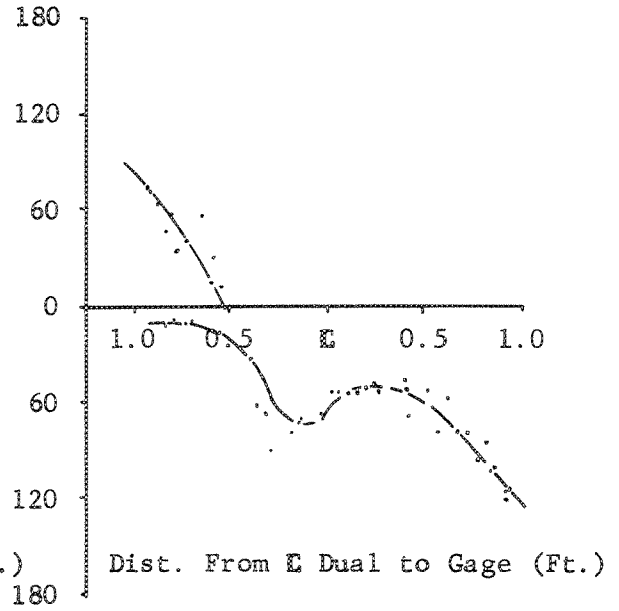


FIGURE 102.--(Cont'd.)



6.5" Depth
Continuous Strain
Gage Readings
E-1-L 11/28/66
Speed * 5 mph
wl. = 188,000
Av. Pave. Temp.
36.5° F.

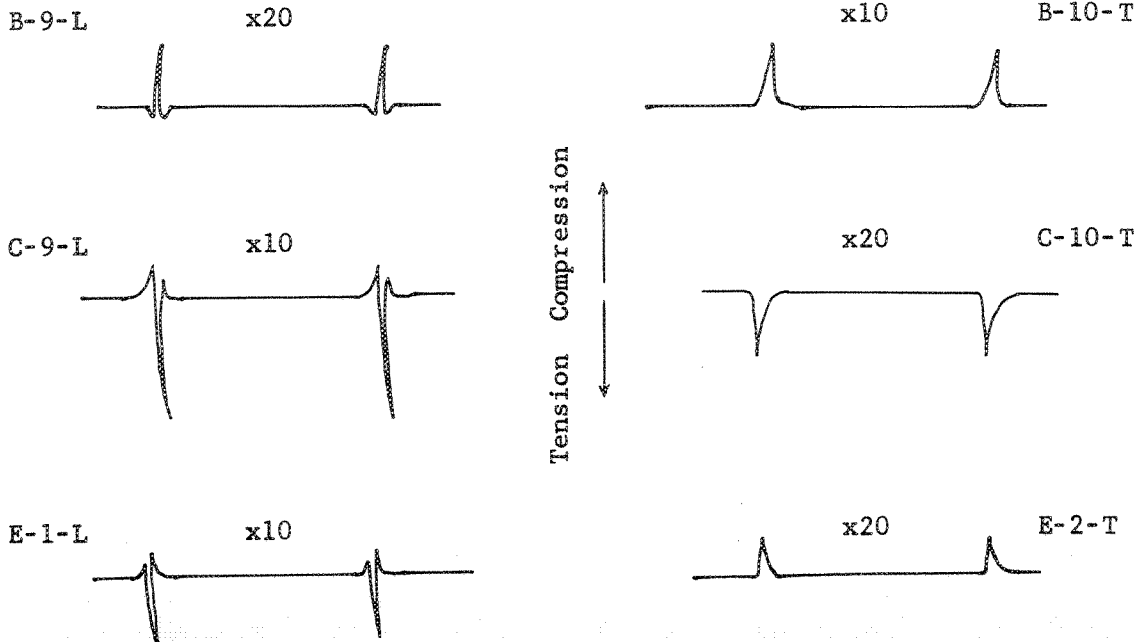
(e)



6.5" Depth
Continuous Strain
Gage Readings
E-2-T 12/1/68
Speed = 5 mph
wl. = 199,000
Av. Pave. Temp.
40.5° F.

(f)

FIGURE 102(g) SOME TYPICAL STRAIN GAGE READINGS
Speed = 10 mph Chart Speed = 5 mm/sec
Distance: 1.05' inside E duals to gage
W. L. = 134,300
Nov. 16, 1966



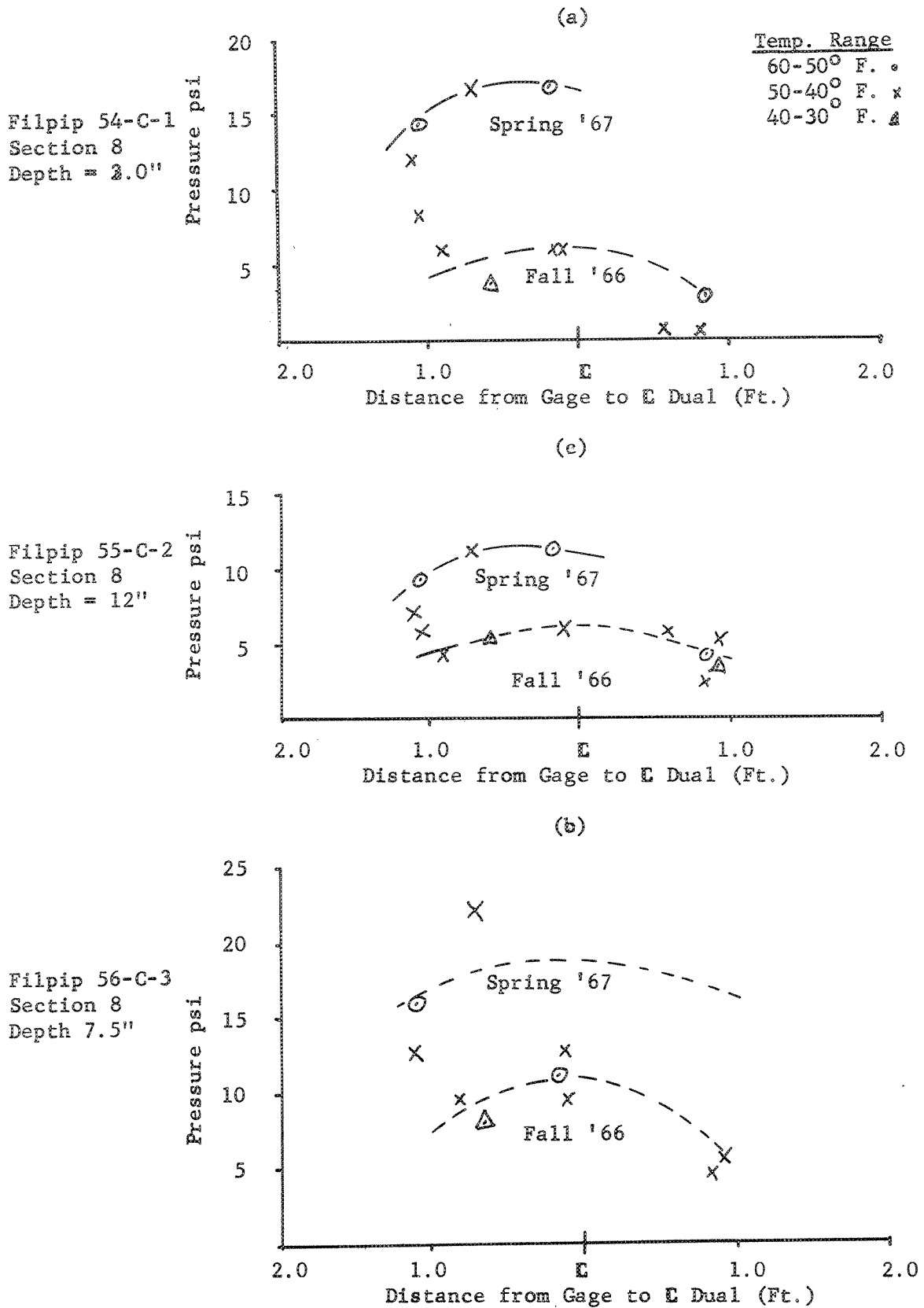
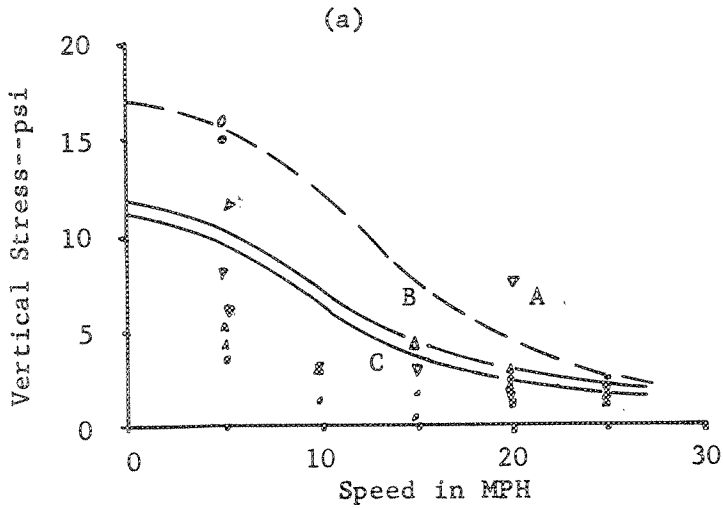


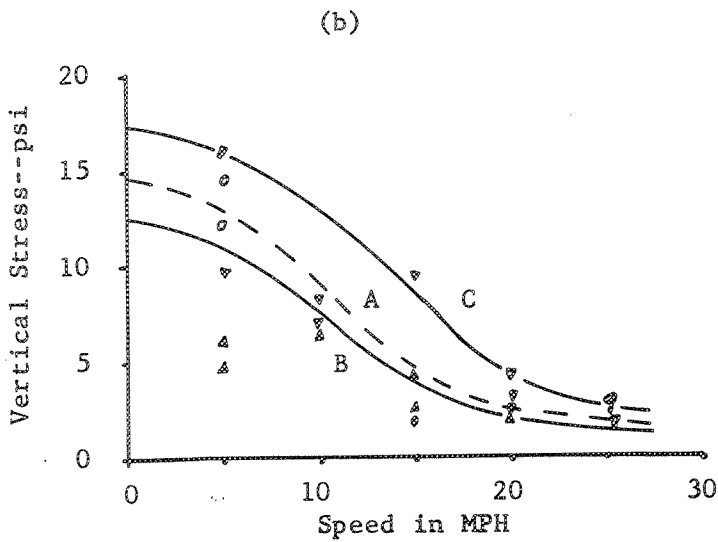
FIGURE 103.--VERTICAL STRESSES MEASURED BY FILPIP TRANSDUCERS WITH RESPECT TO LATERAL WHEEL POSITION

FIGURE 104.--VERTICAL STRESS VS SPEED WSU PRESSURE CELL

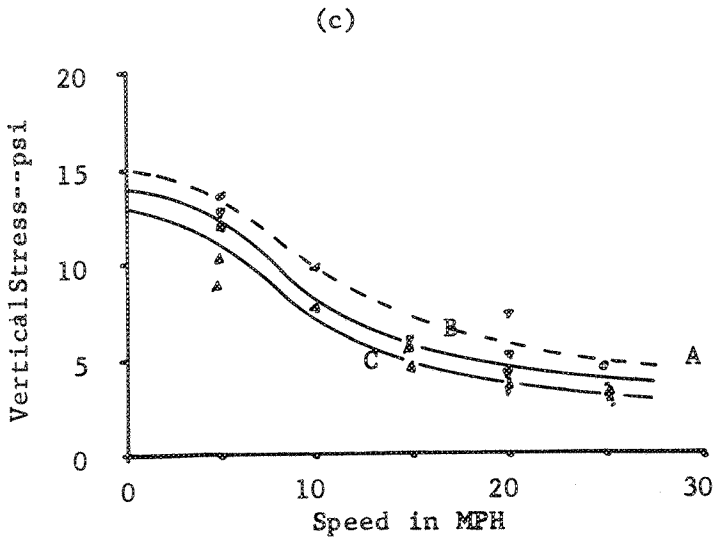


Section 6: 5.0" E.T.B.
 Cell Depth = 3.0"
 WSU Cell #3

Tire Size: 11:00 x 22.5
 Tire Pressure: 80 psi
 Wheel Load: 5,300 lbs.
 Dual Load: 10,600 lbs.



Section 8: 9.0" E.T.B.
 Cell Depth = 3.0"
 WSU Cell #2



Section 8: 9.0" E.T.B.
 Cell Depth = 12.0"
 WSU Cell #1

Legend:
 E Duals ---o---o--- A
 Inside Tire ▲▲▲▲ B
 Outside Tire ▼▼▼▼ C

FIGURE 105.--VERTICAL SUBGRADE¹ STRESS AS A FUNCTION OF BASE MATERIAL, DEPTH² AND ENVIRONMENT

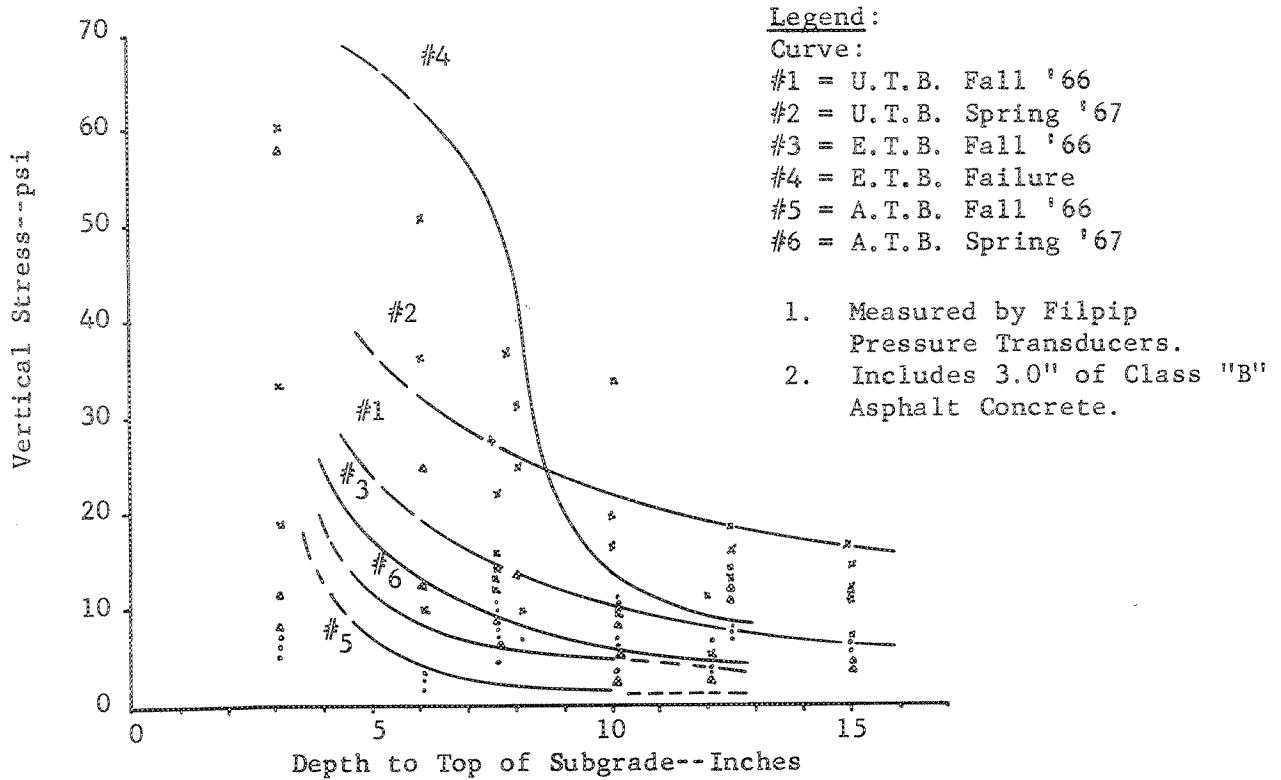
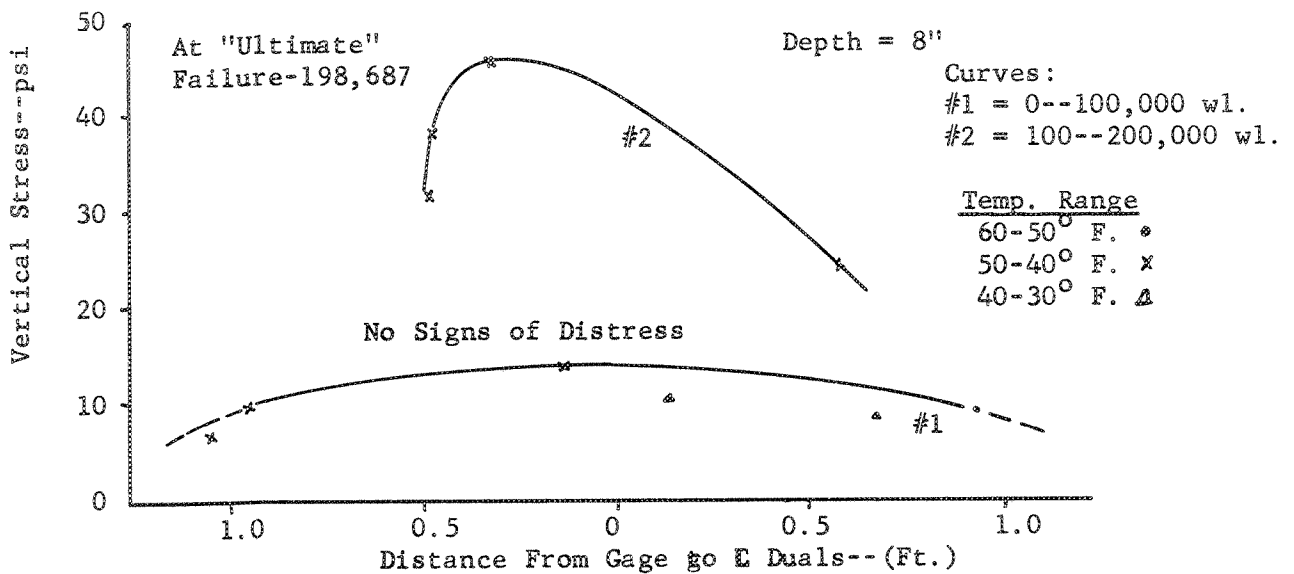


FIGURE 106.--TRANSVERSE VERTICAL STRESS¹ DISTRIBUTION Section 6: 5.0" E.T.B.



1. Measured by Filpip Pressure Transducers.

TABLE XXIII: SUMMARY OF MAXIMUM VERTICAL STRESSES

Section	Period	Gage Depth Inches	Filpip Transducer Readings		MSU Pressure Cell Readings	
			Vertical Stress PSI	Lateral Position of & Duals-Ft.	Vertical Stress PSI	Lateral Position of & Duals-Ft.
1	Spring	7.5	28	0.55		
2	Fall	3.0 ¹	96	0.83		
	Spring	10.0	33.6	0.10		
3	Spring	12.5	18	0.44		
4	Spring	15.0	16.8	0.34		
5	Fall	6.0	62.4	0.30		
6	Fall	3.0 ¹	102.0	0.58	15.9	0.25
	Fall	8.0	46.0	0.32		41
7	Fall	10.0	11.3	Not defined		
8	Spring	3.0 ¹	16.8	0.72	16.0 ²	0.81
	Spring	7.5 ¹	22.4	0.72		41
	Spring	12.0	11.2	0.72	13.5 ²	0.04
9	Spring	5.0	72.4	Not defined		
10	Spring	3.0	8.4	0.28		
	Fall	6.5	7.0	0.55		
12	Spring	3.0 ¹	6.0	0.20		
	Fall	9.5	10.0	0.25		

¹Filpips at this position seem to read erratically.

²Fall period.

TABLE XXIV
STRESS REDUCTION RATIOS¹ FOR DIFFERENT BASE MATERIALS

Base Depth (inches)	Period	Untreated Base		Emulsion Treated ²		Asphalt Treated	
		Stress PSI	Stress Reduction Ratio ²	Stress PSI	Stress Reduction Ratio	Stress PSI	Stress Reduction Ratio
2.0	Fall	24.0		17.5		7.5	
	Spring	37.0		66.5		11.5	
4.0	Fall	16.0	0.33	11.0	0.37	3.0	0.60
	Spring	29.0	0.22	56.0	0.16	7.0	0.39
6.0	Fall	12.0	0.50	7.0	0.60	1.8	0.76
	Spring	24.0	0.35	20.0	0.70	5.0	0.57
8.0	Fall	9.0	0.63	5.0	0.71	1.5	0.80
	Spring	20.5	0.45	11.0	0.83	4.0	0.65
10.0	Fall	7.0	0.71	4.0	0.77	1.0	0.87
	Spring	18.0	0.51	8.0	0.88	3.5	0.70
12.0	Fall	6.0	0.75	4.0	0.77	1.0	0.87
	Spring	16.5	0.55	7.0	0.89	3.5	0.70

¹Taken with respect to the 2.0-inch depth stresses, and includes 3.0 inches of C. "B" asphalt concrete wearing course.

²Spring stresses are stresses obtained at failure and includes both fall and spring periods.

Discussion of Results

The sudden occurrence of distress and failures in the two thinnest emulsion-treated bases (sections 5 and 6) were unexpected. One of the reasons for this surprising development probably was the mixing and construction problems of the emulsion mix. The mix was too wet and proper curing may not have been achieved. Studies done by Monismith, Terrel, and Chan (16) indicate that the modulus of emulsion-treated aggregate varies with the amount of curing and as curing progresses, the modulus will increase. Finn *et al.* in their report (17) and the Chevron Asphalt Company (18) emphasize this property of the emulsion-treated bases. The fact that complete cores could not be obtained may be an indication that curing was in progress. This may mean that the thin sections had not reached their proper strength and that they were too thin to overcome the wheel load effects. Hence, they failed sooner than expected.

Why the second and third thinnest untreated base (sections 2 and 3) developed distress before the thinnest section is conjecture. Early subgrade failure may be the reason. Section 1 was in the path of greatest travel during construction and the subgrade may have become more compacted than either of the two sections. The advent of rain no doubt accelerated the failures as water was able to seep through the cracks, therefore continuously saturating the base and the subgrade. This was borne out by the fact that the subgrade moisture decreased with depth (see the first part of this report).

Why transverse cracks? In many highways longitudinal cracking is the norm, thus indicating that the curvature basin is larger in the transverse direction. The curvature basin is larger in the longitudinal direction in the test track sections, hence higher tensile stresses were developed in this direction. This was partly borne out by strain gage readings. Ring #3 also shows similar development of transverse cracks as initial signs of distress indicating that this

may be a natural condition of the test site and the test (19).

Failures occurring during the spring testing period were spectacular and catastrophic. Deflections were very high--in excess of 0.084 inches. During this period the speed of the apparatus was 10 mph and because of the eccentric mechanism, which is dependent upon the apparatus speed, the wheels took a long time to cross the wheel path width. Hence there was a concentration of wheel load on one part of the pavement. The first few heavy wheel loads probably caused considerable permanent deformation. This phenomena has been reported by the Canadian Good Roads Association (12). The edge location of the observed failures may have been a factor as suggested by the WASHO Test Road Report (20) and reported by Meyerhoff (21). Examination of the subgrade after completion shows that the subgrade was completely saturated. The degree of saturation of the subgrade effects the bearing capacity of flexible pavements as indicated by Broms (22). A reduction in relative density and an increase in degree of saturation which occurs during the spring breakup period reduces the subgrade bearing capacity greatly. This probably occurred in the sections that failed spectacularly in the spring. The fact that rutting occurred also indicates that rutting may have extended into the subgrade soil. Vesic and Domaschuk (23) show that certain maximum vertical stress levels exist and that once these values are reached they may not appreciably increase, thus remaining within the pavement structure. The vertical stresses did increase during the spring period, perhaps indicating that this stress level was exceeded and, hence rutting was extended into the subgrade. Another indication of different mode of failure occurring during the spring was that LVDT and Benkelman beam deflections were two to four times greater than in the fall. Since a relatively weak, compressible subgrade and a strong, well-compacted but thin pavement structure existed, structural failure occurred through punching shear. Therefore it can be said that different

subgrade conditions occurred during fall and spring testing periods causing different conditions and different modes of failure.

Studies of the data obtained by instrumentation reveal that the data was insufficient to show definite results but that certain trends could be discovered. Lateral wheel placement did affect the measured values of stress, strain, and deflection. This has been borne out by other studies (13, 15). Deflections occurring in the untreated bases show that about 48% of the movement occurred within the pavement and base structure and that this increased with wheel loads perhaps indicating a decrease in modulus (24). Deflections increased with wheel loads indicating possible variations in the resilient characteristics of the subgrade due to environmental changes during the life of the pavement. This may be especially true during the spring when deflections increase two- to fourfold.

Strain readings below the pavement show that maximum strain occurred directly under the tire. Strains were higher in the spring than during the fall. Tensile strain increased with depth while compression decreased. Gusfeldt and Dempwold (25), Klomp and Niesman (26) obtained strain results under controlled centered loading and with uniform top to bottom temperatures which were almost similar to that obtained at the test track. Some deviations were observed due to temperature differences between layers and different loading. An attempt to correlate tensile strains and deflection data was unsuccessful due to insufficient data. This was done to try to establish a criterion for measurement of fatigue failure (27). It is hoped that this may be possible as data from the next two rings becomes available.

Work done by Sowers and Vesic (28) and Nijober (29) shows that vertical stress decreases with depth and is affected by the lateral positions of wheels. The different bases had a marked effect on the stress level. During the spring

periods, stresses measured increased two to three times. The significance of this has been previously discussed. Readings obtained from the Filpip transducers seem to be unsatisfactory, especially near the surface. The possibility that the capacitor plates may have become overstressed during compaction does exist. When distress occurred, high pressures were measured indicating that perhaps pressure points may have been established as the pavement section began to act as separate entities.

Equivalencies based on fall and spring testing periods are shown in Table XXV. At the AASHO Road Test, one inch of bituminous surface was equivalent to 3 inches of crushed stone base or to 4 inches of sand-gravel subbase (13). Experience in Canada indicates that ratio of the relative supporting capacity of bituminous concrete surface to granular base may be as low as 2 to 1 (30). Shook and Finn (31), using AASHO Road Test data showed that larger equivalencies of asphalt-concrete surfacing in terms of crushed rock base ranged from 2 to 6.7 depending upon the criteria used. The values shown in Table XXV seem to be reasonable. However, it should be noted that these equivalencies apply only to the materials used in this test and within the range and degree of this experiment and is subject to modification as results from the other rings become available.

TABLE XXV

EQUIVALENCIES IN TERMS OF ATB¹
 (3.0" of C1 "B" A.C. Wearing Course)

Type of Base	Fall '66 ² Inches	Spring '67 ³ Inches	Adjusted ⁴ Spring '67 Inches
UTB	4.75	2.40	1.85
ETB	3.50	1.80	1.38
ATB	1.00	1.00	1.00

- ¹ It should be emphasized that these equivalencies are tentative and are subject to change as results from other rings become available.
- ² These equivalencies are based on the thinnest sections which survived during this period. For example, 2.0 inches of special aggregate asphalt-treated base is equivalent to 7.0 inches of emulsion-treated crushed stone base and 9.5 inches of crushed stone untreated base. (See Table XV).
- ³ These are based on the thickest sections which failed during this time. For example, 5.0 inches of special aggregate asphalt-treated base is equivalent to 9.0 inches of emulsion-treated crushed stone base and 12.0 inches untreated crushed stone base. (See Table XV).
- ⁴ These values were obtained by adjustments which took into account the fact that at "ultimate" failure, both the untreated and emulsion-treated sections were in better condition than the asphalt-treated base. Certain assumptions were made which may or may not be borne out by results from the next test ring, hence judgment should be postponed until then. These assumptions and adjustments are shown in Table XV, Figure 54 and the explanation is on page 64.

Limitations of Test Track Testing

The test track testing is no substitute for full-scale test roads. There are built-in limits. Time effects cannot be evaluated or measured as a test track pavement lasts only 3 to 6 months. Hence, long-term environmental effects cannot be taken into account. Aging of the asphalt pavement cannot be measured. The test track surface is not subjected to traffic wear of a regular road such as skidding, braking, and different random loads and different vehicles. The test track will not give exact answers but relative ideas of the strength and properties of various pavements under test. The test track is an intermediate step between building a full-scale highway and the laboratory. Properly used, highway engineers can obtain an idea of what can be used, its relative performance, and its strength with respect to other standard materials. Laboratory results can be confirmed by test track testing. It is an intermediate step and an economical method of evaluating theories and materials before applying them to full-scale roads such as the AASHO and WASHO road tests.

The relative narrowness and limited lengths of the test sections may disturb some engineers. That boundary conditions may exist because of these limited pavement dimensions is acknowledged. But the question to be answered is when is a test pavement a continuous road? How long does a test section have to be before it duplicates a continuous road? There is no discreet answer. These small pavement sections would give similar relative answers on pavement and material performance even if the test pavement lengths were doubled or tripled.

As much as possible regular construction methods were used for the construction of these pavements. Admittedly the equipment used was perhaps not as large as on some freeway projects and certain deviations from regular construction practice was necessary because of the circular dimensions of the track and the needs of the pavement design, especially the subgrade. Great care was taken to

ensure that the test pavements met Washington State Highway Department specifications.

The test track is open to all weather conditions, hence environmental effects cannot be properly evaluated. This was also true for the AASHO, WASHO, and other road tests. It is very difficult to control the environment unless one has the test pavement protected from the elements and the environment controlled. All that can be done is test the pavement during certain periods-- summer, fall, and spring--and compare results. One will receive relative comparisons between the different seasonal effects. Long-term environmental effects, as mentioned before, cannot be measured because of the nature of the testing operation. Testing is always a compromise between variables as done in the AASHO Road Test (32). The test track was a compromise hence, certain variables cannot be evaluated exactly.

The possibility that weight distribution on the duals may change does exist. This may occur when changes in wheel camber and transverse slope occur. As the latter changes, wheel camber may change thus distributing the weight unevenly. This probably occurs at the test track when the pavement surface deteriorates thus changing longitudinal and transverse slope. This also occurs in highways, especially on roads with poor rideability characteristics.

The diameter of the test track is fixed and only so many feet of pavement can be built. Hence one is limited to a certain radius and length of sections. The fact that the wheels move constantly in a circle might induce centrifugal forces and impose unusual stresses in the pavement was studied and eliminated by the balanced three wheel system. The tight turning radius might cause exceptional scuffing between the tires and the pavement. This effect was studied in Ring #1 and it was concluded that although increased tire wear does occur, this is more an effect of the pavement on the tires rather than the opposite

(33). The fact that the outside tire is free-wheeling minimizes the frictional effect that this tire might have had on the pavement as the duals rotate.

Some boundary effects occur where the concrete tunnel is located by the pavement. The actual effects are as yet incompletely known. Observations of Rings #2 and #3 seem to indicate that temperatures in the soil and pavement are higher in the winter than in the rest of the track. This is due to heat transfer from the tunnel to the track. The concrete wall might also act as a barrier to drainage thus contributing to the saturation of the subgrade. This is being studied and evaluated.

The limitations of the test track findings are obvious. The findings only relate specifically to the soils and the materials actually used in the test pavements, to the conditions under which the materials were placed, and to the environment and climate at the test site. The results relate only to the traffic of uniform wheel loadings applied in this experiment and not to mixed truck and passenger car traffic such as found on normal highways. Time was another limitation. Since this test ring was part of a three test ring series, first evaluations and results await the completion of these rings. Findings here may be later modified.

CONCLUSIONS

Major Conclusions

1. The testing period could be divided into two different periods--fall, 1966 and spring, 1967. Subgrade support was very different during these two periods. Deflections, strains, and stresses were 2 to 4 times higher during the spring period than for the fall period. Investigation revealed that the subgrade was saturated during the spring period, hence indicating a weak subgrade when compared to the fall period. Temperature effects seemed to have been negligible.
2. The modes of failure were different during the two testing periods. In the fall distress was heralded by the appearance of random transverse cracks which increased in length and scope followed by alligator cracking pattern. The time to reach "ultimate" failure was long.
3. Preliminary equivalencies were developed and are summarized in Table XXV. The fall equivalencies are based on the thinnest sections that survived, while the spring equivalencies are based on the thickest sections that failed in "ultimate" failure. These findings are valid only to the test and under test conditions.
4. The untreated crushed stone bases developed cracks early. They continued to stay in test for long periods of time indicating resiliency. In contrast, the asphalt-treated base, once cracking started, failed rapidly. At the end of testing only the thickest special asphalt-treated base (5 inches) was almost intact. It, too, was starting to develop minute transverse cracks.
5. On the basis of this test, the special asphalt-treated base seems to have superior load carrying performance ability compared to the emulsion-

treated and untreated crushed stone bases. The early failures of the thinnest emulsion-treated bases may have been due to improper mixing procedures and incomplete curing.

Minor Conclusions

1. Deflections, strains, and stresses were greatly affected by the lateral position of the dual tires. Temperature effects seem to have negligible effects due to the small temperature range during the testing periods.
2. Definite findings could not be reached due to the lack of sufficient data on deflections, strains, and stresses. Hence trend lines had to be used to obtain some of the results. This indicates the need for a semi-automatic system which can take continuous data. This is being planned for Ring #4.
3. The maximum values of strain, deflection, and stress are of special interest in continuing research to establish failure criteria. Some maximum values have been obtained. The full significance of these values awaits the completion of the next two rings. These findings are sustained by Kingham's report (34).
4. Some modifications in the instrumentation have been based on the findings from Ring #2. Several instruments were found to be unsuitable and have been replaced with more reliable instruments. Experiments with strain gage placement are still continuing. As confidence develops in the reliability of the instruments, fewer changes will be necessary.

PRACTICAL IMPLICATIONS FROM TEST RING #2

The construction techniques and the control exercised in Test Ring #2 were unusual, unusual in the sense when compared to normal practices used in typical highway construction jobs. Even so, with all this care, problems arose because of non-uniform subgrade condition. By this it is meant that although the subgrade met density specifications, the non-uniformity of density may cause problems. Uniformity of subgrade density may be more important than meeting density specifications. This has practical implications for highway departments in that even if one designs a very thick pavement, a poor job or even a careful one on a subgrade preparation, that is the lack of obtaining uniformity of density, may cause the pavement to fail. Once again, this points out that subgrade preparation and density uniformity are of the utmost importance, and that one cannot correct this even by using over-designed pavements.

Emulsion-treated bases have an advantage in that they can be cold-mixed either in a plant or right on the job. There may be a cost advantage in areas where plants are not available. However, some care is needed. The proper amount of moisture must be added otherwise curing problems may arise as in Ring #2. Before another layer is applied, the lower layer has to be cured properly otherwise the necessary strength will not be developed. In fact, one can say that curing is important in obtaining the desired strengths in emulsion-treated bases.

The results from Rings #1 and #2 indicate that the use of non-fractured screened aggregate is feasible. This type of base is apparently equal to many other types. Economies can be achieved as crushing would not be necessary. Since similar type of aggregates exist on the west coast, both contractors and highway departments could save money using these aggregates. Complete equivalencies and comparative strengths will have to await the results from Rings #3 and #4.

The equivalencies shown in Table XXV have practical implications to the pavement designer. He can now compare the equivalent strengths of the different materials used. The engineer must design pavements to be able to weather the most critical periods and environments. Results from Ring #2 show that conditions during the spring thaw are most critical; hence, this should be recognized in design problems.

Benkelman beam measurements can be used to predict where and to some extent when distress may occur. This would mean correlating deflections with pavement distress. This has practical implications for maintenance. As soon as one knows that a pavement has reached a critical stage, an overlay can be planned. This would require studying deflections for all thicknesses and types of roads, and setting up deflection limits. When these limits are reached, the maintenance department would plan on laying an overlay. This would be economical in that overlays would not have to be applied before necessary. Maximum life of existing pavements could then be achieved. It is hoped that results from Rings #3 and #4 will help in developing critical deflection values for pavements.

Deflections, strains, and stresses obtained from LVDT's, strain gages, and pressure cells will be useful in helping to evaluate strength parameters in pavements. Data from Ring #2 showed some interesting trends, which may be further clarified as data from Rings #3 and #4 become evaluated and available. This may lead to the development of critical values for pavement deflections, strains and stresses so that failure and design pavement theories can be formulated. In the long run, this may lead to better and more economical pavements.

REFERENCES

1. Theodore W. Horner. Experimental Design and Analysis of Experiments for Comparison of Paving Materials, Engineering Analysis Section, The Asphalt Institute, Booz Allen Applied Research, Inc., August, 1965.
2. Standard Specifications for Road and Bridge Construction--1963, Washington State Highway Commission, Department of Highways, Olympia, Washington.
3. Specifications for Paving and Surfacing of Pavement Test Track, Washington State University, Project No. 918, June 24, 1966.
4. Milan Krukar. "Highway Test Track, Research Project Y-993," Quarterly Report No. 2, Washington State University, September 30, 1967.
5. Pavement Instrumentation Studies for San Diego County Experimental Base Project, The Asphalt Institute, Materials and Research Development (a division of Woodward, Clyde, Sherard and Associates), Oakland, California, February, 1966.
6. D. Crony and J. D. Coleman. "Pore Pressure and Suction in Soil," Proceedings, Pore Pressure and Suctions in Soils Conference, 1960, Buttersworth, 1961.
7. Milan Krukar. Instrumentation of Test Ring No. 2, Preliminary Report, Washington State University, October, 1965.
8. Milan Krukar. "Pavement Test Track, Project Y-651," Monthly Progress Reports No. 35-46, Washington State University, July, 1966 to June, 1967.
9. Milan Krukar. "Pavement Test Track, Project Y-651," Quarterly Progress Reports No. 11-14, Washington State University, September, 1966 to June, 1967.
10. Climatological data from U. S. Department of Commerce, Environmental Science Service Administration, Washington, D.C., 1966-67.
11. Milan Krukar. Density and Moisture Content Report, Ring #2, Special report to the Asphalt Institute, Washington State University, December 2, 1966.
12. "Pavement Evaluation Studies in Canada," Technical Publication No. 19, Canadian Good Roads Association, Ottawa, Canada, September, 1963.
13. "The AASHTO Road Test, Report 5, Pavement Research," Special Report 61E, Highway Research Board, Washington, D.C., 1962.
14. R. Ian Kingham. Report on Strain and Deflection Data--Washington State University Test Track--Test Ring #2, Special Projects Section, The Asphalt Institute, October, 1962.
15. "Three-Year Evaluation of Shell Avenue Test Road," Highway Research Record No. 117, Shell Avenue Test Road Committee, Highway Research Board, Washington, D.C., 1965.

16. C. L. Monismith, R. L. Terrel, and C. K. Chan. "Load Transmission Characteristics of Asphalt-Treated Base Courses," Proceedings, Second International Conference of the Structural Design of Asphalt Pavements, University of Michigan, Ann Arbor, August, 1967.
17. F. N. Finn, R. G. Hicks, W. J. Kari, and L. D. Coyne. Design of Emulsified Asphalt Treated Bases, Highway Research Board, Annual Meeting, Washington, D.C., 1968.
18. Bituminal Base Treatment Manual, Chevron Asphalt Company, 1967.
19. Milan Krukar. "Highway Test Track, Project Y-993," Quarterly Progress Report No. 3, Washington State University, December, 1967.
20. "The WASHO Road Test, Part 2 Test Data Analyses Findings," Special Report No. 22, Highway Research Board, Washington, D.C., 1955.
21. G. G. Meyerhoff. "Influence of Shoulders on Flexible Pavement Strength," Proceedings, Canadian Good Roads Association Meeting, 1960.
22. Bengt. B. Broms. "Effects of Degree of Saturation on Bearing Capacity of Flexible Pavements," Highway Research Record No. 71, Washington, D.C., 1965.
23. A. S. Vesic and L. Domaschuk. "Theoretical Analysis of Structural Behavior of Road Test Flexible Pavements," National Cooperative Highway Research Program Report 10, Highway Research Board, Washington, D.C., 1964
24. H. B. Seed, F. G. Mitry, C. L. Monismith, and C. K. Chan. "Prediction of Flexible Deflections from Laboratory-Repeated Load-Tests," National Cooperative Highway Research Program Report 35, Highway Research Board, Washington, D.C., 1967.
25. K. H. Gusfeldt and K. R. Dempwolff. "Stress and Strain Measurements in Experimental Road Sections Under Controlled Loading Conditions," Proceedings, Second International Conference on the Structural Design of Asphalt Pavements, University of Michigan, Ann Arbor, August, 1967.
26. A. J. G. Klomp and Th. W. Niesman. "Observed and Calculated Strains at Various Depths in Asphalt Pavements," Proceedings, Second International Conference on the Structural Design of Asphalt Pavements, University of Michigan, Ann Arbor, August, 1967.
27. Hyoungkey Hong. "Fatigue Characteristics of Flexible Pavement," Proceedings of the American Society of Civil Engineers, Journal of the Highway Division, April, 1967.
28. G. F. Sowers and A. B. Vesic. "Vertical Stresses in Subgrade Beneath Statically Loaded Flexible Pavements," Highway Research Board Bulletin 342, Washington, D.C., 1962.
29. L. W. Nijober. "Testing Flexible Pavements Under Normal Traffic Loadings by Means of Measuring Some Physical Quantities Related to Design Theories," Proceedings, Second International Conference on the Structural Design of Asphalt Pavements, University of Michigan, Ann Arbor, August, 1967.

30. Report on AASHO Road Test, Canadian Good Roads Association, Ottawa, Canada, 1962.
31. J. F. Shook and F. N. Finn. "Thickness Design Relationships for Asphalt Pavements," Proceedings, First International Conference on the Structural Design of Asphalt Pavements, University of Michigan, Ann Arbor, August, 1962.
32. W. N. Carey, Jr. "Extending the Findings of the AASHO Road Test," 49th Annual Convention of the National Sand and Gravel Association and the 35th Annual Convention of the National Ready Mixed Concrete Association, Miami Beach, Florida, January 26, 1965.
33. Milan Krukar. "A Study of Truck Tire Wear on the Pavement Test Track," Circular 37, Technical Extension Service, College of Engineering, Washington State University, 1966.
34. R. Ian Kingham. Report on Preliminary Performance Findings, Washington State University Test Track, Special Projects Section, The Asphalt Institute, October, 1967.